THE INTERACTION BETWEEN PHYTOPLANKTON AND BACTERIA IN RESPONSE TO OIL AND DISPERSANT; IMPLICATIONS FOR MICROBIAL MUTUALISM AND CARBON CYCLING

A Thesis

by

SAMANTHA PATRICIA SETTA

Submitted to the Office of Graduate and Professional Studies of
Texas A&M University
in partial fulfillment of the requirements for the degree of

MASTER OF SCIENCE

Chair of Committee,	Antonietta Quigg
Co-Chair of Committee,	Jessica Labonté
Committee Member,	Jason Sylvan
Head of Department,	Anna Armitage

August 2018

Major Subject: Marine Biology

ABSTRACT

Microbial communities play a vital role at the base of the food web providing and recycling essential nutrients and carbon for larger organisms. Phytoplankton in the ocean are responsible for approximately 50% of global primary production. After phytoplankton leeching, lysis, or death, this fixed carbon can be recycled by bacterial communities. During the 2010 Deep Water Horizon (DwH) oil spill in the Gulf of Mexico, on site researchers and responders recorded unprecedented formations of marine snow. In the presence of oil or oil plus dispersants, microbial communities also produced marine oil snow (MOS); aggregates in which oil has become entrapped. In order to determine key players in phytoplankton–bacterial interactions responding to oil spills, natural microbial communities were collected from two sites in the Gulf of Mexico, an 'open ocean' site near the Flower Garden Banks, and a 'coastal' site off the coast of Louisiana. Mesocosm tanks (~100 L) were used to examine impact of oil spill both with and without the dispersant on the microbial (prokaryotic and eukaryotic) community composition. The eukaryotic community composition was driven by the type of water mass (open ocean vs. coastal) and treatment, while the prokaryotic community composition was primarily influenced by treatment. Interactions between microbial communities were compared using statistical associations in a co-occurrence network. Key players in the interaction between phytoplankton and bacteria include putative hydrocarbon degraders (mainly Alpha- and Gammaproteobacteria), especially *Methylophaga*, and *Pseudalteromonas*. The *Methylophaga* and *Pseudalteromonas* interacted with Bacillariophyceae and Dinophyceae based on water mass (open ocean vs. coastal) and treatment. Heterotrophic *Paraphysomonas*, and mixotrophic Dinophyceae interacted with other phytoplankton and bacteria and appeared to be especially

resilient to oil spills. Bacillariophyceae dominated in the coastal experiment, and both Bacillariophyceae and Dinophyceae, which release EPS in response to stressors, were more interconnected in the dispersed oil network analysis. The interaction between microbial organisms is shaped by oil/dispersant and/or EPS production. Competition and resiliency to oil spills was also a key component in the response of Fungi and grazers. By identifying the key players in response to oil spills, further studies can elucidate the microbial response.

ACKNOWLEDGEMENTS

Thank you to my committee members, chair Antonietta Quigg & co-chair Jessica Labonté, as well as Jason Sylvan, and Zoe Finkel for helping with data, advice, and support. Thank you for all the help from the Quigg lab members, Finkel Lab, and Sylvan Lab, especially Shawn Doyle, Amanda Achberger, and Genmei Lin. And thank you to everyone on the ADDOMEx team. Special thanks to Blair Sterba-Boatwright for help with statistics. I thank GOMRI ADDOMEx consortium for making this research possible.

CONTRIBUTORS AND FUNDING SOURCES

Contributors

Sample collection was done by Shawn Doyle, Genmei Lin, Emily Whittaker, and Jason Sylvan. Extractions and sample prep were done in assistance of Shawn Doyle, Genmei Lin, and Amanda Achberger in the Sylvan Lab. Processing was done on the Sylvan lab server with assistance from Shawn Doyle, Genmei Lin, and Amanda Achberger. Advisement by special appointment from Zoe Finkel.

All other work conducted for the thesis was completed by the student independently.

Funding Sources

This research was made possible by a grant from The Gulf of Mexico Research Initiative to support consortium research entitled ADDOMEx (Aggregation and Degradation of Dispersants and Oil by Microbial Exopolymers) Consortium. Data is publicly available through the Gulf of Mexico Research Initiative Information and Data Cooperative (GRIIDC) at http://data.gulfresearchinitative.org (doi: 10.7266/N7C53JDP, doi: 10.7266/N77D2SPZ, doi: tbd, doi:tbd).

TABLE OF CONTENTS

LIST OF FIGURES

LIST OF TABLES

INTRODUCTION

THE DEEPWATER HORIZON AND MOS

On April 20, 2010 the Deepwater Horizon (DwH) Oil Spill began when a platform explosion led to a malfunction in the blowout preventer at the sea floor and ended when the well was sealed on July 15, 2010 (Crone & Tolstoy, 2010). During the 84 days of the DwH, between 4.1 and 4.4 million barrels of Sweet Louisiana Light oil (after accounting for BP's collection effort) were released into the Gulf of Mexico off of the coast of Louisiana (Atlas & Hazen, 2011; Crone & Tolstoy, 2010; McNutt et al., 2012; Reddy et al., 2012). Several attempts were made to clean up the oil on site, including direct recovery from the wellhead, large skimmers, fire booms, and both aerial and deep sea application of dispersants (U.S. Coast Guard, 2011). Approximately 8% of the oil released was chemically dispersed using both COREXIT 9500A and 9527 (U.S. Coast Guard, 2011). Dispersants have been used previously in the Gulf of Mexico and are meant to increase solubility of the oil (U.S. Coast Guard, 2011; Pace et al., 1995) and prevent it from reaching the shore line where critical habitats could otherwise be impacted.

Oil droplets, rather than slicks, are readily degraded by the marine microbial community (Atlas & Hazen, 2011). Light oil, like the Louisiana Sweet Oil released during the DwH spill, is also more easily degraded by the microbial community than crude oil released in other major spills (Atlas & Hazen, 2011). Because of this, Corexit was deemed appropriate to use for the DwH spill for bioremediation efforts (Atlas & Hazen, 2011; U.S. Coast Guard, 2011). Corexit 9500A and Corexit 9527 are considered safe to apply to marine ecosystems when following set guidelines for dispersal period and volume released (U.S. Coast Guard, 2011). However, there have been questions raised about the effectiveness and toxicity of chemically dispersed oil (including Corexit 9527 mixtures) in natural environments. Dispersed oil uptake increases in some organisms like fish, crustaceans, and phytoplankton, while others like oil-degrading

bacteria, thrive in dispersed oil (Hook & Osborn, 2012; Ramachandran et al., 2004; Parsons et al., 1984).

In turn, the fate of oil and Corexit in the marine environment can be affected by extracellular polymeric substances (EPS) released by the microbial community (Quigg et al., 2016). EPS are excreted by both bacteria and phytoplankton under normal conditions, but their production can be exacerbated in response to stressors (Myklestad, 1995). These exudates can take three different forms, marine gels, marine snow, and transparent exopolymeric substances (TEP) (Thornton, 2002). A variety of macromolecules including proteins and acidic polysaccharides make up EPS (Quigg et al., 2016; van Eenennaam et al., 2016). EPS that encompasses oil molecules can either emulsify oil and Corexit or the relative 'stickiness' of the EPS can cause aggregation (Alldredge & Silver, 1988; Passow, 2016; Quigg et al., 2016). During oil spills, aggregates formed are known as marine oil snow (MOS) and serve as substrates for bacterial degradation (Quigg et al., 2016). Unprecedented amounts of marine snow were observed during the Deepwater Horizon oil spill and were attributed to environmental conditions, use of Corexit, and oil present (Passow et al., 2012; Quigg et al., 2016). After the DwH, Passow et al., (2012) concluded there were three main mechanisms in which MOS formed (1) mucous hanging from surface waters at which active microbial degradation eventually lead to pieces falling off and sinking, (2) collision of particles in the water column following the Coagulation Theory, and (3) *Trichodesmium* spp. aggregation (Passow et al., 2012). Minerals can also increase aggregation and sedimentation of marine snow (Daly et al., 2016). The Mississippi River discharge was higher than average in the months before and after the DwH oil spill and resulted in increased suspended sediment and minerals which may have led to increased marine snow formation (Daly et al., 2016). Furthermore, research into the effects of Corexit on

MOS formation have shown both a decrease in overall aggregation and increasing oil concentrations in aggregates, resulting in increased oil sedimentation (Passow, 2016; Passow, Sweet, & Quigg, 2017). MOS sedimentation and microbial recycling during the DwH oil spill transported important carbon, nutrients, minerals, oil, and Corexit to the deep ocean (Passow, 2016; Quigg et al., 2016).

THE MICROBIAL LOOP AND CARBON CYCLE

Throughout the descent of aggregates in the water column, the microbial community affects the degradation of oil and Corexit, as well as the aggregates themselves (Quigg et al., 2016). The breakdown of organic matter by the microbial community is part of the 'microbial loop', first defined by Azam et al., (1983) and more recently, redefined by Jiao et al. (2010). The microbial loop in turn is an important part of the carbon cycle that recycles carbon within the marine environment (Azam et al., 1983; Jiao et al., 2014; Jiao et al., 2010). The carbon cycle begins as inorganic carbon in the form of CO_2 fixed by phytoplankton during photosynthesis and is subsequently available in phytoplankton biomass for larger organisms (Field, 1998; Jiao et al., 2010). Not only can phytoplankton provide carbon as a food source, they also produce nutrients and the aforementioned EPS that can be utilized by bacteria as a carbon source (Amin et al., 2009; Bell & Sakshaug 1980; Lau et al., 2007). Approximately 50% of the carbon produced by phytoplankton is taken up by the bacterial community (Azam et al., 1983).

Additionally, predation on phytoplankton results in release of organic matter by sloppy feeding in either dissolved or particulate form (Jiao et al., 2014). Organic matter can also be released by cell lysing viruses that create a 'viral shunt' of organic matter towards the microbial loop (Wilhelm & Suttle, 1999; Jiao et al., 2014). Particulate organic matter (POM) can still be used by other organisms and enter back into biogeochemical cycling (Jiao et al., 2014).

However, a fraction of the dissolved organic matter (DOM) is too small for the microbial community to recycle (Azam et al., 1983; Jiao et al., 2014). For example, recalcitrant dissolved organic matter (RDOM) is more readily produced in ecosystems with low nutrient input, where the C:N content of cells is higher and therefore more difficult to metabolize (Jiao et al., 2010). Some of the RDOM will aggregate as it sinks into a form large enough for the microbial community to break down (Jiao et al., 2014). The rest of the RDOM that escapes consumption and degradation sinks to depth and is sequestered into long-term carbon storage known as the microbial pump (Azam et al., 1983; Jiao et al., 2010).

The initial draw-down of atmospheric CO_2 by the phytoplankton community and subsequent sinking of particulate organic carbon (POC) to depth is known as the biological pump (Jiao et al., 2014). Although both the microbial carbon pump and biological carbon pump work in unison in both nutrient-rich and oligotrophic water, the microbial carbon pump is dominant in the latter (Jiao et al., 2014). During the months surrounding the DwH oil spill satellite images revealed high chlorophyll in the spill area indicating a phytoplankton bloom (Daly et al., 2016; Hu et al., 2011). With a large phytoplankton biomass and oil spill hydrocarbons available for bacterial consumption, both the microbial and biological carbon pump made similar contributions to long-term carbon storage (Fenchel, 2008; Guidi et al., 2016; Hu et al., 2011; Joye et al., 2014). Furthermore, the sedimentation of aggregates formed by exudates of both phytoplankton and bacteria provides an additional mechanism for oil and dispersant transport to long-term storage (Jaio at al., 2014; Quigg et al., 2016).

PHYTOPLANKTON

Phytoplankton play a vital role at the base of the food web and account for approximately 50% of global primary productivity and fix 45 gigatons of carbon per year (Falkowski et al., 1998; Field, 1998). Phytoplankton growth can be limited by both nutrients and light in the open ocean (Field, 1998; Moore et al., 2013). Because they are dependent on light, they reside in the euphotic zone at depths where ≥1% of surface irradiance is available, and have adaptations to promote buoyancy and decrease cell density (Graham et al., 2016). However, some species of phytoplankton sink out of the euphotic zone as part of their life cycle and exudates might be an evolutionary adaptation for aggregation and subsequent sedimentation (Passow et al., 1994; Thornton, 2002). Moreover, aggregation might increase uptake of nutrients, which are also limiting to phytoplankton (Thornton, 2002).

According to Liebig's law of the minimum, the essential nutrient present in the lowest concentration in an ecosystem limits growth even if other nutrients are in excess (Danger et al., 2008). However, more recent research indicates co-limitation occurs especially in high nutrient low chlorophyll regions in the world's oceans (Martin, 1988; Moore et al., 2013; Wells et al., 2005). In the northern Gulf of Mexico where the DwH oil spill occurred, phytoplankton communities can be nitrogen-limited (Zhao & Quigg, 2014) or phosphate-limited (Sylvan et al. 2007; 2011), or both, along different parts of the shelf (Quigg et al. 2011) and/or depending on the river discharge. As mentioned in the preceding section, river discharge from the Mississippi River during the oil spill was higher than average and contributed to high phytoplankton biomass (Hu et al., 2011). Interestingly, release of EPS has been shown to increase during periods of stress and nutrient limitation (Shniukova & Zolotareva, 2015; van Eenennaam et al., 2016).

While phytoplankton growth and EPS release can be limited by bottom-up trophic interactions (nutrients and light), there are also top-down controls on phytoplankton biomass and aggregation (Graham et al., 2016; Prowe et al., 2012). Grazing by heterotrophic ciliates, zooplankton, and small crustaceans can affect both the density and diversity of the phytoplankton community (Graham et al., 2016; Prowe et al., 2012). Infection and lysis by viral communities found in the water column were also discovered to impact algal communities during phytoplankton blooms (Wilhelm & Suttle, 1999). These grazers are an important part of the biological carbon pump and release particulate and dissolved organic matter for use in the microbial pump (Jiao et al., 2010). During the DwH oil spill, low grazing density by zooplankton likely impacted the high satellite chlorophyll *a* measurements seen directly after the spill (Brussaard et al., 2016; Hu et al., 2011).

Not only can both bottom-up and top-down trophic interactions impact the structure and community composition of phytoplankton, but also the added stressors of oil and Corexit during oil spills. Many studies have been done on the effects of oil and dispersed oil on phytoplankton community composition. After the oil spill, as mentioned above, there was an observed phytoplankton bloom in August near the site of the spill (Hu et al., 2011). Comparisons between phytoplankton community composition before, after, and during the oil spill showed an overall decrease in phytoplankton abundance (Parsons et al., 2015). Community composition was dominated by diatoms, cryptomonadas, dinoflagellates, and cyanobacteria during the year of the oil spill compared to pre- and post-oil spill composition (Parsons et al., 2015). Gonzalez et al. (2009) did a study to tease apart the effects of oil on algal communities in both oceanic and coastal environments. Autotrophic nanoflagellates increased in both open ocean and coastal communities, while picophytoplankton decreased, and diatoms showed a unique response

depending on size (González et al., 2009). Harrison et al., (1986) used experimental enclosures and revealed a microflagellate dominated eukaryotic community similar to results of Gonzalez et al., (2009). In 1 L bottles a set of experiments was conducted to replicate conditions during the oil spill for ten different diatom species (Bretherton et al., 2018). *Synechococcus elongates*, *Dunaliella tertiolecta*, *Phaeodactylum tricornutum*, *Navicula* sp., and Skeletonema grethae CCMP775 were found to be tolerant of oil and dispersed oil treatments (Bretherton et al., 2018). However, the centric diatoms, *Thalassiosira pseudonana*, *Lithodesmium undulatum*, and *Skeletonema costatum* were sensitive to oil and dispersed oil treatments, while *Odeontella mobiliensis* was only sensitive to dispersed oil (Bretherton et al., 2018).

While phytoplankton community composition can be affected by oil and dispersant additions, other studies looked at a combination of factors that could be affecting phytoplankton. In an experiment by Ozhan et al. (2014), toxicity measurements taken during lab experiments found different responses based on phytoplankton functional communities and size. At lower oil concentrations dinoflagellates were better adapted while diatoms did better at higher concentrations (Ozhan et al., 2014). Corexit additions in the same experiment not only increased oil uptake and toxicity to phytoplankton, but also were toxic when added without oil to these communities (Ozhan et al., 2014). In a set of experiments involving concurrent sanctioned oil release in the water column and a set of microcosms on-board a vessel, Brussard et al., (2016) discovered lower chlorophyll *a* measurements, phytoplankton viability, and community composition in oil treatments. Salinity, temperature, sunlight, and nutrients can also affect oils toxicity to phytoplankton communities. Phototoxicity, or the weathering of oil by sunlight, also increased the negative impact of oil on different phytoplankton species (Ozhan et al., 2014; Lee et al., 2003). Oil spills create a slick in surface waters which can reduce light and decrease gas

exchange for phytoplankton (Ozhan & Bargu, 2014). Haung et al., (2011) found increased uptake of oil by *Skeletonema costatum* during warmer months and hypothesized it to be the result of increased metabolic activity. Furthermore, investigations have also been conducted on toxicity pathways in phytoplankton (Deasi et al., 2010; Garr et al., 2014; Hook & Osborn, 2012). Dispersed oil can cause membrane damage, result in damage to DNA, and decrease cell division and motility (Deasi et al., 2010; Garr et al., 2014; Hook & Osborn, 2012). Phytoplankton have a range of sensitivities to oil and Corexit depending on species and environmental conditions, therefore further research needs to be done to expand upon the effects of oil on these vital algal communities.

INTERACTIONS BETWEEN PHYTOPLANKTON AND BACTERIA

As susceptible as some species of phytoplankton are to both oil and Corexit, natural microbial communities in the marine environment include hydrocarbon degraders that can diminish these toxic effects (McGenity et al., 2012). Hydrocarbon degraders are present in the Gulf of Mexico throughout the water column and in the sediment, which resulted in a microbial response at the blow out preventer and in the deep water plume (Dubinsky et al., 2013; Valentine et al., 2010). In fact, biodegradation, or the breakdown of oil by hydrocarbon degraders, is the primary source of remediation during oil spills (McGenity et al., 2012). Oil released during an oil spill contains a mix of hydrocarbons including alkanes, mono-aromatic hydrocarbons, and polycyclic aromatic hydrocarbons (PAHs) (McGenity et al., 2012). The main hydrocarbon degraders found during the DwH oil spill included species of *Oceanospirilalles, Colwellia, Cyclocalasticus, Flavobacteria, Rhodobacteriales,* and *Alcanivorax* (Hu et al., 2017; Joye et al., 2014). There is a recognized community succession in the event of added hydrocarbons (oil

spills), although the main degraders may change depending on environment (McGenity et al., 2012; Mckew et al., 2007). This succession typically starts with *Alcanivorax*, which degrade branched alkanes, followed by *Cycloclasticus* degrading PAHs, and *Thalassiolituus* degrading *n*-alkanes (McKew et al., 2007). While these are the known main players in hydrocarbon degradation, there is still research to be done on the effects of Corexit on the DwH oil spill microbial communities; evidence thus far indicates a negative impact (Joye et al., 2014).

Bacterial communities are known to interact with phytoplankton communities in the euphotic zone competitively, synergistically, and as parasites (Amin et al., 2012). Some bacteria are endosymbiotic with certain phytoplankton, especially those that are nitrogen fixers (Cole et al., 1982). These interactions help provide further explanation behind the 'paradox of the plankton', or that diverse populations of phytoplankton reside within the same space and time regardless of the accepted ecological theory of resource partitioning (Amin et al., 2012; Hutchinson, 1961). Resource partitioning now includes recycled nutrients from the associated bacterial communities, as well as the minerals and vitamins they provide (Amin et al., 2012). The bacterial community associated with phytoplankton reside in an area immediately surrounding the phytoplankton cells known as the 'phycosphere' in which transport of nutrients and minerals is governed by diffusive models (Amin et al., 2012; Cole, 1982; Cooper & Smith, 2015; McGenity et al., 2012).

The diffusive boundary layer in the phycosphere allows for transfer of nutrients, metabolites, and vitamins between species (Amin et al., 2012; Cole et al., 1982). Bacterial-symbionts detect phytoplankton using three proposed methods: 1) Quorum sensing, 2) Pheromones released by phytoplankton, and 3) Using other compounds and metabolites (Amin et al., 2012). Communities associated with phytoplankton are specialized compared with bacterial

communities that are free-living in the water column and can include *Pseudomonas, Flavobacterium, Marinobacter, Roseobacter,* and *Achromobacter* (Cole et al., 1982). Both *Proteobacteria* and *Bacteroidetes* are found to be commonly associated with diatom species (Amin et al., 2012; Gardes et al., 2011). An aforementioned type of EPS, TEP, was also discovered to be a tool for bacterial recruitment by phytoplankton and serve as a food source for these symbionts (Amin et al., 2012). A study by Gardes et al., (2011) demonstrated the necessity of the bacterial symbiont for the release of TEP (type of EPS) and the aggregation of the diatom *Thalassiosira weissflogii*. Additionally, hydrocarbons released by phytoplankton communities can be used by hydrocarbon degrading associated microbes, in the absence of an oil spill (Acuna et al., 2009). As mentioned previously, TEP released by algal cells can act as a dispersant for oil and further increase biodegradation (McGenity et al., 2012). Lau et al., (2007) found a diel pattern in transcription of the *glcD* gene which is used to monitor bacterial uptake of glycolate, a phytoplankton exudate. This was one of the first studies that demonstrated proof of the use of algal exudates by bacteria at the molecular level (Lau et al., 2007).

On top of the release of these organic exudates by phytoplankton to encourage recruitment of bacterial symbionts, bacterial species also provide beneficial compounds, nutrients, and vitamins (Amin et al., 2012). One of these, vitamin B_{12} (cobalamin) provides a vital nutrient that's essential to phytoplankton growth but is scarce in the marine environment (Croft et al., 2005). Another experiment, conducted by Foster et al., (2011), demonstrated the importance of nitrogen fixing bacteria for phytoplankton–bacterial interactions in low-nitrogen environments, like that found in the open ocean. N-fixing bacterial symbionts convert nitrogen gas into ammonium which can be taken up by algal cells (Amin et al., 2012; Foster et al., 2011). Iron is also a micronutrient vital to phytoplankton growth, however a binding complex is

generally required for uptake by both phytoplankton and bacteria (Amin et al., 2009). Bacteria were discovered to release an iron-siderophore that converts Fe (II) into a form that can be transported into an algal cell, while also can still be competitively scavenged (Amin et al., 2009). Most of these studies used diatom-bacterial interactions, which is applicable to coastal waters as diatoms are generally dominant (Amin et al., 2012). Antagonistic interactions between phytoplankton and bacteria are also known to occur: some algal species release antibiotic substances, while bacteria can release algacidal compounds (Cole et al., 1982).

Although all of the previous examples take place in the algal associated phycosphere, it is important to note that phytoplankton communities can also interact with free-living communities that vary from that of the bacterial symbionts (Cole et al., 1982). When looking at the community structure during a disturbance like that of an oil spill, it's important to consider both the 'free-living' bacterial communities as well as the algal associated communities (Amin et al., 2012; Cole et al., 1982). Network analysis of community structure over time, and in response to environmental variables like that by Fuhrman & Steele (2008), are especially helpful in this kind of comparison. Fuhrman et al., (1980) found a correlation between algal standing stock to bacterioplankton in the marine environment. This implies that released dissolved organics were most important in the interaction between the two and not the vitality of the phytoplankton communities (Fuhrman & Azam, 1980). The seasonality of both phytoplankton blooms and the highest bacterial density also correlate and can be evaluated using this type of network analysis (Cole et al., 1982; Fuhrman & Steele, 2008). These sources highlight the significant interactions between phytoplankton and the free living bacterial community.

All of these mutualistic interactions provide important resources to both the hydrocarbon degraders and primary producers. Together, these communities play a large role in the carbon

cycle and microbial carbon pump and produce exudates known as TEP. TEP is an EPS that allows aggregation of particulate matter and oil during oil spills to form marine oil snow. As sedimentation occurs, the biomass of MOS associated microorganisms, oil and dispersant are transported to the deep ocean impacting the fate and degradation of these compounds. All of the processes that lead to the formation of MOS during oil spills are dependent on community composition and the interaction between the phytoplankton and bacteria. In order to elucidate the mechanisms of unprecedented MOS production observed during the DwH oil spill, community composition and other molecular techniques were used during a mesocosm experiment in which DwH oil spill conditions were replicated.

QUESTIONS AND ASSOCIATED HYPOTHESES

Overall objective: To determine the key players in phytoplankton–bacterial interactions responding to oil spills in both open ocean and coastal zones of the Gulf of Mexico.

Hypothesis #1: In response to oil, bacterial growth will increase rapidly and communities will shift to species that degrade branched alkanes (e.g., *Alcanivorax*), followed by those that degrade PAHs (e.g., *Cycloclasticus*), and finally *n*-alkane degraders (e.g., *Thalassiolituus*) based on the results of McKew et al. (2007).

Hypothesis #2: Phytoplankton community composition in order of highest abundance to lowest will include diatoms, phytoflagellates, cryptomonads, cyanobacteria, and dinoflagellates in mesocosms conducted during spring/summer in coastal zones and dominated by picoplankton in the open ocean experiment according to Gonzalez et al. (2009).

Hypothesis #3: Changes in phytoplankton communities will be paralleled by those in bacterial communities and driven heavily by treatment; any divergences in this trend will be driven by the water masses (open ocean versus coastal) in phytoplankton communities and treatment in bacterial communities.

METHODS

EXPERIMENTAL DESIGN

In order to test the hypotheses listed above, natural microbial communities were collected with the R/V Trident from an (1) open ocean and (2) coastal environment off of the TX coast using a pump to pull surface water into storage containers on deck. The open ocean sample was collected by the west Flower Garden Banks at 27° 53'41.8" N, 94° 02'20.2" W and used for the mesocosm 3 experiment (Figure 1). The coastal microbial community was sampled off of the coast of Louisiana at 29° 22'52" N, 93° 23'06" W and was used for the mesocosm 4 experiment (Figure 1).

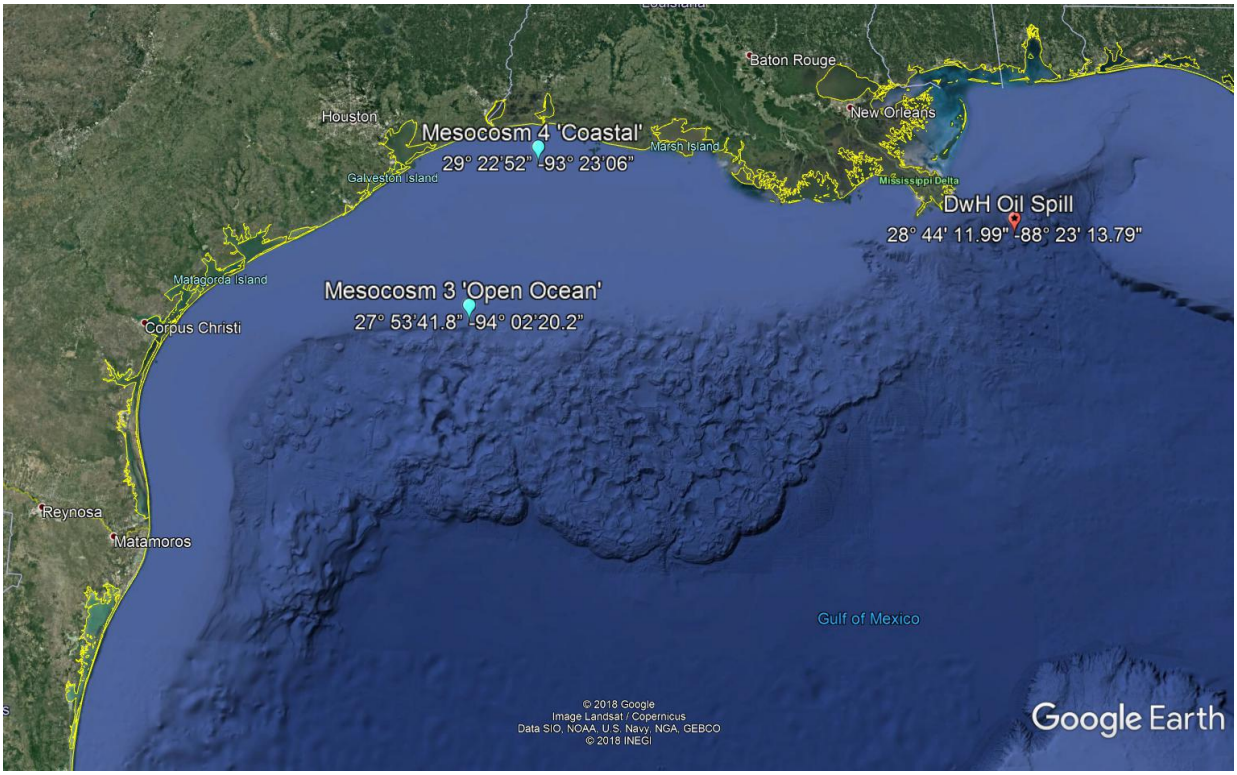

Figure 1: Map of both open ocean (mesocosm 3 experiment) and coastal (mesocosm 4 experiment) sites in the Gulf of Mexico near the location of the Deepwater Horizon Oil spill (DwH Oil Spill) produced using Google Earth ©. Coordinates are shown under the labeled experiments and DwH oil spill locations.

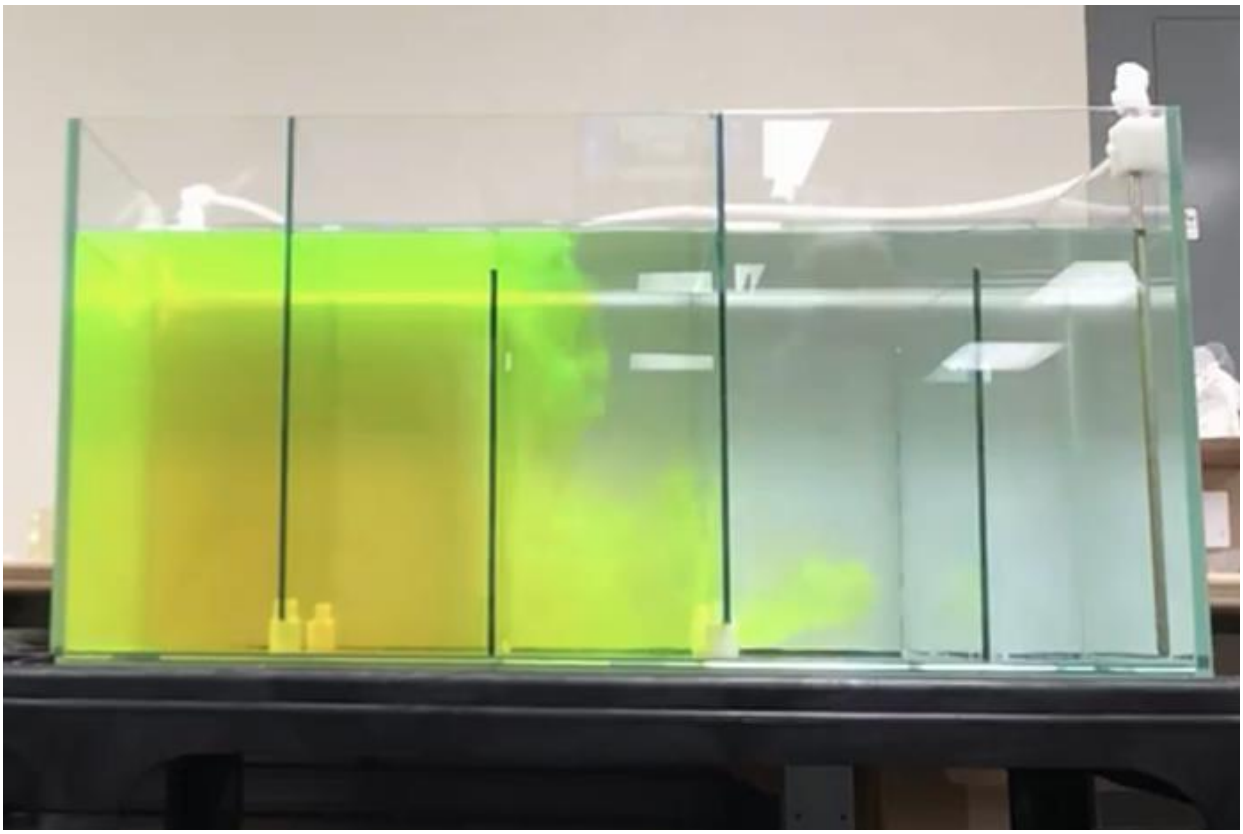

Figure 2: Demonstrating the baffled circulation tank that were used to mix the oil, Corexit, and natural microbial communities for each treatment.

Storage containers were transported back to Texas A&M University at Galveston (TAMUG), where a temperature controlled room in the Sea Life Facility was used to conduct both sets of experiments. Upon arrival at TAMUG, natural communities were added to a baffled recirculation tank (BRT) (Figure 2). These tanks were filled with unfiltered 130 L surface water including any microbial communities and Macondo surrogate oil, with COREXIT 9500 additions depending on treatment (Morales-McDevitt et al., 2017; Wade et al., 2017). While representative of the Gulf of Mexico natural microbial community, the unfiltered community includes grazers and predators that can affect bacterial and phytoplankton community composition.

There were four treatments run in triplicate for both mesocosm experiments with one control and three experimental as detailed below (Figure 3). The control included only the natural community collected at the open ocean or coastal site and were not added to the baffled circulation tanks. The three experimental treatments included water accommodated fraction of Macondo oil (WAF), chemically enhanced water accommodated fraction of Macondo oil (CEWAF), and diluted chemically enhanced WAF (Figure 3) (DCEWAF). Adding Macondo surrogate oil to baffled recirculation tanks allowed the water accommodated fraction or water soluble fraction to dissolve into the sample water, while the insoluble component remains at the surface. The addition of COREXIT 9500 with Macondo oil results in a chemically-enhanced water accommodated fraction with more oil dissolved in the water (Lessard & Demarco, 2000). To mix the WAF treatment, a total of 25 mL of Macondo oil was added to the 130 L of collected natural microbial community in the baffled circulation tank by adding 5 mL every 30 minutes for 2.5 hours. WAF mixing continued for 24 hours following the first addition, to saturate the water with soluble oil. To create the CEWAF, 25 mL of a 1:20 ratio of Corexit:Oil was mixed together, then 5 mL of this mixture was added to 130 L of seawater every 30 minutes for 2.5 hours and left to mix for 21.5 additional hours, for a total of 24 hours. For the diluted CEWAF treatment (DCEWAF) 9 L of the CEWAF mixture described above was added to 78 L of the collected natural microbial community. The final volume in all tanks was 87L. The 130 L of each treatment combined in the BRT tanks were divided for the triplicate tanks to ensure water from each BRT was well mixed. Multiple BRT tanks for each respective treatment and a mixture of BRT tanks for each triplicate were used to ensure similar WAF concentrations. To avoid the confounding effects of nutrient limitation, nutrients were added in f/20 concentrations. All tanks were kept on a Light: Dark cycle of 12:12. The experiments ran for 3-4 days depending

on the health of the phytoplankton community. It is important to note the 0 hr timepoint is in relation to when microbial communities were added to the treatment tanks after the 24 hour mixing period.

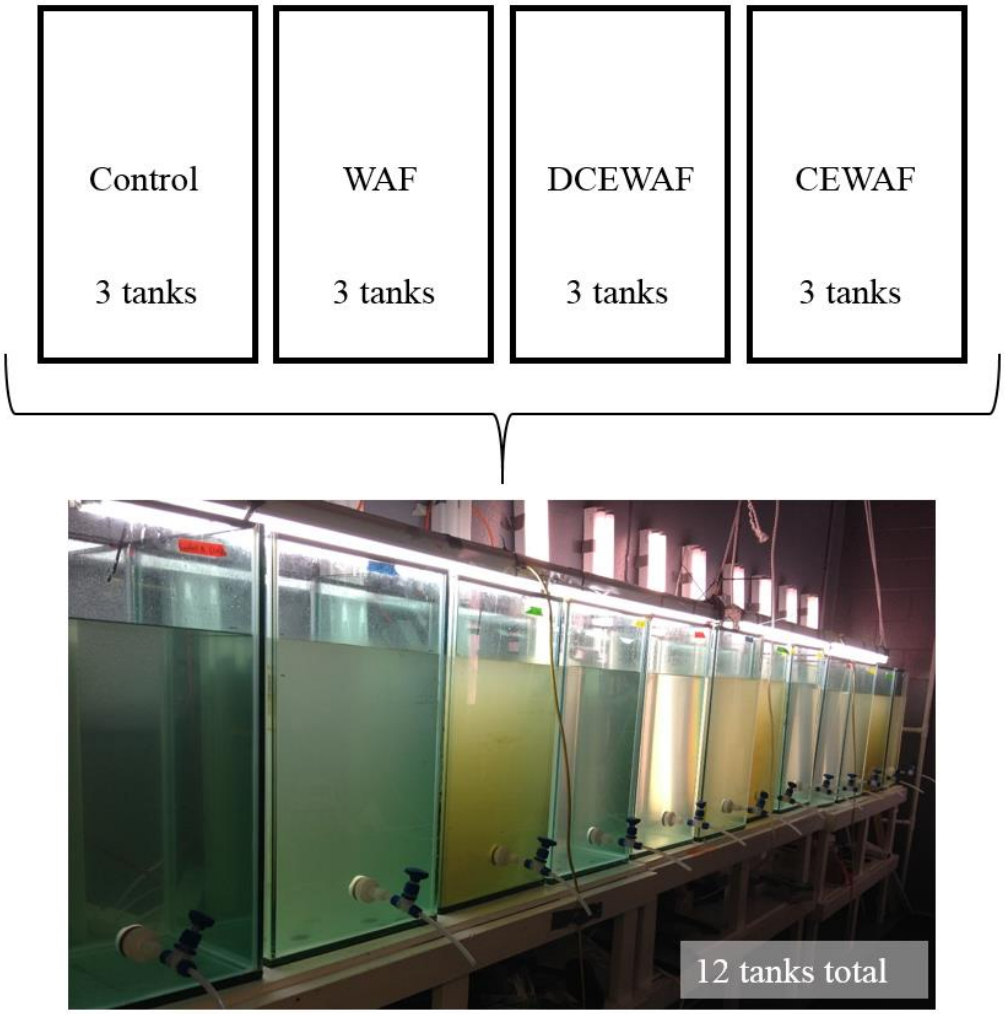

Figure 3: Illustrates the experimental design for both mesocosm 3 and mesocosm 4. Control tanks will be used to compare to three treatments; WAF or water accommodated fraction of oil, DCEWAF diluted chemically enhanced water accommodated fraction, and CEWAF or chemically enhanced water accommodated fraction. There will be three control tanks, and three tanks for each treatment for a total of twelve tanks.

COMMUNITY COMPOSITION USING SMALL SUBUNIT RIBOSOMAL RNA AMPLICON SEQUENCING

In order to determine microbial community composition throughout the experiment, samples were taken every 12 hours from each tank and filtered through 10 um polycarbonate filters by collaborators in the Sylvan Lab from Texas A&M University (TAMU), after which the filtrate were filtered through a 0.2 μm polycarbonate filters. Filters were immediately frozen in a -80 C freezer until extraction. Samples were extracted in Sylvan Lab at TAMU using the MP Bio FastDNA SPIN Kit for Soil according to the manufacturer, with three unused filters for blanks. Both eukaryotic (18S rRNA) and bacterial (16S rRNA) small ribosomal subunits were amplified using polymerase chain reaction (PCR). The PCR amplifications were preformed using GoTaq Flexi DNA polymerase (Promega) following the methods of Caporaso et al., 2012. Samples were run in triplicates of 25μL and cycled at 95˚C for 3 min, then 30 cycles total of 95˚C for 45 s, 50˚C for 60 s (56˚C used for 18S rRNA extractions), and 72˚C for 90 s, followed by elongation at 72˚C for 10 min. After PCR amplification, sample triplicates were combined and run on a 1.5% agarose gel to confirm amplification and quantified using the QuantiFluor dsDNA System (Promega).

Illumina MiSeq analysis on both 16S rRNA (V4 region) and 18S rRNA (V8/V9) hypervariable regions were used to identify bacterial and phytoplankton community composition, respectively (Apprill et al., 2015; Walters et al., 2015). Hypervariable regions although common throughout eukaryotic and bacterial lineages, can better identify to lower taxonomic levels depending on region. Amplification of the 16S rRNA V4 hypervariable region was used to determine bacterial community composition from the aforementioned extracted DNA samples by collaborators in the Sylvan Lab at TAMU according to Doyle et al., 2018. The

primer pair 515F and 806R were used with Golay barcodes and adaptors, and modifications to reduce biases in Crenarchaeota lineage, Thaumarchaeota lineage, and the SAR11 clade (Apprill et al., 2015; Parada et al., 2015, Walters et al., 2015). Bradley et al., (2016) did a comprehensive study to compare differences in phytoplankton community when using the V4, V8, and V9 regions and concluded the V8/V9 combination more accurately represented true community composition (Amaral-Zettler et al., 2009; Bradley et al., 2016; de Vargas et al., 2015). Therefore, dual-barcoded primers were used to amplify the V8/V9 hypervariable regions of the 18S rRNA gene. Three replicates of PCR products were pooled to reduce bias, quantified using the QuantiFluor dsDNA System (Promega), combined into one library, and purified with an UltraClean PCR Clean-Up Kit (MoBio Laboratories) following the methods in Caporaso et al., (2012). A negative PCR was controlled with each PCR run, and procedural controls were included in the final MiSeq library for Illumina MiSeq sequencing (v2 chemistry, PE250 reads) at the Georgia Genomics Facility (Athens, GA, USA).

A similar data analysis pipeline to Bradley et al., (2016) was used to examine sequences and is included in Figure 4. Mothur v.1.39.1, an open-source bioinformatics software was used to edit, trim, and analyze all sequences (both 16S and 18S rRNA hypervariable regions) simultaneously (Kozich et al., 2013). The methods described in the MiSeq SOP (https://www.mothur.org/wiki/MiSeq_SOP) were followed for the analysis of both the eukaryotic and bacterial communities (Kozich et al., 2013). This process trims low quality portions of the sequenced reads and enables the user to assemble, align, and identify operational taxonomic units (OTUs) within each sample. The SILVA 128 database was used for phytoplankton OTU identification with later use of the PR2 database for confirmation of

eukaryotic identification, while bacterial OTUs were identified using only the SILVA 128 database (Edvardsen et al., 2016; Guillou et al., 2013; Quast et al., 2013; Tragin et al., 2016).

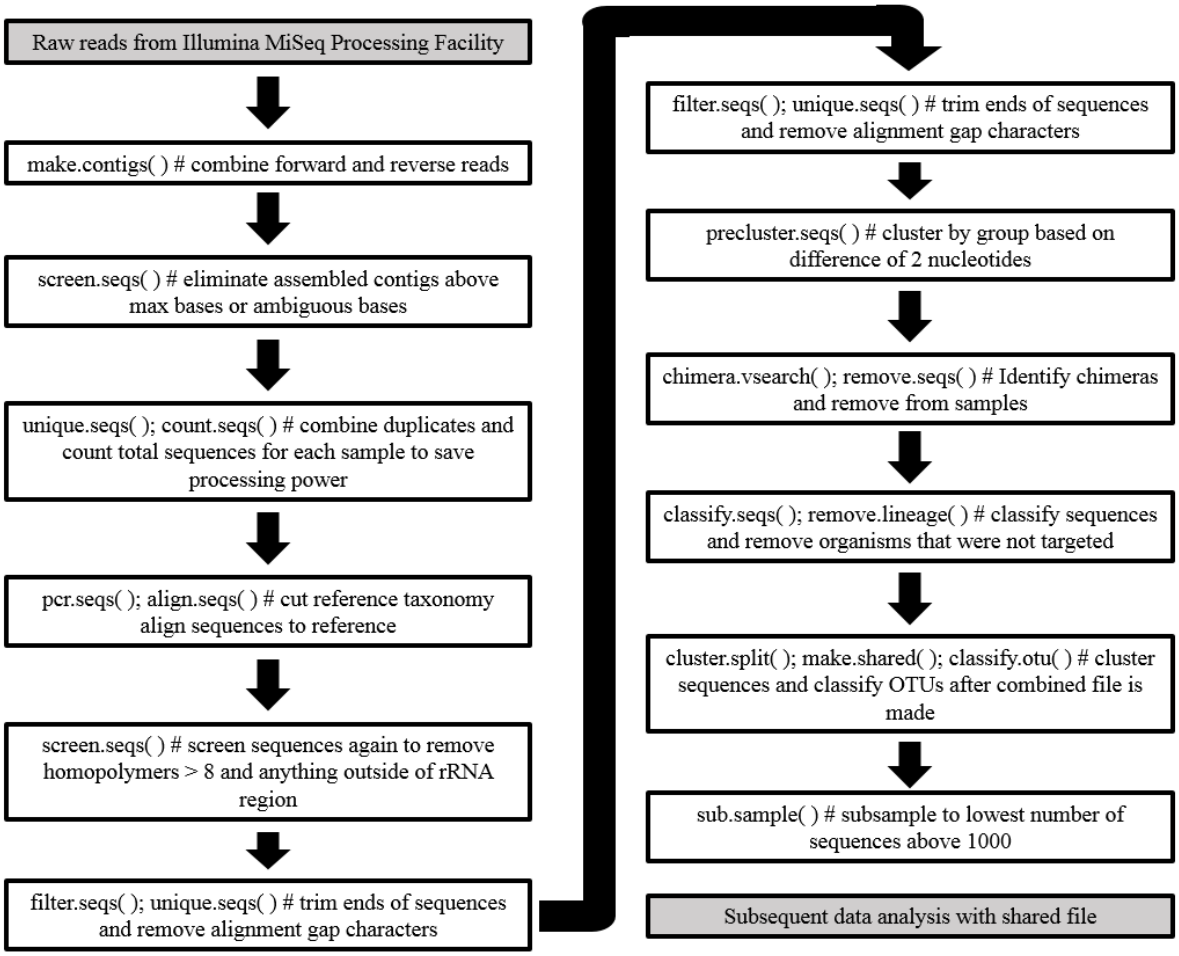

Figure 4: Flowchart describing the sequence processing using the bioinformatics software mothur (Schloss et al., 2009). Each box shows a step in processing with the commands listed and description of steps commented out with a number sign (#). Grey boxes at the beginning and end show the input and output steps.

STATISTICAL ANALYSIS

After identification of major OTUs in each experiment and treatment, the rarefaction curves from each community and experiment were then used to determine the number of sequences to use for sub-sampling from the original community to prevent sequencing depth bias in further analyses

(Weiss et al., 2017). The vertical lines in each rarefaction curve represent the number of sequences used for sub-sampling in each experiment, using the mothur command sub.sample (Figure 4) (Weiss et al., 2017). In the eukaryotic community the sequences were randomly sub-sampled in mother to 8196, while in the prokaryotic community they were sub-sampled to 1114. These numbers were chosen as they were the smallest number of sequences per sample above 1000, for both the prokaryotes and eukaryotes. These sub-sampled communities were then used for the stacked bar graph, NDMS plots, statistical tests and all subsequent analyses (Hughes et al., 2001).

Diversity measures (Inverse Simpson, Chao1 index, and ACE index), and rarefaction curves were calculated using mothur (Appendix Figure A-1 & A-2). Three diversity metrics were used to describe community composition changes in both prokaryotes and eukaryotes; (1) Inverse Simpson, (2) Chao Index, and (3) Abundance Coverage Estimator (ACE). The (1) Inverse Simpson diversity measures evenness in community composition, and is therefore low with only a few dominant species and high with many dominant species (Castro-Nallar et al., 2015). Both the (2) Chao index and (3) ACE measure changes in rare individuals heavily influenced by singletons/doubletons and OTUs with less than ten individuals, respectively (Hill et al., 2003; Hughes et al., 2001). These three diversity metrics give a comprehensive view of community diversity by measuring changes in both the dominant community and rare members of the community (Castro-Nallar et al., 2015; Hill et al., 2003). To compare diversity metrics between experiments and across treatments over time an ANOVA multi-level linear model with a split-plot design was used. Split-plot designs take into account any variation that occurs due to random tank affects. Each tank was a random blocking factor, and Time-point, Treatment, and Environment (Mesocosm3 = Open Ocean, Mescosm4 = Coastal) were included as categorical

predictors (Quinn & Keough, 2002). Another assumption of an ANOVA test includes orthogonal contrasts, which refers to evenness across the sampling matrix. In order to ensure samples were orthogonal, type III Sum of Squares with helmert contrasts were used for categorical predictors (Quinn & Keough, 2002). Whole-plot (environment and treatment) factors aggregated by tank and split-plot (time-point) were tested for homoscedascity (Brown-Forsythe Levene (BFL) and Breusch-Pagan (B-P) tests) and normality (shapiro-wilkes test and qqplots) (Quinn & Keough, 2002). Homoscedascity refers to the ANOVA test assumption that all samples have equal variation. Additionally, the interaction between tank and time-point was also tested (Tukey's non-additivity test) to ensure a random blocking design was appropriate (Quinn & Keough, 2002). Models that seemed to indicate non-linearity in the fitted vs. residuals plot were tested using squared terms of both time-point (after converting to a continuous predictor) and the y-value, however none of these models did significantly better based on Akaike information criterion (AICc). AICc values are used to compare models, while taking into account explained variation and model complexity. Auto-correlation and generalized least squares (GLS) were tested against the regular ANOVA model to correct for repeated sampling over time and deviations from homoscedasticy, respectively (Zuur et al., 2009). AICc values were compared to determine the best model, which generally included either autocorrelation or GLS for homoscedascity (Quinn & Keough, 2002, Zuur et al., 2009).

The relative abundance of each OTU was then compared across time-points and represented using stacked bar graphs. Additionally, the community composition change in each experiment and treatment over time was shown using Bray-Curtis Dissimilarity and Jensen-Shannon Divergence and represented in a non-metric multi-dimensional scaling (NMDS) plot of

which only Jensen-Shannon Divergence will be shown since the two metrics gave similar results (Arumugam et al., 2011; Koren et al., 2013; Martin-Platero et al., 2018).

NETWORK ANALYSIS

A network analysis was conducted using Cytoscape (www.Cytoscape.org) (Shannon et al., 2003). This analysis determines positive and negative correlations between microbial communities and can include environmental parameters such as EOE, salinity, nutrients and/or chlorophyll *a* concentrations (Fuhrman & Steele, 2008). A Local Similarity Analysis (LSA) by Ruan et al. (2006) was used to investigate correlations between abundant microbes. Because microbes were randomly subsampled to the same number of sequences per OTU (see above), the OTUs in the top 1% relative abundance were further filtered to above 300 sequences (prokaryotes) and phytoplankton communities (eukaryotes). The resulting network included approximately 70 OTUs that were shared across treatment. Each experiment (open ocean vs. coastal) was run separately using an LSA in ELSA (bioinformatics software (Ruan et al., 2006)). An LSA includes lag time and therefore can reveal pairwise relationships between groups of microbes that otherwise would be missed (Fuhrman & Steele, 2008). In Cytoscape the LSA network files produced by ELSA are used and then additional attributes are added, such as treatment, classification, etc. A network analysis visualized in cytoscape displays each OTU as a node and correlations as 'edges' or lines connecting nodes. Lag-time correlations are represented with arrows and indicate a lag in the response of one organism to the abundance of another (Xia et al., 2011). In order to filter the number of edges, only those with the strongest correlations of Spearman's absolute rho values greater than 0.5, p-values of greater than 0.05, and q-values of greater than 0.05 were used, according to the methods from Cram et al. (2015)

(Cram et al., 2015). Networks were then separated by treatment and OTUs that were highlighted as potential associations with other microbial communities in NMDS plots, relative abundance bargraphs, and diversity indices were the focus of the network discussion. Although there has been a multitude of research on the bacterial communities in response to oil, there are few studies that detail the response of both the eukaryotic and prokaryotic communities and their interaction (Buchan et al., 2014; Gärdes et al., 2011; Fuhrman et al., 2008; Ozhan et al., 2014). Through a network analysis with Cytoscape of the aforementioned microbial communities, relationships and correlations can be drawn between eukaryotes and prokaryotes during the event of an oil spill.

RESULTS

RAREFACTION CURVES AND SUB-SMAPLING WITHIN COMMUNITIES

Rarefaction curves were compared across mesocosm experiments and treatment to determine the diversity of the communities in each treatment. The asymptote of the rarefaction curve can indicate the degree to which the total microbial diversity was sampled. Each rarefaction curve includes a vertical line to show the number of sequences used to subsample in each experiment and treatment (Figures 9, 10, 11, & 12). The number of sequences was determined using the lowest number of sequences per sample above 1000 (see methods). Rarefaction curves of the eukaryotic community in the open ocean experiment reach an asymptote in most samples by the number used for subsampling except for a few highly diverse samples in the DCEWAF and CEWAF experiments (Figure 5). The coastal experiment was subsampled within the plateau in OTUs with increasing number of individuals sampled, implying true diversity is well represented (Figure 6). Additionally, the plateau in the CEWAF treatment was much smaller compared to control, WAF and DCEWAF (Figure 6). The prokaryotic community in the open ocean experiment had a higher asymptote for all four treatments, with the highest in the WAF treatment (Figure 7). The DCEWAF and CEWAF treatments in these open ocean rarefaction curves also had a few outlier samples that began to reach an asymptote at much higher values (Figure 7). Finally, the rarefaction curves for the prokaryotes in the coastal experiment had some of the highest asymptotes compared to each experiment and community (Figure 8). Comparable to the open ocean experiment, there were a few samples within both the DCEWAF and CEWAF treatments with high asymptotes (Figure 8). The prokaryotic community had higher asymptotes representing total diversity compared to

eukaryotes, the samples were rarified according to the methods and these samples were used for all subsequent analyses.

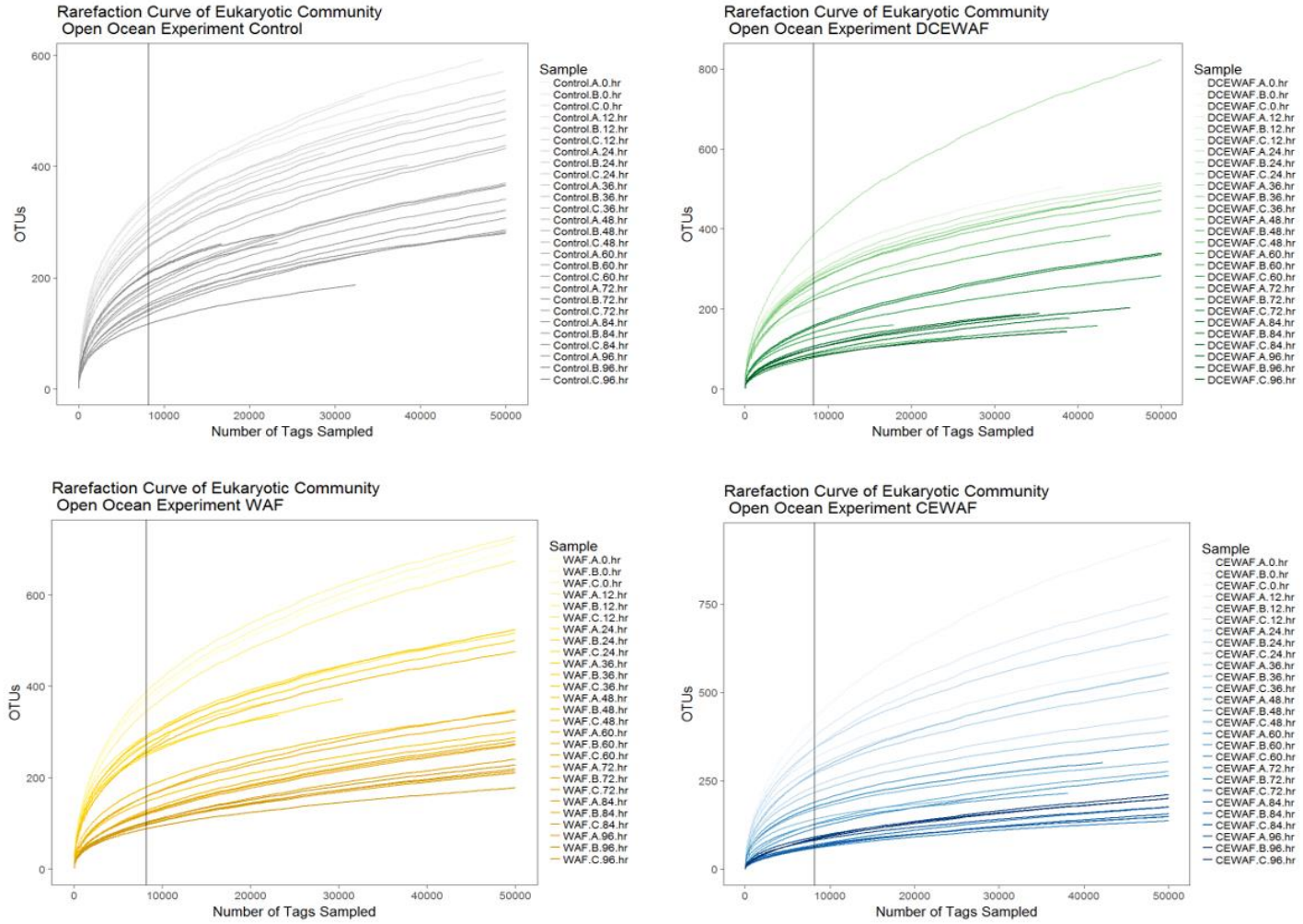

Figure 5: Rarefaction curves of the eukaryotic communities in the open ocean experiment. Briefly, from the top-left counter-clockwise, control samples (grey), WAF (yellow), CEWAF (blue), and DCEWAF (green). The black line drawn in each graph represents the number of reads sub-sampled from the eukaryotes (8196).

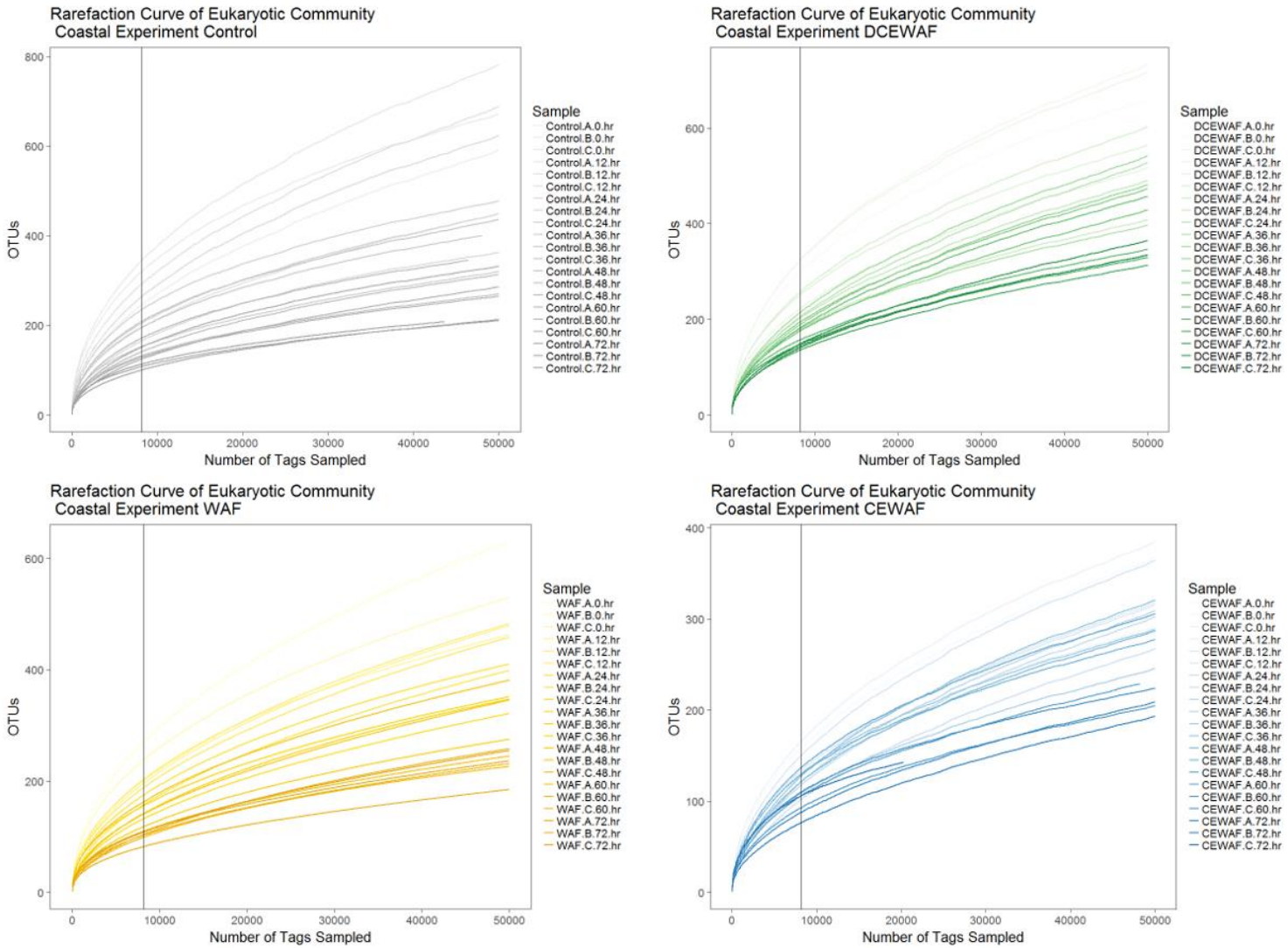

Figure 6: Rarefaction curves of the eukaryotic communities in the coastal experiment. Briefly, from the top-left counter-clockwise, control samples (grey), WAF (yellow), CEWAF (blue), and DCEWAF (green). The black line drawn in each graph represents the number of reads sub-sampled from the eukaryotes (8196).

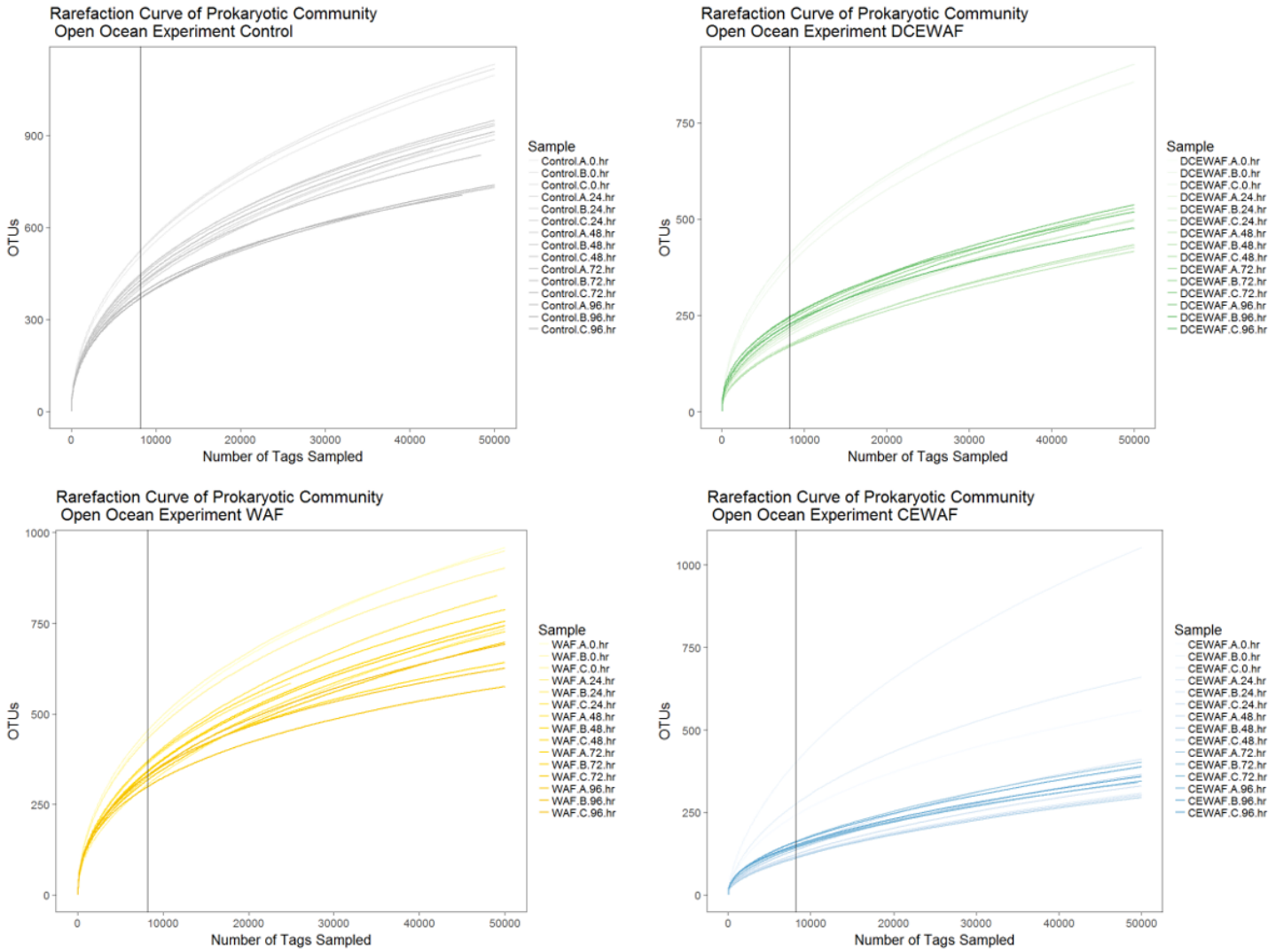

Figure 7: Rarefaction curves of the prokaryotic communities in the open ocean experiment. Briefly, from the top-left counter-clockwise, control samples (grey), WAF (yellow), CEWAF (blue), and DCEWAF (green). The black line drawn in each graph represents the number of reads sub-sampled from the eukaryotes (1114).

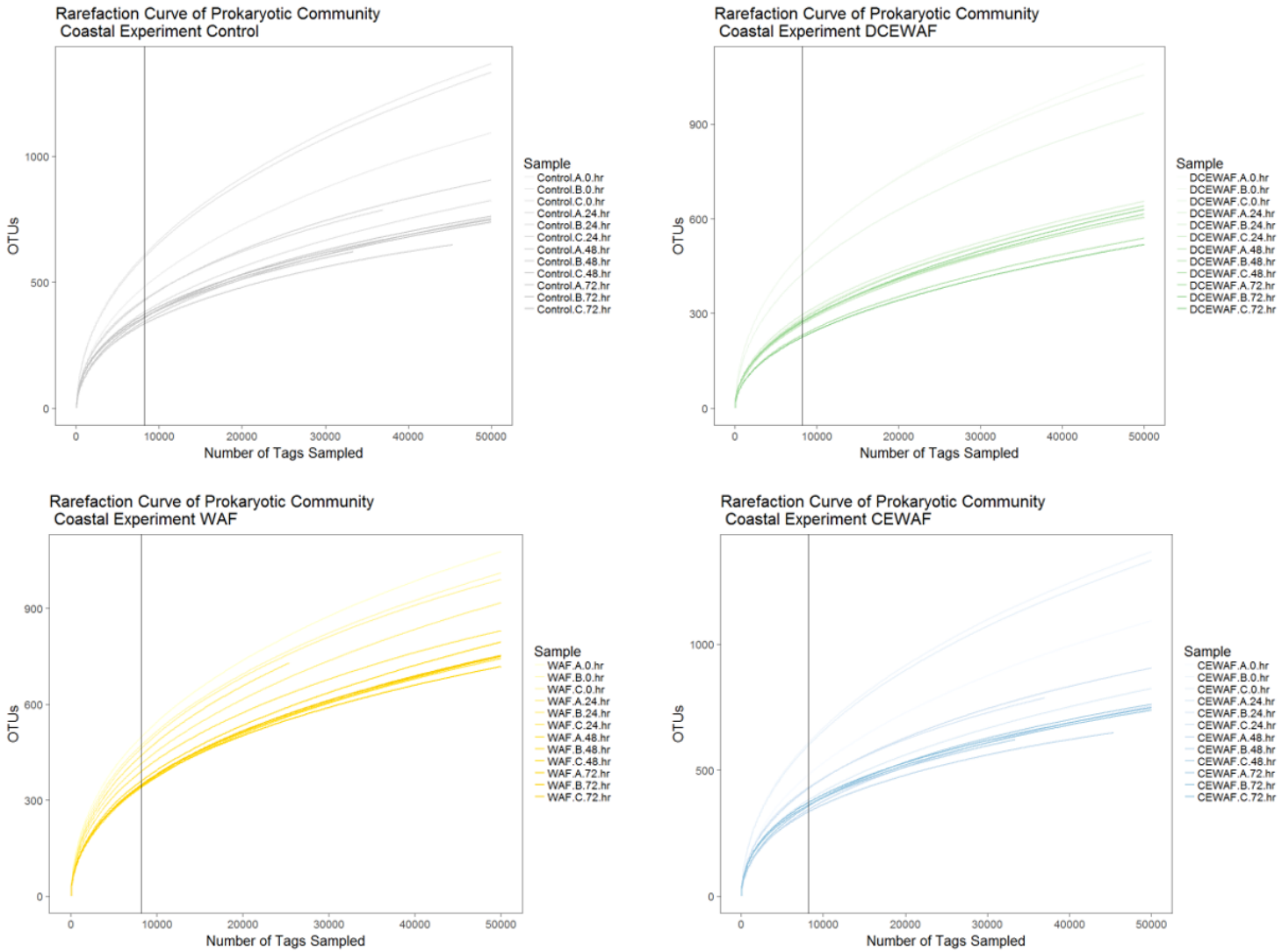

Figure 8: Rarefaction curves of the prokaryotic communities in the coastal experiment. Briefly, from the top-left counter-clockwise, control samples (grey), WAF (yellow), CEWAF (blue), and DCEWAF (green). The black line drawn in each graph represents the number of reads sub-sampled from the prokaryotes (1114).

NMDS PLOTS

Non-metric multidimensional scaling (NMDS) plots were used to display the community composition change between treatments and over time in both the open ocean and coastal experiments. Within the overall community NMDS plot, the two communities are circled to highlight the separation between points (Figures 13 & 16). Additionally, stress is indicated on each NMDS plot in the top right corner and is a measure of similar the true multi-dimensional trends are represented in 2-dimensional space (Clarke et al., 1993). A stress below 0.20 is considered reliable, NDMS plots with stress above this value is considered too high to trust grouping between points (Clarke et al., 1993). The eukaryotic community composition between the two experiments grouped similarly and changed over time with a stress of 0.12 (Figure 9). Additionally, the open ocean community had more separation between points in the NMDS plots than the coastal community indicating more variability within the open ocean community (Figure 9).

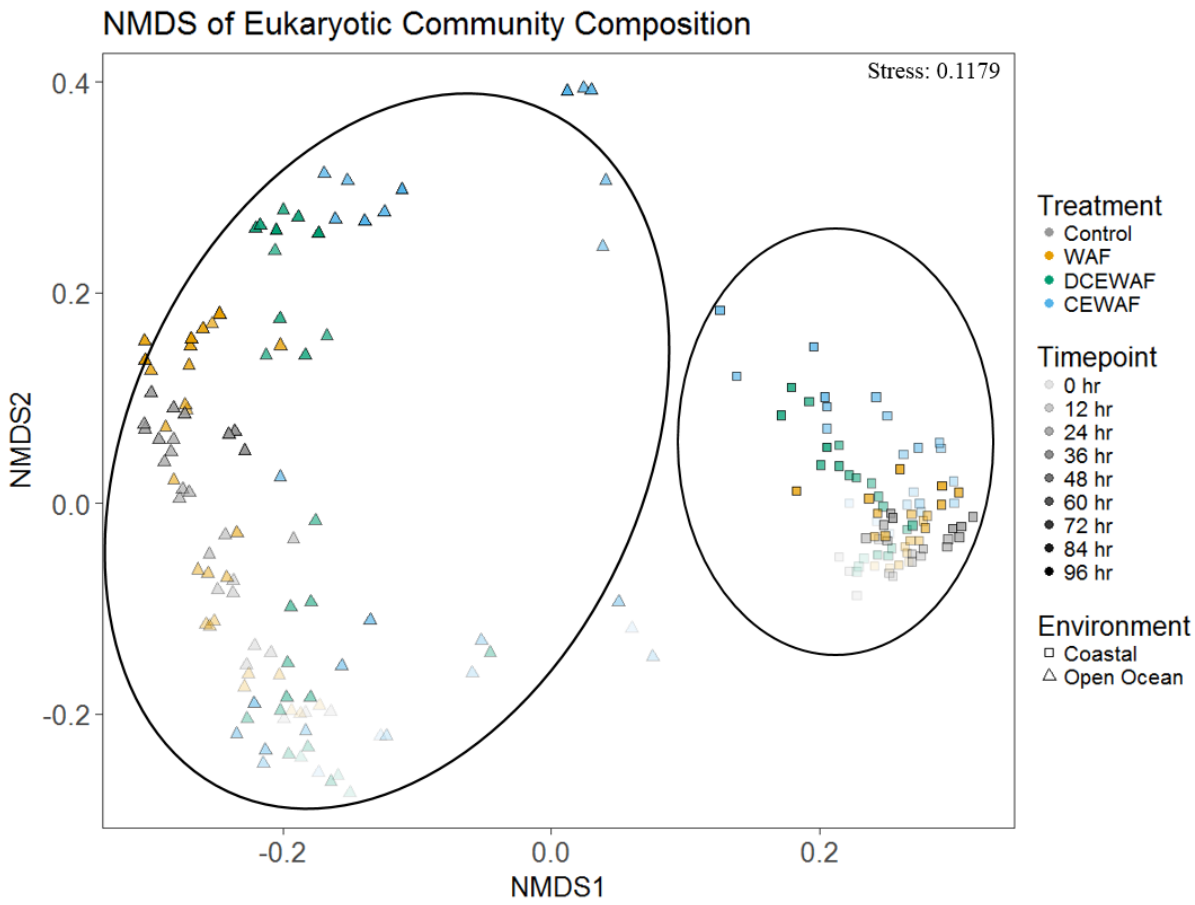

Figure 9: Non-metric multidimensional scaling (NMDS) plot of the eukaryotic community composition. Environments are separated by coastal (squares) and open ocean (triangles), each treatment is shown with different colors, control (grey), WAF (yellow), DCEWAF (green), and CEWAF (blue). Time-point is illustrated from early to late using light to dark shading. Stress is indicated in the upper right corner of the plot. The circles around points in the plot were drawn onto the plot to highlight the separation between open ocean and coastal experiments.

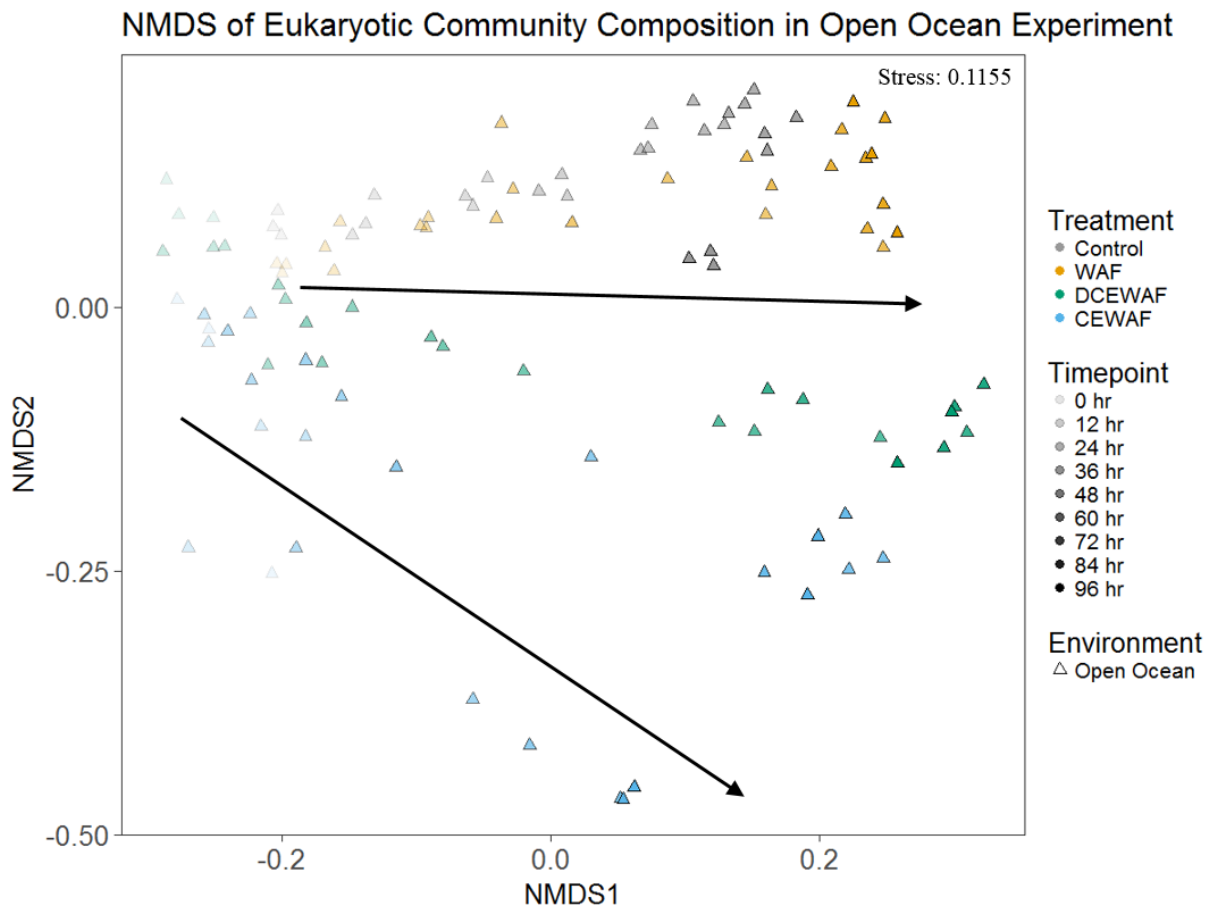

Figure 10: Non-metric multidimensional scaling (NMDS) plot of the eukaryotic community composition of the open ocean environment. Each treatment is shown with different colors, control (grey), WAF (yellow), DCEWAF (green), and CEWAF (blue). Time-point is illustrated from early to late using light to dark shading. Arrows indicate the change in Jensen-Shannon Dissimilarity, or shifting community composition over time. Stress is indicated in the top-right of the NMDS plot.

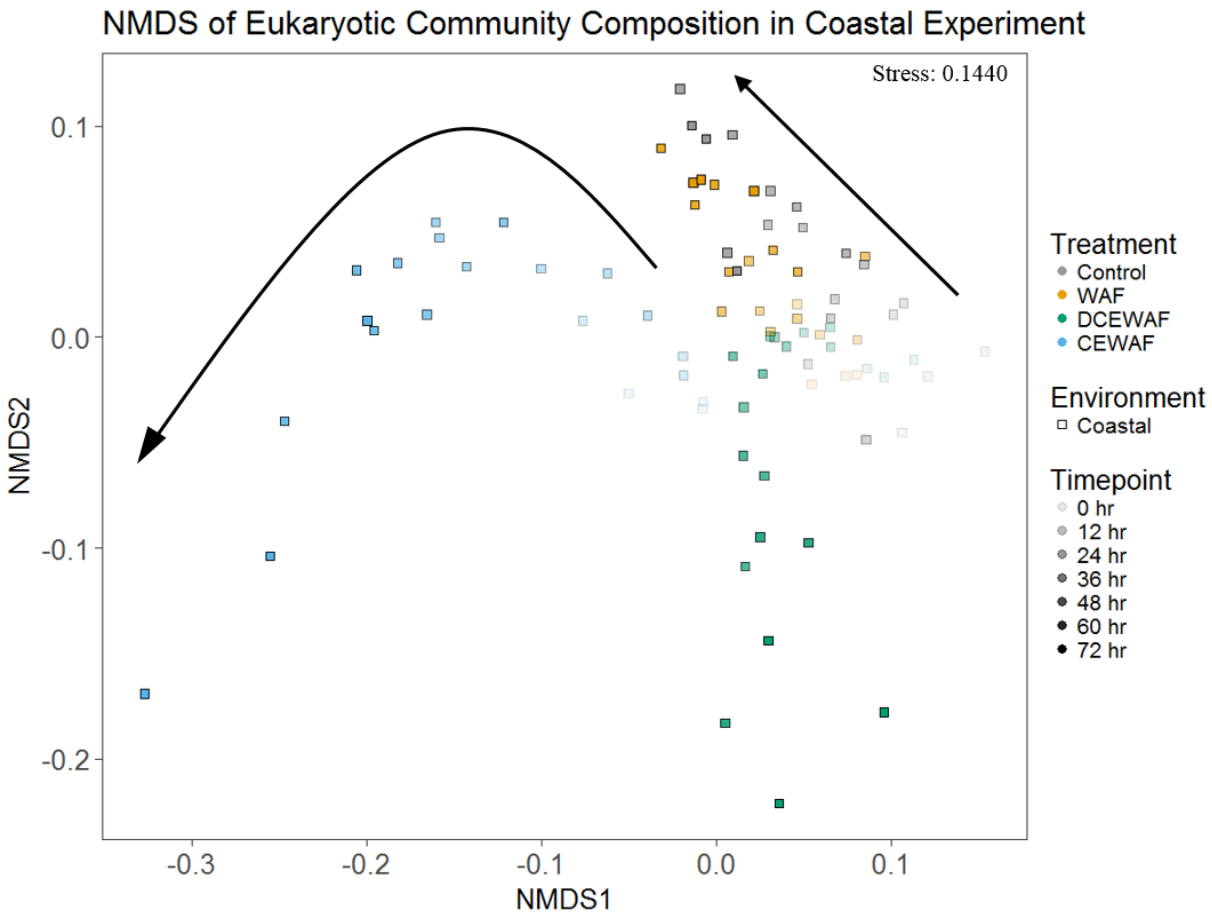

Figure 11: Non-metric multidimensional scaling (NMDS) plot of the eukaryotic community composition of the coastal environment. Each treatment is shown with different colors, control (grey), WAF (yellow), DCEWAF (green), and CEWAF (blue). Time-point is illustrated from early to late using light to dark shading. Arrows indicate the change in Jensen-Shannon Dissimilarity, or shifting community composition over time. Stress is indicated in the top-right of the NMDS plot.

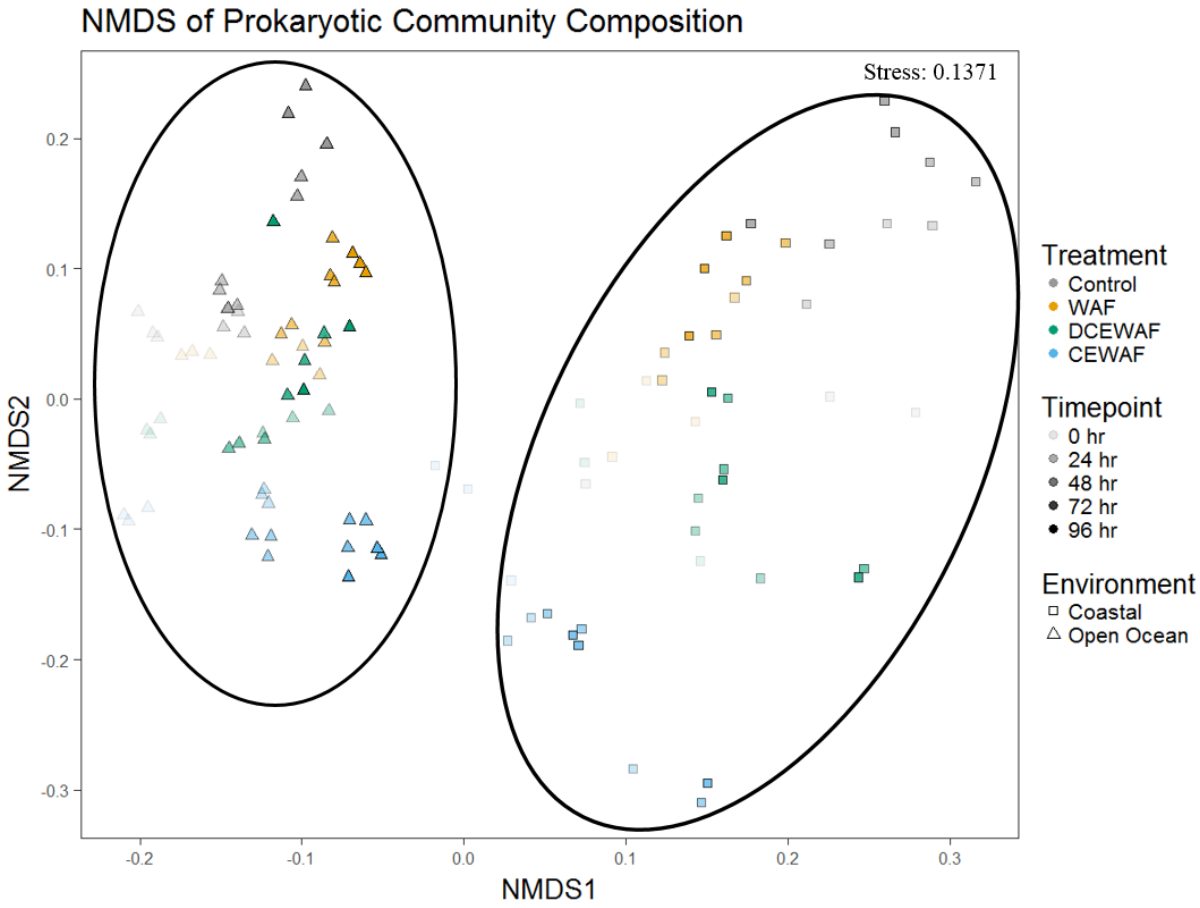

Figure 12: Non-metric multidimensional scaling (NMDS) plot of the prokaryotic community. Environment is displayed using squares for the coastal community, and triangles for the open ocean community. Each treatment is shown with different colors, control (grey), WAF (yellow), DCEWAF (green), and CEWAF (blue). Time-point is illustrated from early to late using light to dark shading. Stress is indicated in the top-right of the NMDS plot. The circles around points in the plot were drawn onto the plot to highlight the separation between open ocean and coastal experiments.

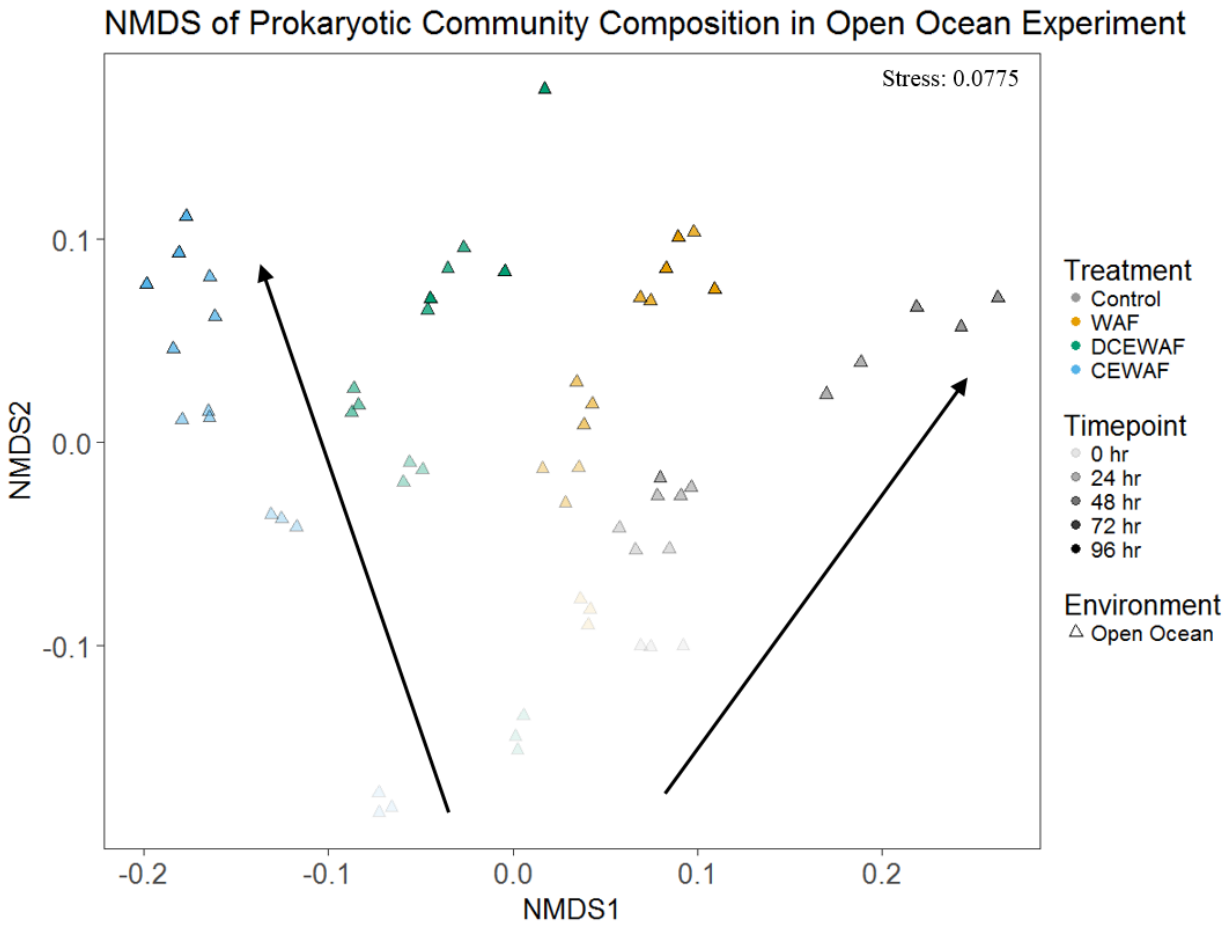

Figure 13: Non-metric multidimensional scaling (NMDS) plot of the prokaryotic community in the open ocean environment. Each treatment is shown with different colors, control (grey), WAF (yellow), DCEWAF (green), and CEWAF (blue). Time-point is illustrated from early to late using light to dark shading. Arrows indicate the change in Jensen-Shannon Dissimilarity, or shifting community composition over time. Stress is indicated in the top-right of the NMDS plot.

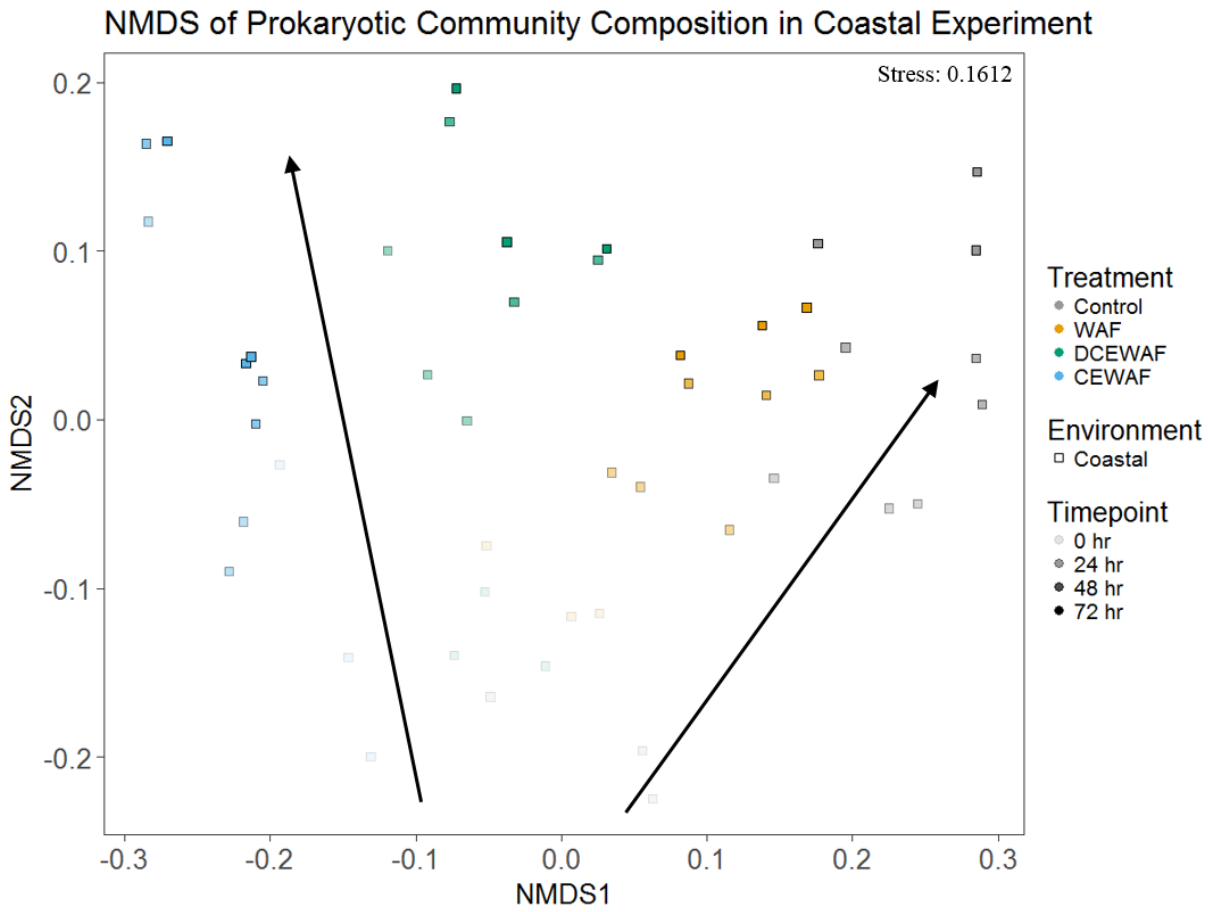

Figure 14: Non-metric multidimensional scaling (NMDS) plot of the prokaryotic community in the coastal environment. Each treatment is shown with different colors, control (grey), WAF (yellow), DCEWAF (green), and CEWAF (blue). Time-point is illustrated from early to late using light to dark shading. Arrows indicate the change in Jensen-Shannon Dissimilarity, or shifting community composition over time. Stress is indicated in the top-right of the NMDS plot.

Within the Eukaryotic community, the open ocean experiment grouped by treatment with increase in the separation over time (arrows) (stress of 0.11), with the most similarity between control and WAF (Figure 10). In the coastal experiment the DCEWAF and CEWAF grouped separately, and the control and WAF again grouped similarly with a stress of 0.14 (Figure 11). The coastal community DCEWAF and CEWAF treatments change over time separated in different directions within the NMDS space, unique to the eukaryotic community coastal

experiment (Figure 11). The change in community composition over time at first was similar to that of the control and WAF (straight arrow), but later moved in a new direction indicating a different type of change in community composition (curved arrow) (Figure 11). Compared to the eukaryotic community response, the prokaryotic community NMDS plots had lower stress values and a stronger clustering of points within each treatment (Figures 13 & 16). Again, both the coastal and open ocean experiment grouped separately in the NDMS of prokaryotic community composition over time and across treatments with a stress of 0.14 (Figure 12). However, the separation between points was slightly larger in the coastal experiment, in contrast to the pattern seen for the eukaryotes (Figure 12). Community composition in the open ocean experiment changed over time (0 hr – 96 hr) and grouped by treatment, with the greatest difference between the control and CEWAF treatments (stress of 0.08) (Figure 13). Over time, the separation between treatments was enhanced (arrows) (Figure 13).

The separation between the control and WAF treatment was unique to the prokaryotic open ocean community compared to the eukaryotic community, in which control and WAF grouped similarly (Figures 13 & 17). The NMDS plot of the prokaryotic community in the coastal experiment showed a grouping between treatments similar to that of the NMDS of the eukaryotic community (Figure 14). Like that of the open ocean community NMDS plot, in the coastal experiment the separation between treatments was enhanced over time (arrows) (Figure 14). These NMDS plots display a clear pattern over time and across treatments highlighting some potentially influencing factors that will be explored in the next few sections.

RELATIVE ABUNDANCE IN THE OPEN OCEAN EXPERIMENT

The overall eukaryotic relative abundance in the open ocean experiment was more varied compared to the coastal experiment which contained a dominant community (Figures 19 & 20). At the 0 hour time-point the community in the open ocean experiment was relatively diverse across all four treatments and was primarily comprised of the classes Bicoecea, Icthyosporea, Dothideomycetes, Eurotiomycetes, Microbotryomycetes, Chlorarachnea, and the Infra-Kingdom Stramenopiles (Figure 15). Within the open ocean experiment, the most abundant eukaryote in both the control and WAF treatment was of the class Bicoecea in the phylum Bigyra (Figure 15). Bicoecea was also present in the DCEWAF and CEWAF treatments but dwindled to relative zero by the later time-points in the CEWAF treatment (Figure 15). In the open ocean DCEWAF and CEWAF treatments Oligohymenophorea was most abundant (Figure 15). However, Oligohymenophorea was present at a lower relative abundance in both the control and WAF treatment compared to Bicoecea (Figure 15). Granofilosea, a naked amoeboid, had a high relative abundance in only the CEWAF treatment. The last three time-points the CEWAF eukaryotic community composition was dominated almost exclusively by these two aforementioned grazers, Granofilosea and Oligohymenophorea (Figure 15). Additionally, Icthyosporea decreased to relative zero in all treatments except the CEWAF in which it increased and persisted for longer (Figure 15).

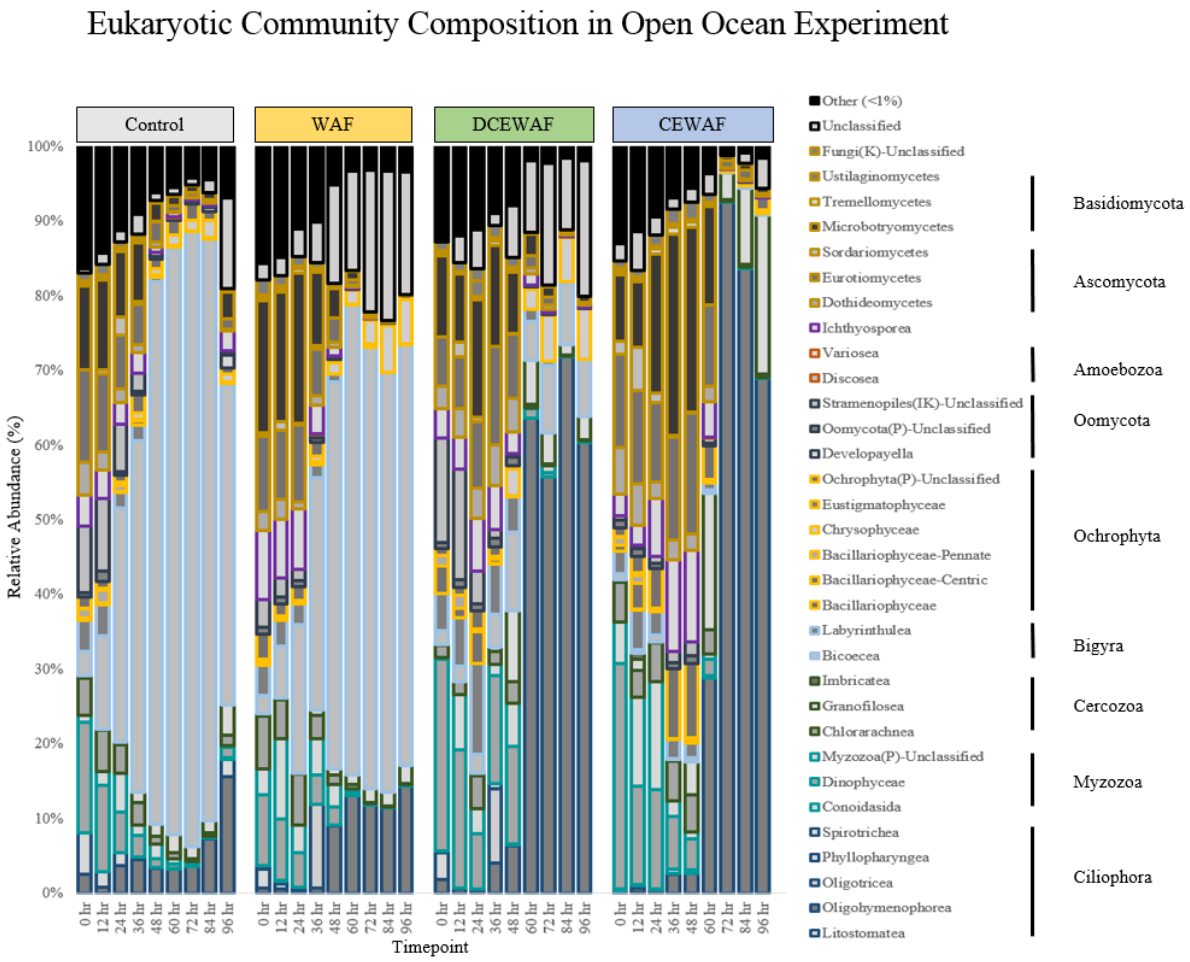

Figure 15: Stacked bar graphs of the eukaryotic community in the open ocean experiment showing change over time (x-axis) of percent relative abundance (y-axis) in each class (left key in the legend to the right) divided by treatment on the top of each bar graph. Each class is colored with different shades of grey within the same phylum, denoted by different outline colors and labeled on the right key in the legend to the right. Letters within class names indicates the taxonomic level if class couldn't be identified, K = Kingdom, IK = Infrakingdom, P = Phylum. Unclassified contains any individuals that couldn't be classified, while other is comprised of individuals that were each less than 1 % of the total relative abundance.

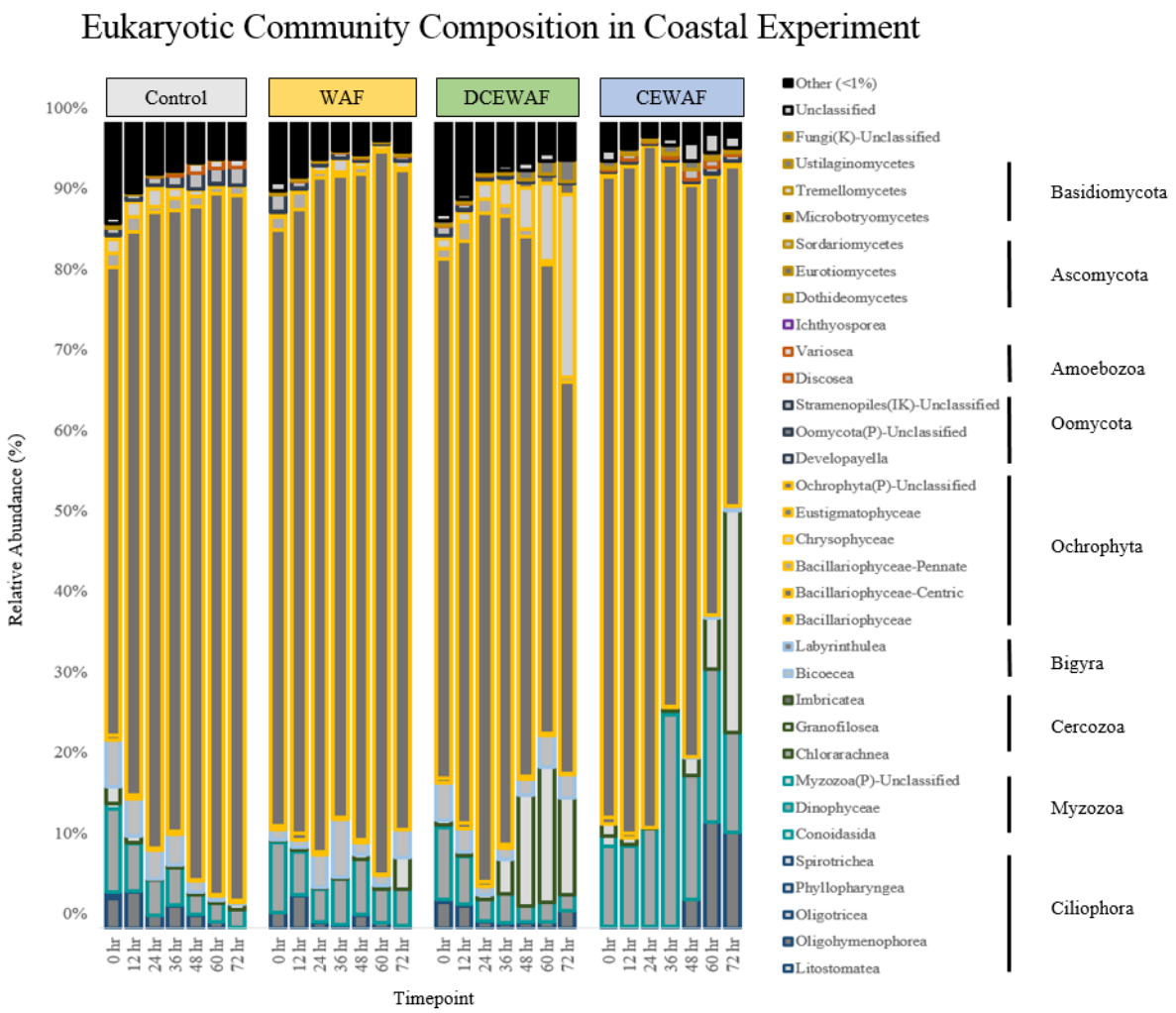

Figure 16: Stacked bar graphs of the eukaryotic community in the coastal experiment showing change over time (x-axis) of percent relative abundance (y-axis) in each class (left key in the legend to the right) divided by treatment (top of each bar graph). Each class is colored with different shades of grey within the same phylum, denoted by different outline colors and labeled on the right key in the legend to the right. Letters within class names indicates the taxonomic level if class couldn't be identified, K = Kingdom, IK = Infrakingdom, P = Phylum. Unclassified contains any individuals that couldn't be classified, while other is comprised of individuals that were each less than 1 % of the total relative abundance.

One unexpected result from the open ocean experiment was the high relative abundance of Fungi in earlier time-points (Figure 15). Four classes of marine fungi were present in the open ocean experiment, Dothideomycetes, Eurotiomycetes, Sordariomycetes, and Microbotryomycetes (Figure 15). Both Dothideomycetes, and Eurotiomycetes increase in relative abundance in DCEWAF and CEWAF compared to the control and WAF treatments with the most drastic changes in the CEWAF treatment (Figure 15). Sordariomycetes had a higher relative abundance in CEWAF, and persisted longer in both of the dispersed oil treatments (Figure 15). Microbotryomycetes was present in all treatments but persisted in the CEWAF (Figure 15).

Finally, phytoplankton groups within the open ocean experiment comprised of Bacillariophyceae, Chloroarachnea, Chrysophyceae, and Dinophyceae (Figure 17). Centric Bacillariophyceae were most abundant in the CEWAF treatment, contrastingly pennate Bacillariophyceae had the highest relative abundance in the control treatment (Figure 17). Chlorarachnea had the lowest relative abundance in the DCEWAF treatment throughout all of the time-points (Figure 17). In the WAF treatment Chlorarachnea had a high relative abundance at the 0 hr time-point, while at the later time-points its relative abundance decreased (Figure 17). Overall Chlorarachnea relative abundance decreased over time in all treatments, until the final time-point in which the control and CEWAF treatments had comparatively lower relative abundances (Figure 17). Chrysophyceae increased over time in all four treatments, first the relative abundance increased in the control and WAF, followed by an increase in DCEWAF and a slight increase in CEWAF (Figure 17). By the final time-point the relative abundance of Chrysophyceae in the control decreased, and the CEWAF treatment had a higher relative abundance than the control (Figure 17).

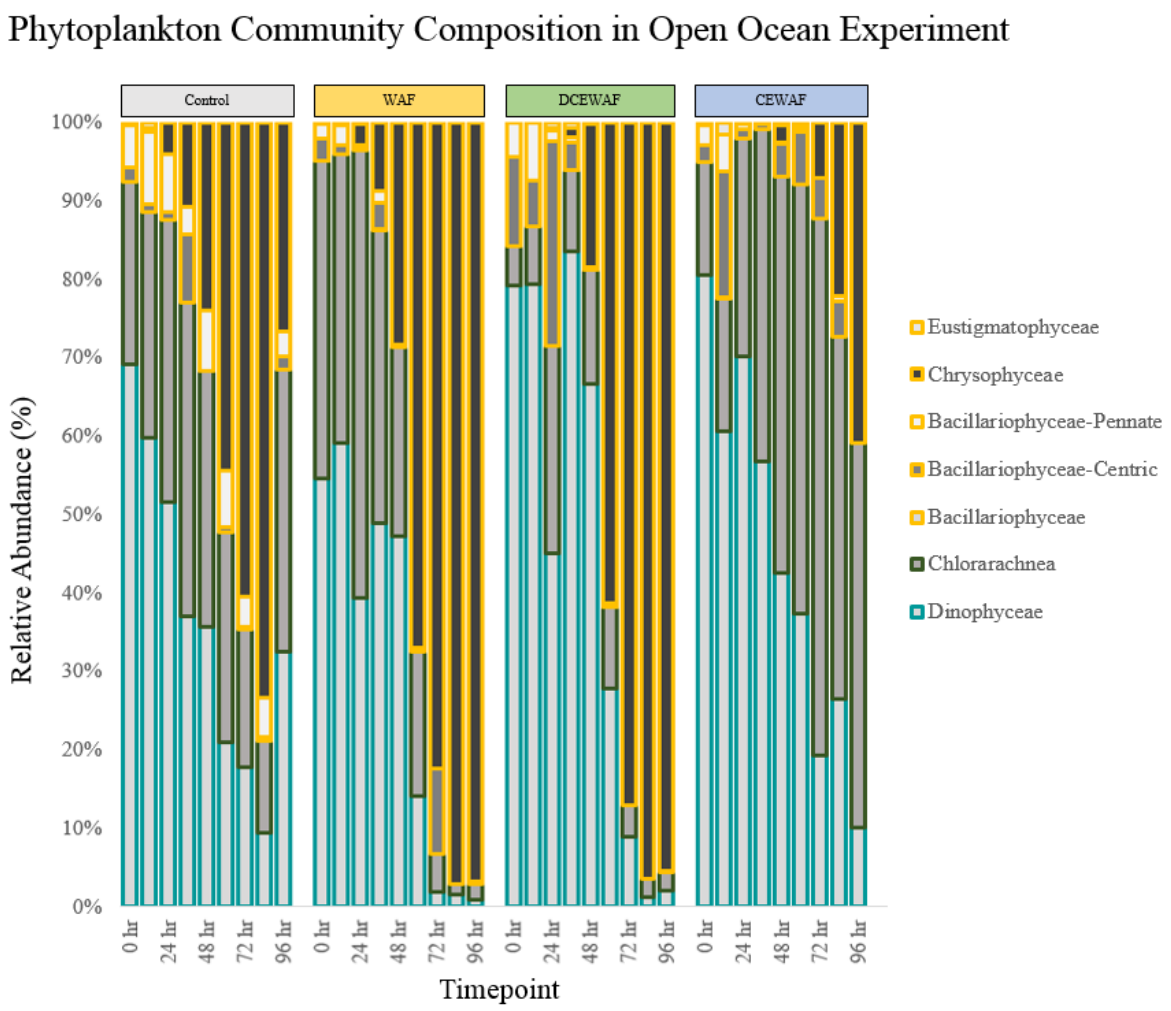

Figure 17: Stacked bar graphs of the phytoplankton community in the open ocean experiment showing change over time (x-axis) of percent relative abundance (y-axis) in each class (left key) divided by treatment (top of each bar graph). Each class is represented by the same colors from the outline in the whole eukaryotic community stacked bar graphs (Figure 15). The remainder of the stacked bar graphs represented by white space are individuals with less than 1 % relative abundance. In the DCEWAF T8, there were only two replicates and therefore the relative abundance is out of 200 %.

Dinophyceae had the lowest relative abundance in the WAF treatment (Figure 17). In the earlier time-points from 0 hr to 48 hr, the highest relative abundance fluctuated between the control, DCEWAF and CEWAF treatments (Figure 17). At the later time-points in the open ocean experiment the relative abundance of Dinophyceae decreased in all treatments, but the control and CEWAF relative abundances were similar by the final time-point (Figure 17).

Throughout the open ocean experiment, Gammaproteobacteria were the most abundant class of organisms in all four treatments (Figure 18). With the Gammaproteobacteria, Alteromonodales had the highest relative abundance that increased with increasing oil and dispersed oil concentration, i.e. the relative abundance ranked from highest to lowest was CEWAF, DCEWAF, WAF and control (Figure 18). Additionally, within the Gammaproteobacteria the orders Xanthomonadales and Thiotrichales had the highest relative abundance in the WAF and DCEWAF, respectively (Figure 18). The relative abundance of Xanthomonadales was high at early time-points and decreased to relative zero by the final time-point (Figure 18). Asymmetrically, in the WAF, CEWAF, and DCEWAF treatments, Thiotrichales increased in relative abundance relative to the decrease in Xanthomonadales (Figure 18). Oceanospiralles had a high relative abundance in treatments without dispersed oil, while Cellvibrionales showed the opposite response and was the most abundant in the DCEWAF and CEWAF (Figure 18).

Pseudomonadales was consistent across the control, WAF, and DCEWAF treatments, while in CEWAF the relative abundance was relatively low at the 0 hr time-point and increased over time (Figure 18). Among the prokaryotes, the Alphaproteobacteria also had high relative abundance in all four treatments (Figure 18).

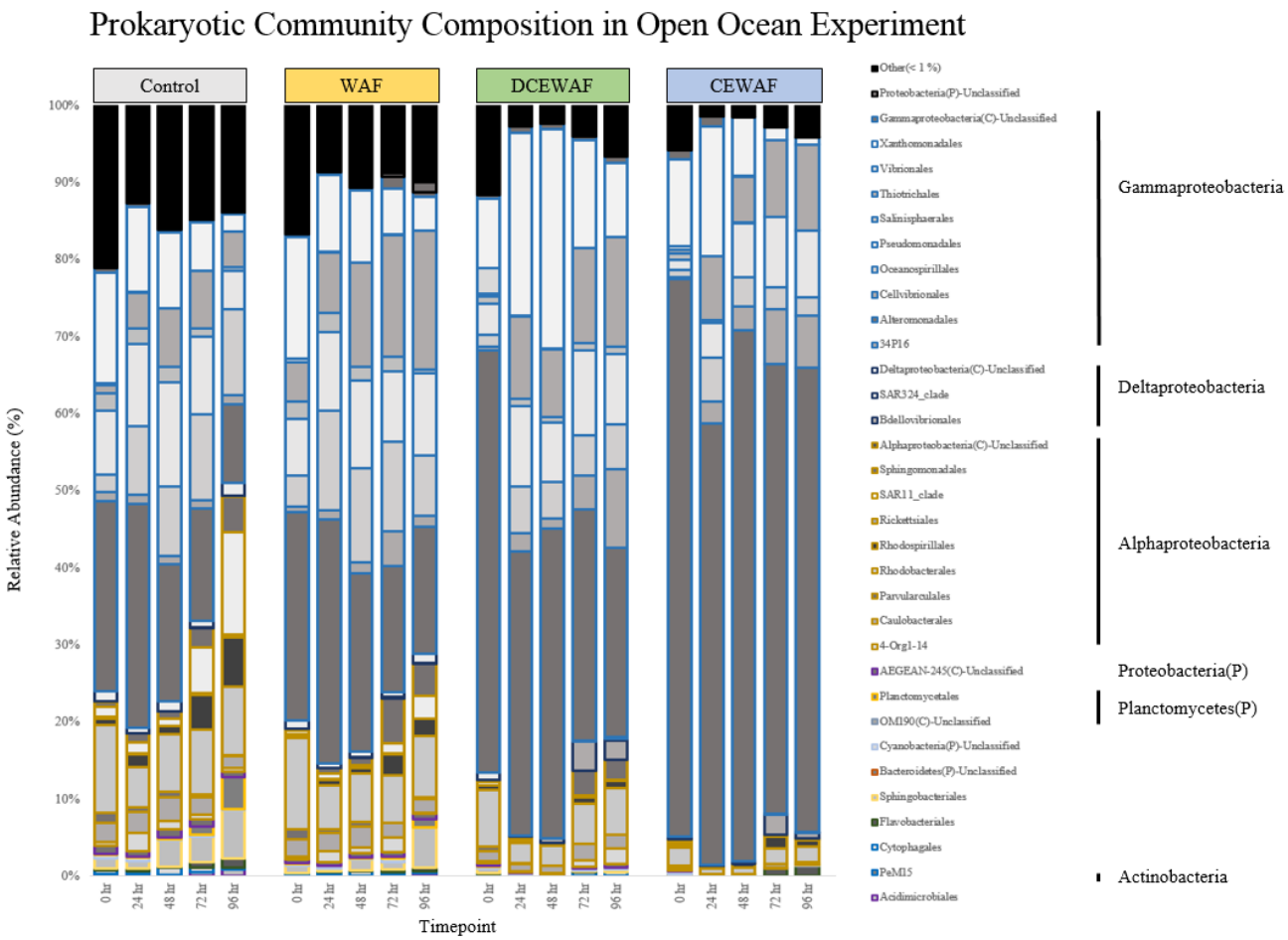

Figure 18: Stacked bar graphs of the prokaryotic community in the open ocean experiment showing change over time (x-axis) of percent relative abundance (y-axis) in each order (left key in the legend to the right) divided by treatment (top of each bar graph). Each order is colored with different shades of grey within the same order, denoted by different outline colors and labeled on the right key in the legend to the right. Letters within class names indicates the taxonomic level if class couldn't be identified, K = Kingdom, IK = Infrakingdom, P = Phylum. Unclassified contains any individuals that couldn't be classified, while other is comprised of individuals that were each less than 1 % of the total relative abundance.

Of the Alphaproteobacteria, the SAR11 Clade and Rhodobacterales dominated in the control, WAF, and DCEWAF (Rhodobacterales only) (Figure 18). Moreover, Rhodobacterales decreases with increasing oil and dispersed oil (control > WAF > DCEWAF > CEWAF), suggesting a sensitivity to dispersed oil (Figure 18). While Sphingobacteriales increases over time in the control and WAF treatments (Figure 18). The relative abundance of prokaryotes in these communities reflected the treatment in which they grew, and changed minimally over time.

RELATIVE ABUNDANCE IN THE COASTAL EXPERIMENT

The coastal eukaryotic community composition was much more consistent across treatments and time-points (Figure 16). This consistency was due to the dominance of centric Bacillariophyceae in all four treatments (Figure 16). The eukaryotes in the coastal experiment were comprised primarily of phytoplankton (Figure 16). After centric Bacillariophyceae, the highest relative abundance of eukaryotes included Bicoeceae, Oligohymenophorea, Granofilosea, Dinophyceae, and Chyrsophyceae (Figure 16). The relative abundance of Bicoeceae remained consistent across the control, WAF, and CEWAF treatments (Figure 16). Similar to the open ocean experiment, Bicoeceae was not present in the DCEWAF (Figure 16). Oligohymenophorea had the highest relative abundance in the CEWAF treatment compared to the control, WAF, and DCEWAF in which the relative abundance was similar (Figure 16). Granofilosea, had the highest relative abundance in dispersed oil treatments (DCEWAF, and CEWAF) and at later time-points (Figure 16).

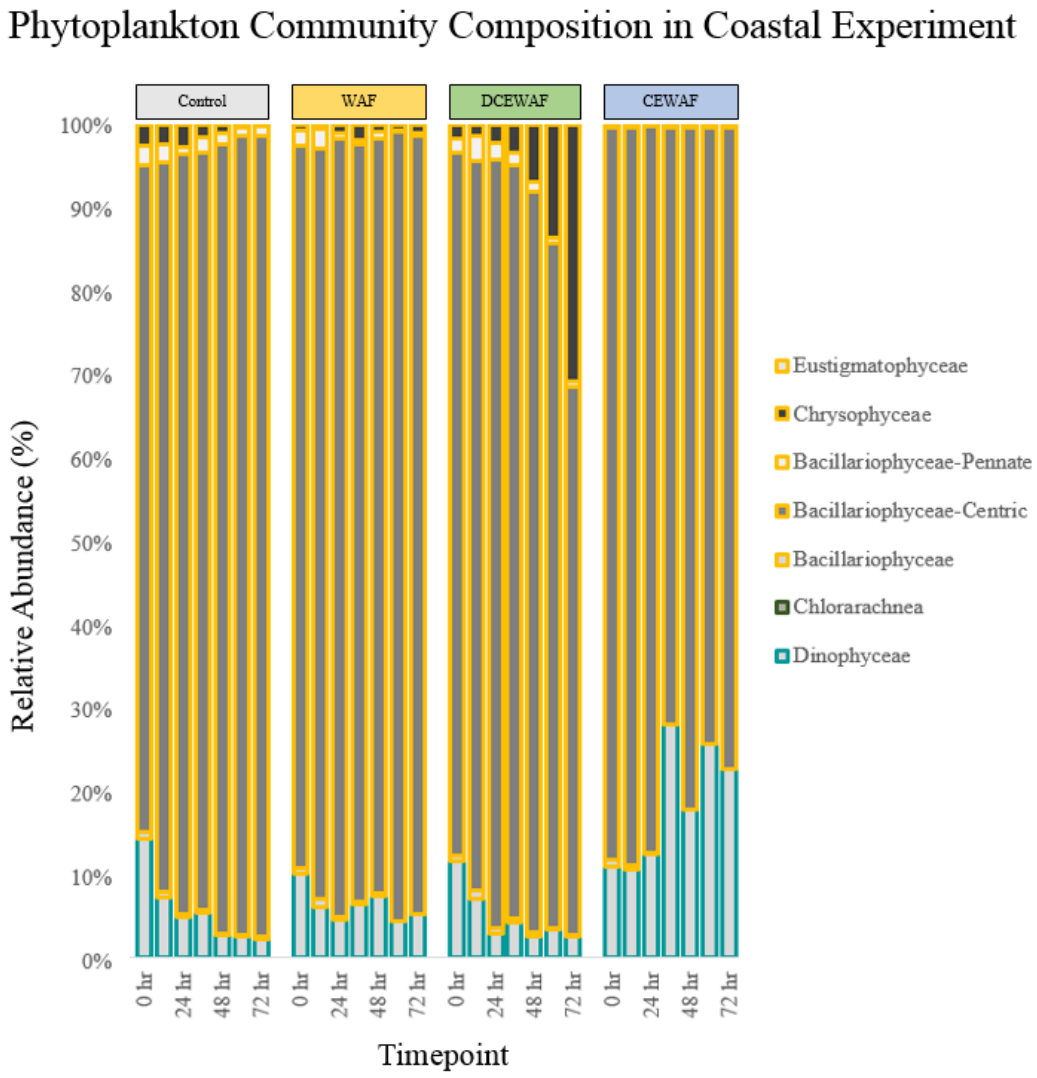

Figure 19: Stacked bar graphs of the phytoplankton community in the coastal experiment showing change over time (x-axis) of percent relative abundance (y-axis) in each class (left key) divided by treatment (top of each bar graph). Each class is represented by the same colors from the outline in the whole eukaryotic community stacked bar graphs (Figure 16). The remainder of the stacked bar graphs represented by white space are individuals with less than 1 % relative abundance.

After Bacillariophyceae, the two most abundant phytoplankton in the coastal experiment were the aforementioned Dinophyceae, and Chrysophyceae (Figure 19). Both groups had similar relative abundances at the first time-point, however over time differences between treatments were distinct (Figure 19). Dinophyceae had a higher relative abundance in the CEWAF treatment at the final time-point, decreased relative abundance in the control and WAF, and a constant relative abundance in DCEWAF (Figure 19). Comparatively, the relative abundance of Chrysophyceae increased over time in the CEWAF treatment, while remaining at relative zero in the control, WAF, and CEWAF (Figure 19). Compared to the open ocean experiment, fungi were not present in high relative abundance in the coastal experiment (Figure 16). Although the eukaryotic community was dominated by a single class, the prokaryotic community varied across treatment and time.

The starting community of the prokaryotes in the coastal experiment was comprised of the orders Thiotrichales, Alteromonodales, Pseudomonadales, Oceanospiralles, Cellvibrionales, SAR11 Clade, Rhodobacterales, Cyanobacteria, Flavobacteriales, and Acidimicrobiales (Figure 20). Alteromonodales had the highest abundance at time-point zero in all four treatments, however after the first 24 hours Thiotrichales had the highest abundance in both the control and WAF (Figure 20). Interestingly, the DCEWAF had a higher abundance of Thiotrichales than CEWAF, although the relative abundance in DCEWAF was still much lower than either the control or WAF treatments (Figure 20). The relative abundance of Alteromonodales seemed to be the antithesis of Thiotrichales as the highest abundance of Alteromonadales was in the DCEWAF and CEWAF treatments, which also had the lowest abundance of Thiotrichales (Figure 20). As previously mentioned, Thiotrichales had the highest abundance in the dispersed oil treatments, along with Alteromonadales (Figure 18). This discrepancy between open ocean

and coastal experiments with Thiotrichales & Alteromonodales could be a result of competitive exclusion in the control and WAF of the open ocean experiment or a beneficial interaction with the eukaryotic community (Amin et al., 2012; Hibbing et al., 2010).

Among the remaining Gammaproteobacteria the most abundant were the Pseudomonodales, Oceanospiralles, and Cellvibrionales which all increased with increasing oil and dispersed oil after the first time-point (Figure 20). The relative abundance of Pseudomonadales remained consistent over time in all treatments except for the control, in which the abundance was at relative zero (Figure 20). Although the relative abundance of Pseudomonadales was slightly higher in the CEWAF treatment, the starting community relative abundance was also slightly higher and remained relatively consistent even in the higher concentration of dispersed oil (Figure 20). The relative abundance of Oceanospiralles went down over time in the control and WAF treatments, while in the DCEWAF and CEWAF the abundance went up and peaked by the 48-hour time-point before decreasing again at the last time-point (Figure 20). The order Cellvibrionales decreased in abundance in all treatments over time, except DCEWAF in which the relative abundance slightly increased after the first 24 hours and proceeded to decrease thereafter (Figure 20).

In the coastal experiment, the Alphaproteobacteria were comprised primarily of SAR11 and Rhodobacterales with the highest abundance in treatments without dispersed oil (control & WAF) (Figure 20). SAR11 clade, had a consistent response and decreased across time in all treatments (Figure 20). Similarly, Rhodobacterales decreased over time in all treatments, and the abundance in CEWAF dropped to relative zero after the first time-point (Figure 20).

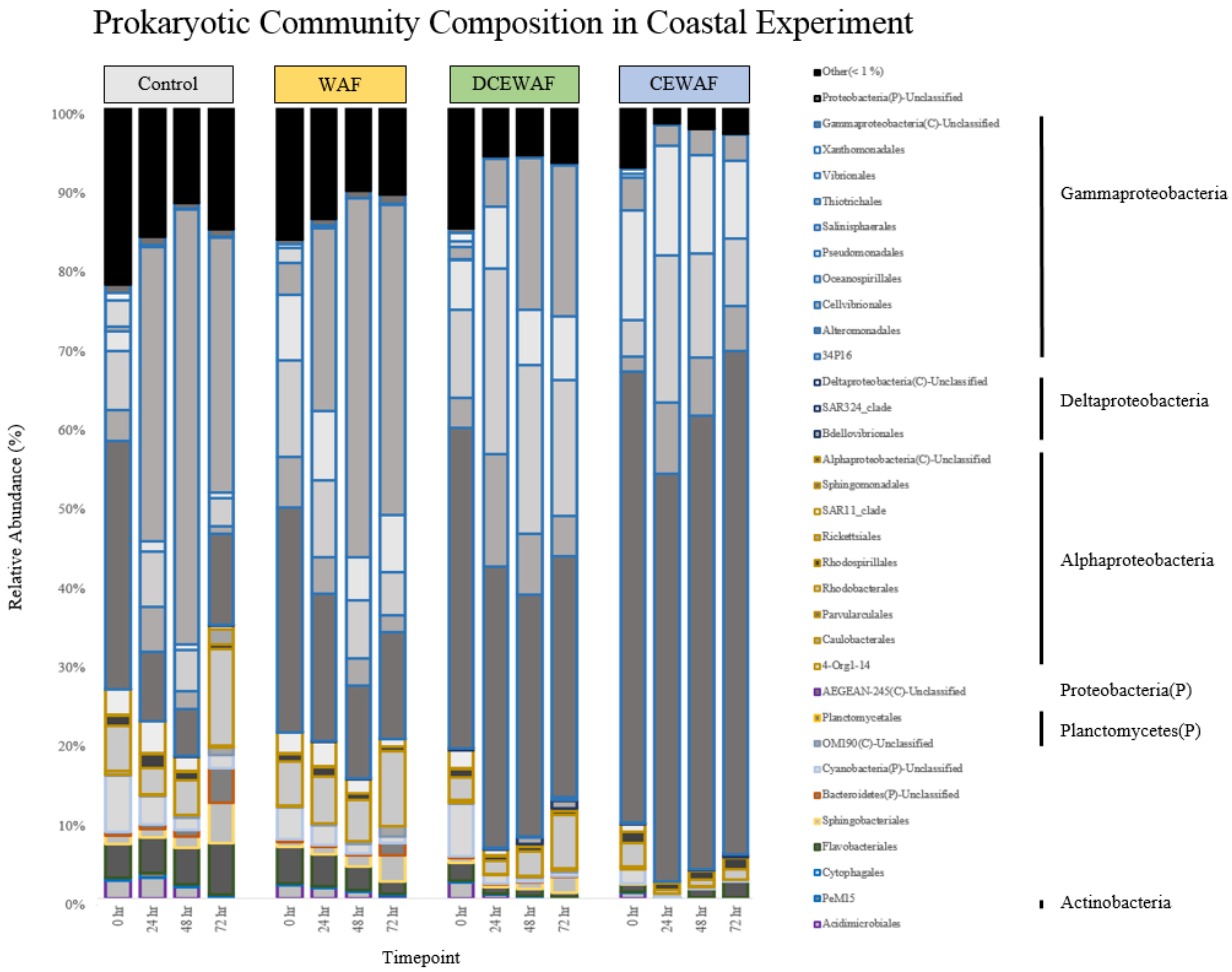

Figure 20: Stacked bar graphs of the prokaryotic community in the coastal experiment showing change over time (x-axis) of percent relative abundance (y-axis) in each order (left key in the legend to the right) divided by treatment (top of each bar graph). Each order is colored with different shades of grey within the same order, denoted by different outline colors and labeled on the right key in the legend to the right. Letters within class names indicates the taxonomic level if class couldn't be identified, K = Kingdom, IK = Infrakingdom, P = Phylum. Unclassified contains any individuals that couldn't be classified, while other is comprised of individuals that were each less than 1 % of the total relative abundance.

However, in the control, WAF, and DCEWAF treatments the relative abundance began to increase at the last time-point (72 hour) (Figure 20). Several other microbes were also present in low abundance that were sensitive to dispersed oil based on relative abundance (Figure 20). The Cyanobacteria (Phylum), Flavobacteriales, and Acidimicrobiales all decreased in abundance with increasing oil and dispersed oil (control > WAF > DCEWAF > CEWAF) (Figure 20).

STATISCAL ANALYSIS OF DIFFERENCES IN DIVERSITY

Above, NMDS plots and stacked bar graphs of eukaryotic and prokaryotic community composition over time reveal a potential effect of both treatment (control, WAF, CEWAF, and DCEWAF) and environment (open ocean vs. coastal) over time. Following these analyses, ANOVA statistical tests were run on each community (prokaryotes vs. eukaryotes) to determine the most important drivers in alpha diversity. Three alpha diversity metrics were used to represent different aspects of community diversity (1) Inverse Simpson for community evenness influenced by dominant individuals (2) Chao1 index and (3) Abundance Coverage Estimator (ACE), both estimators of community richness (see methods). All three were considered as they highlight diversity of highly abundant organisms (Inverse Simpson), and rare members (Chao & ACE) therefore providing a complete picture of overall diversity.

Inverse Simpson Diversity Index

In the eukaryotic community, the highest diversity according to the Inverse Simpson index is in the open ocean control. A decrease over time in diversity was observed in both the coastal and open ocean experiment with no clear trend across treatment (Figure 21).

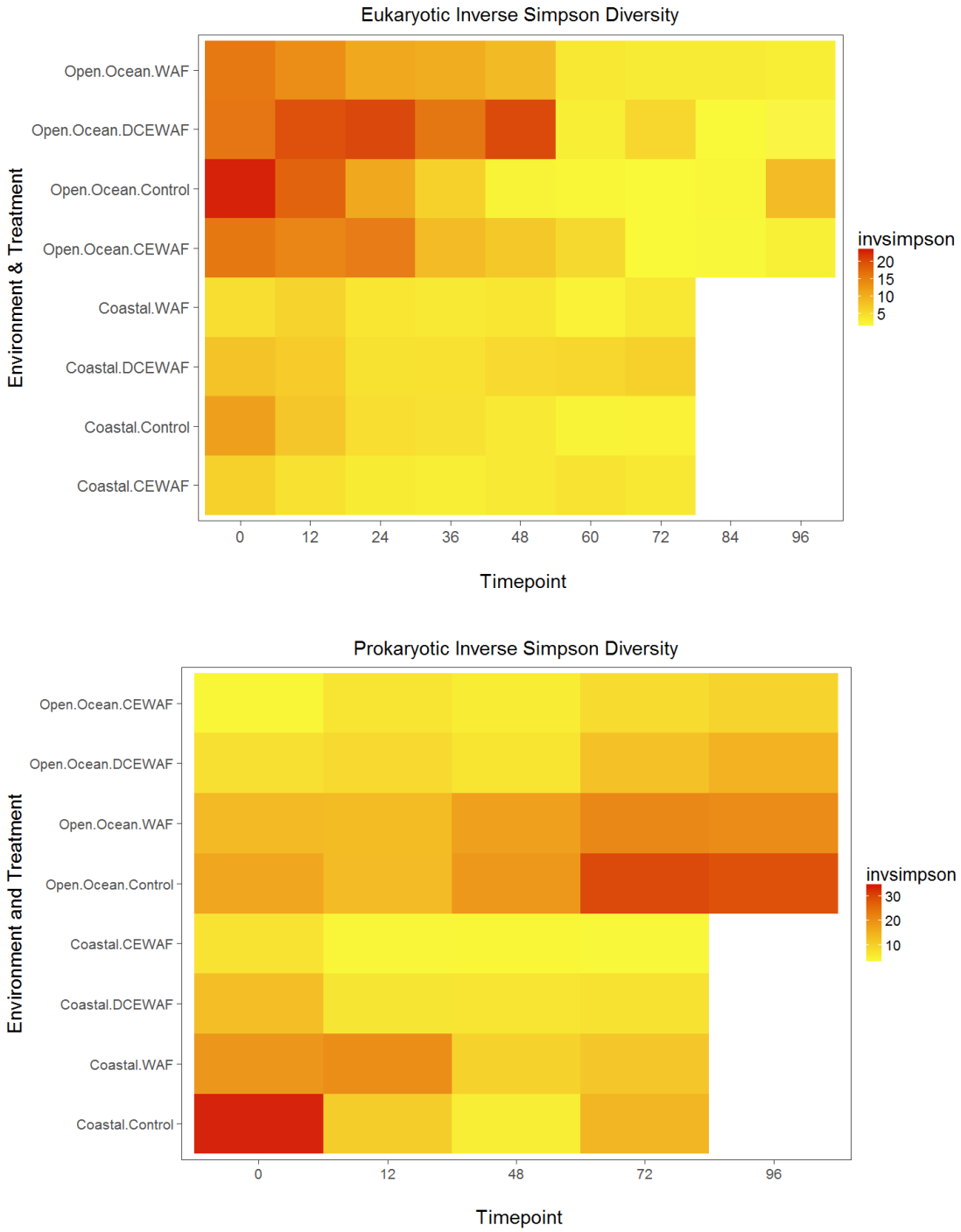

Figure 21: Eukaryotic community (top) and prokaryotic community (bottom) Inverse Simpson diversity for the eukaryotic community with time-point on the x-axis, and each variation of environment and treatment on the y-axis. The Inverse Simpson index goes from low (light yellow) to high (dark red) and is shown with corresponding numbers on the key to the right.

Within each heatmap, the diversity represented can be different at the 0 hr timepoint as an artifact of experimental design. Although we sampled at the 0 hr time-point, the baffled recirculation tanks (BRTs) were circulating with the natural communities for 24 hours prior (see methods). Using an ANOVA split-lot design with GLS for deviations from homoscedascity, the interaction between environment, treatment, and time-point was significant ($F_{3,159} = 2.75$, $p = 0.045$) but only slightly at an alpha of 0.05 (Table 1). Additionally, the interaction between environment and time-point ($F_{1,159} = 52.50$, $p = < 0.0001$) and treatment and time-point were both significant ($F_{3,159} = 9.00$, $p = < 0.0001$) (Table 1). However, the interaction between environment and treatment was not significant ($F_{3,16} = 0.13$, $p = 0.94$) (Table 1).

Table 1: Eukaryotic Inverse Simpson ANOVA table, each factor is shown to the left of the bar. The values for between group degrees of freedom (Df), within group degrees of freedom (Df), F-value, and p-value are shown in the table. The x symbol indicates an interaction between variables. The asterisks on p-values indicate significance at an alpha of 0.05 (**), and one weakly significant value at an alpha of 0.1 (*).

ANOVA table	Between Group Df	Within Group Df	F-value	p-value
Environment	1	16	50.4498	< .0001**
Treatment	3	16	9.1827	0.0009**
Timepoint	1	159	89.0386	< .0001**
Environment x Treatment	3	16	0.1327	0.9392
Environment x Timepoint	1	159	52.4918	< .0001**
Treatment x Timepoint	3	159	8.9980	< .0001**
Environment x Treatment x Timepoint	3	159	2.7452	0.0449*

Therefore, each level of environment and treatment was significantly different between time-points indicating community change with all three factors (environment, treatment, and time-point) (Figure 21). The assumptions were met for whole-plot levels of homoscedascity in environment (BFL p-value = 0.70) and treatment (BFL p-value = 0.23), and had problems with

normality (Shapiro-Wilkes p-value = 0.003) however a length of 24 allowed assumptions of normality to be met (Quinn & Keough, 2002). There were problems with split-plot factor homoscedascity assumptions with the fitted vs. residuals (B-P p-value = 0.0022), treatment-time-point vs. residuals (BFL p-value = 1.11e-12), and environment-time-point vs. residuals (BFL p-value = 0.0009). The time-point vs. residuals (B-P value = 0.56) as well as normality with a shapiro-wilkes (S-W) p-value of 1.58e-08 and length of 191 did meet assumptions (Quinn & Keough, 2002). The interaction between tank and time-point was significant (Tukey's non-additivity p-value = 7.83e-05), but this was largely due to open ocean DCEWAF and CEWAF (Quinn & Keough, 2002).

The prokaryotic Inverse Simpson index contrasts to the eukaryotes in that the highest diversity is in the last time-point of the open ocean experiment (Figure 21). The coastal experiment showed the opposite pattern as the highest Inverse Simpson values were in the earliest time-points of the coastal community (Figure 21). The prokaryotic community inverse Simpson diversity had a very significant p-value for the interaction between environment, treatment, and time-point ($F_{3,76} = 4.39$, $p = 0.0067$) compared to the eukaryotes (Table 2) when using an ANOVA split-plot design with GLS for deviations from homoscedascity. Similarly, the interaction between environment and time-point ($F_{1,76} = 47.67$, $p = < 0.0001$) and treatment and time-point ($F_{3,76} = 3.43$, $p = 0.021$) were significant (Table 2).

Table 2: Prokaryotic Inverse Simpson ANOVA table, each factor is shown to the left of the bar. The values for between group degrees of freedom (Df), within group degrees of freedom (Df), F-value, and p-value are shown in the table. The x symbol indicates an interaction between variables. The asterisks on p-values indicate significance at an alpha of 0.05 (**), and weakly significant values at an alpha of 0.1 (*).

ANOVA table	Between Group Df	Within Group Df	F-value	p-value
Environment	1	16	4.7569	0.0445*
Treatment	3	16	83.9763	< .0001**
Timepoint	1	76	76.8664	< .0001**
Environment x Treatment	3	16	2.7286	0.0784
Environment x Timepoint	1	76	47.6745	< .0001**
Treatment x Timepoint	3	76	3.4317	0.0211*
Environment x Treatment x Timepoint	3	76	4.3882	0.0067**

Again, environment and treatment were not significant ($F_{3,16} = 2.73$, $p = 0.078$) (Table 2). Therefore, the Inverse Simpson's diversity changed over time within each environment and each treatment (Figure 21). Assumptions for the ANOVA test were met for whole-plot factors of environment (BFL p-value = 0.30), treatment (BFL p-value = 0.12) and the combined factors environment-treatment (BFL p-value = 0.59) with a shapiro-wilkes p-value of 0.40 and length of 24. Like the split-plot assumptions for eukaryotes, there were also problems with the fitted vs. residuals (B-P p-value = 0.005), and environment-time-point vs. residuals (BFL p-value = 0.0022). However, time-point vs. residuals (B-P p-value = 0.1), treatment-time-point vs. residuals (B-P p-value = 0.21), and normality S-W p-value of 2.3e-4 and length 108 met assumptions (Quinn & Keough, 2002). The interaction between the random blocking factor (tank) and time-point was not significant with a Tukey's non-additivity p-value of 0.74. Overall, in both the eukaryotes and prokaryotes the inverse Simpson index was significantly different at each level of environment, treatment, and across time-point suggesting the interaction of each factor is important.

Chao Index

Compared to the Inverse Simpson index which is heavily influenced by dominant community members, the Chao index takes into account both singletons and doubletons and represents the rare individuals present within the community. In the eukaryotic community, the Chao index was higher in earlier time-points in both the coastal and open ocean experiments (Figure 22). Within the coastal experiment, the DCEWAF treatment had the highest Chao index, while the lowest was in the CEWAF treatment (Figure 22). The Chao index was significantly different in the eukaryotic community for the interaction between environment, treatment, and time-point ($F_{3,159} = 9.84$, $p = < 0.0001$) (Table 3) using an ANOVA split-plot design. The assumptions for whole-plot level factors aggregated by tank were met in treatment (BFL p-value = 0.26), and environment-treatment (BFL p-value = 0.62), normality was met due to a length of 24 with a S-W p-value of 0.41. However, within the whole-plot factors the assumption for homoscedascity was not met for environment (BFL p-value = 0.019). Assumptions for split-plot level factors were met in the fitted vs. residuals plot (B-P p-value = 0.12), time-point vs. residuals (B-P p-value = 0.26), environment-treatment vs. residuals (BFL p-value = 0.51), treatment-time-point vs. residuals (BFL p-value = 0.85), and normality with S-W p-value of 3.07e-10 and a length of 191. The interaction between the random blocking factor (tank) and time-point was significant with a Tukey's non-additivity p-value of 0.0036, however this was again mainly due to one time-point and treatment, the open ocean control at 36 hours (Quinn & Keough, 2002).

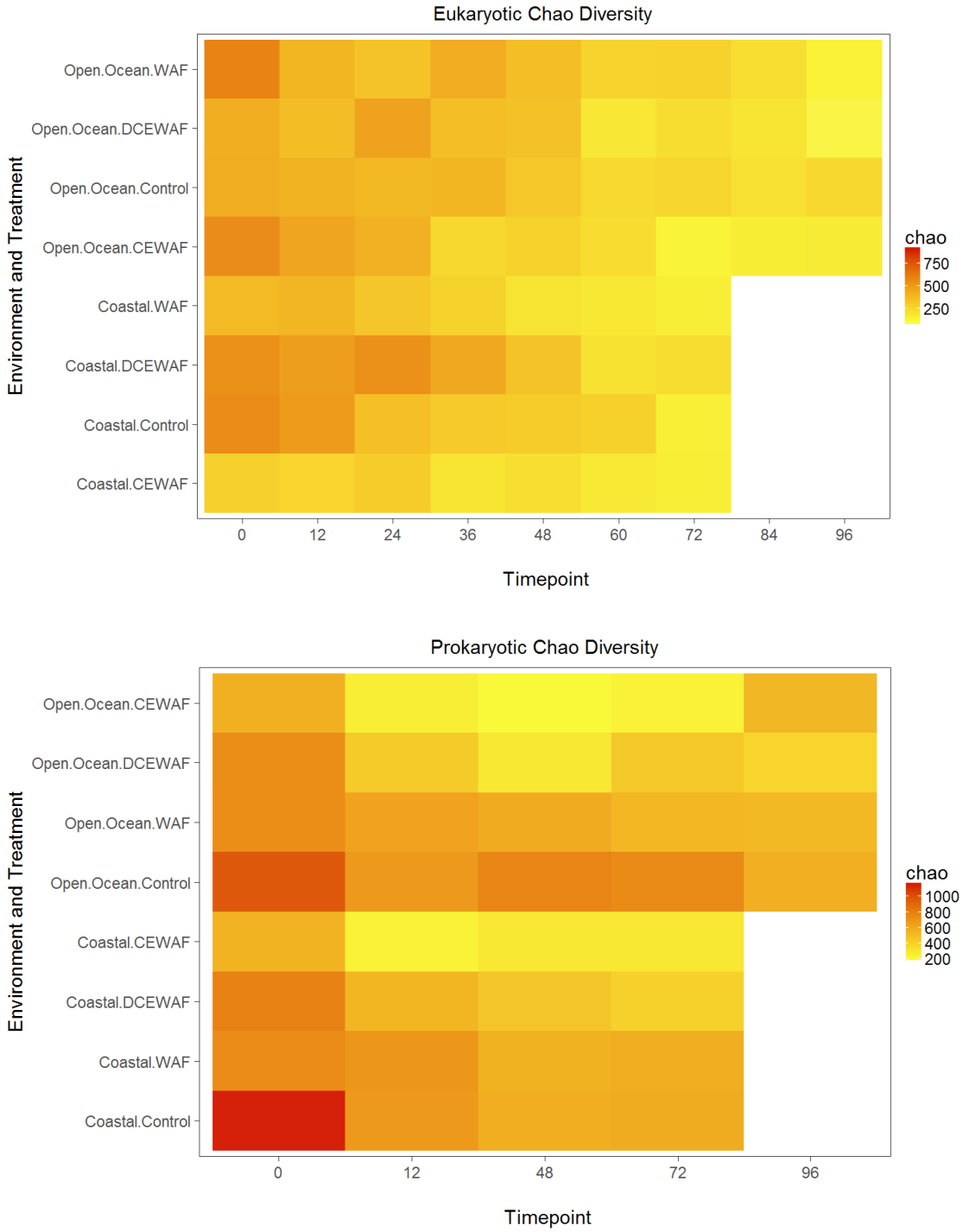

Figure 22: Eukaryotic (top) and prokaryotic (bottom) community Chao diversity for the eukaryotic community with time-point on the x-axis, and each variation of environment and treatment on the y-axis. The Chao goes from low (light yellow) to high (dark red) and is shown with corresponding numbers on the key to the right.

Table 3: Eukaryotic Chao Index ANOVA table, each factor is shown to the left of the bar. The values for between group degrees of freedom (Df), within group degrees of freedom (Df), F-value, and p-value are shown in the table. The x symbol indicates an interaction between variables. The asterisks on p-values indicate significance at an alpha of 0.05 (**), and weakly significant values at an alpha of 0.1 (*).

ANOVA table	Between Group Df	Within Group Df	F-value	p-value
Environment	1	16	0.0003	0.9860
Treatment	3	16	3.8177	0.0308*
Timepoint	1	159	306.8544	< .0001**
Environment x Treatment	3	16	6.2300	0.0052**
Environment x Timepoint	1	159	0.1358	0.7130
Treatment x Timepoint	3	159	0.6000	0.6159
Environment x Treatment x Timepoint	3	159	9.8393	< .0001**

Therefore, within environment each level of treatment across time-point was significantly different indicating environment and treatment interact to influence community changes overtime (Table 3 & Figure 22).

Contrastingly the Chao diversity index over time in the prokaryotes decreased in only the coastal experiment, while the diversity was variable in later time-points of the open ocean experiment (Figure 22). Additionally, the diversity was highest in the control and lowest in the CEWAF treatment in both experiments (Figure 22). The interaction between environment, treatment, and time-point was not significant ($F_{3,76} = 0.042$, $p = 0.99$) (Table 4) using an ANOVA split-plot design.

Table 4: Prokaryotic Chao Index ANOVA table, each factor is shown to the left of the bar. The values for between group degrees of freedom (Df), within group degrees of freedom (Df), F-value, and p-value are shown in the table. The x symbol indicates an interaction between variables. The asterisks on p-values indicate significance at an alpha of 0.05 (**).

ANOVA table	Between Group Df	Within Group Df	F-value	p-value
Environment	1	16	1.8055	0.1978
Treatment	3	16	44.1713	< .0001**
Timepoint	1	76	55.3768	< .0001**
Environment x Treatment	3	16	1.6646	0.2145
Environment x Timepoint	1	76	3.9158	0.0515
Treatment x Timepoint	3	76	1.1032	0.3531
Environment x Treatment x Timepoint	3	76	0.0420	0.9885

The only significant factors for the Chao diversity in prokaryotes were treatment ($F_{3,16} = 44.17$, $p = < 0.0001$) and time-point ($F_{1,76} = 55.38$, $p = < 0.0001$) (Table 4). The open ocean vs. coastal experiment (environment) was not significant ($F_{1,16} = 1.81$, $p = 0.20$) suggesting the rare taxa are heavily influenced by treatment over time rather than environment (Table 4 & Figure 22). The assumptions for the whole-plot factors in this ANOVA were met in environment (BFL p-value = 0.51), treatment (BFL p-value = 0.15), and environment-treatment ((BFL p-value = 0.51), with an S-W p-value of 0.2 and length of 24. The split-plot assumptions were met for the fitted vs. residuals plot (B-P p-value =0.71), treatment-time-point vs. residuals (BFL p-value = 0.86), environment-time-point vs. residuals (BFL p-value = 0.58), and normality with a length of 108 and S-W p-value of 0.0027. However, there were problems with the time-point vs. residuals (B-P p-value = 0.015), but this was only weakly significant at an alpha = 0.05 (Quinn & Keough, 2002). The interaction between tank and time-point was significant with a p-value of 0.002, but again was mainly due variability at the 12 hour time-point.

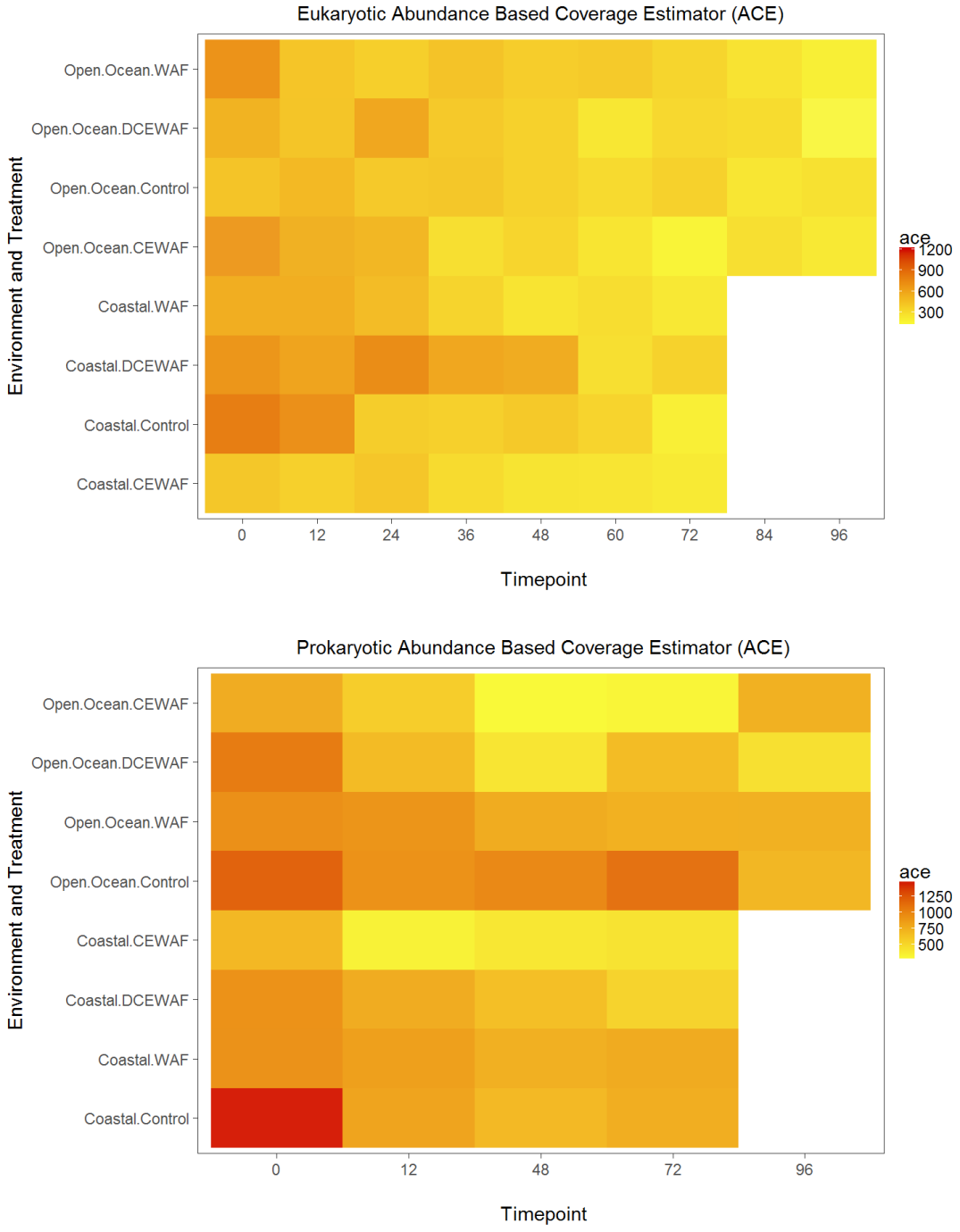

Figure 23: Eukaryotic (top) and prokaryotic (bottom) community Abundance Based Coverage Estimator (ACE) diversity for the eukaryotic community with time-point on the x-axis, and each variation of environment and treatment on the y-axis. The ACE index goes from low (light yellow) to high (dark red) and is shown with corresponding numbers on the key to the right.

Both the prokaryotic and eukaryotic communities are significantly influenced by treatment and change significantly throughout the time points sampled (Table 3 & Table 4). The interaction with environment and treatment over time significantly affects the community composition in eukaryotes, whereas in prokaryotes the community composition is not affected by environment (open ocean vs. coastal) (Table 3 & Table 4).

ACE Index

The ACE index is used to measure diversity while taking into account rare taxa and OTUs with 10 or fewer individuals per OTU, compared to the singletons and doubletons used for the Chao index (Hill et. al., 2003). In the eukaryotic community, the ACE index was highest in the earlier time-points and in the coastal experiment (Figure 23). Within the eukaryotic community in the coastal experiment the control and DCEWAF had the highest ACE diversity (Figure 23). Similarly, to the Inverse Simpson and the Chao diversity metrics, there was a significant interaction between environment, treatment, and time-point for the ACE index ($F_{3,159}$= 7.9140, p = 0.0001) (Table 5) using an ANOVA split-plot design with auto-correlation between time-points. The assumptions for whole-plot factors were met for environment (BFL p-value = 0.14), treatment (BFL p-value = 0.081), environment-treatment (BFL p-value = 0.57), and normality with a S-W p-value of 0.06632 and length of 24. The split-plot level assumptions were met for most factors including time-point vs. residuals (B-P p-value = 0.065), environment-time-point (BFL p-value = 0.59), treatment-time-point (BFL p-value = 0.31), and normality with an S-W p-value of 3e-4 and length 191.

Table 5: Eukaryotic Abundance Based Coverage Estimate (ACE) Index ANOVA table, each factor is shown to the left of the bar. The values for between group degrees of freedom (Df), within group degrees of freedom (Df), F-value, and p-value are shown in the table. The x symbol indicates an interaction between variables. The asterisks on p-values indicate significance at an alpha of 0.05 (**), and weakly significant values at an alpha of 0.1 (*).

ANOVA table	Between Group Df	Within Group Df	F-value	p-value
Environment	1	16	4.2165	0.0568
Treatment	3	16	3.0153	0.0607
Timepoint	1	159	152.2226	< .0001**
Environment x Treatment	3	16	7.0184	0.0032**
Environment x Timepoint	1	159	3.7268	0.0553
Treatment x Timepoint	3	159	0.4033	0.7508
Environment x Treatment x Timepoint	3	159	7.9140	0.0001**

Assumptions for homoscedascity in the fitted vs. residuals (B-P p-value = 0.002) were not met, however the spread for the fitted vs. residuals plot deviated because of potential non-linearity which was deemed inferior when tested against the linear model using AICc. Finally, the interaction between the random blocking factor (tank) and time-point was significant, with a Tukey's non-additivity p-value of 1.9e-4 but was again due to two tanks at the 0 hr time-point. These results and the consistency across indices representing different aspects of the overall community structure suggest environment, treatment, and time all play a significant role in changing diversity (Table 5 & Figure 23).

The prokaryotic community diversity decreases and then increases at later time-points (Figure 23). While the overall diversity is not significantly different in either environment ($F_{1,16}$ = 0.042, p = 0.84), the lowest diversity is seen in the CEWAF treatment (Table 6 & Figure 23) using an ANOVA split-plot design. Treatment ($F_{3,16}$ = 28.71, p = < 0.0001) and time-point ($F_{1,76}$ = 55.56, p = < 0.0001) were significantly different indicating that treatment is the main driver of community composition change over time (Table 6 & Figure 23).

Table 6: Prokaryotic Abundance Based Coverage Estimate (ACE) Index ANOVA table, each factor is shown to the left of the bar. The values for between group degrees of freedom (Df), within group degrees of freedom (Df), F-value, and p-value are shown in the table. The x symbol indicates an interaction between variables. The asterisks on p-values indicate significance at an alpha of 0.05 (**).

ANOVA table	Between Group Df	Within Group Df	F-value	p-value
Environment	1	16	0.0422	0.8398
Treatment	3	16	28.7132	< .0001**
Timepoint	1	76	55.5621	< .0001**
Environment x Treatment	3	16	1.3090	0.3059
Environment x Timepoint	1	76	0.2631	0.6095
Treatment x Timepoint	3	76	0.8393	0.4765
Environment x Treatment x Timepoint	3	76	0.0440	0.9876

The assumptions for whole-plot factors in this experiment were met for environment (BFL p-value = 0.58), treatment (BFL p-value = 0.41), environment-treatment (BFL p-value = 0.95), and normality S-W p-value of 0.38 and length of 24. The split-plot level factor assumptions were also met for fitted vs. residuals (B-P p-value = 0.82), time-point vs. residuals (B-P value = 0.28), treatment-time-point (BFL p-value = 0.91), environment-time-point (BFL p-value = 0.55), and finally normality with a S-W p-value of 9e-4 and length of 108. The interaction between tank and time-point was not significant with a p-value of 0.081. The results from ACE diversity metrics are comparable to the Chao diversity, both metrics that include rare taxa, the prokaryotic community is driven by treatment and time-point, while changes in the eukaryotic community are also dependent on the environment (open ocean vs. coastal). The inverse Simpson index shows environment, treatment and time-point are important drivers for abundant members of the both the prokaryotic and eukaryotic community.

In the prokaryotes, the Chao and ACE diversity indices highlight the similarity between the coastal and open ocean environment, however the Inverse Simpson index suggests dominant communities are impacted by environment (Figures 25, 26, & 27). Conversely, in the eukaryotes all three factors (environment, treatment, and time-point) had a significant interaction for all three diversity metrics indicating both dominant and rare members of the community are impacted by all three (Figure 21, 27, & 29).

NETWORK ANALYSIS

Network analysis in Cytoscape reveals negative and positive correlations within the highest abundance prokaryotes and phytoplankton (Shannon et al., 2003). Lag-time correlations between groups of interest are highlighted among the many interactions between organisms, as they help determine key players in MOS formation in these experiments. During these analyses Operational Taxonomic Unit (OTU) are used as a proxy for individuals, and each organisms OTU is paired with Prok for prokaryotes and Euk for eukaryotes. Lag-time correlations indicate if the abundance of one OTU affects the abundance of another OTU at an earlier or later time-point represented by solid (positive lag-time), and dashed (negative lag-time) lines. A negative lag-time correlation indicates an increase in the first OTU at one time-point and a decrease in the second OTU at later time-points representation by green (positive) and red (negative).

In the open ocean control treatment interaction between groups of diatoms and dinoflagellates with bacteria were common (Figure 24). In particular, the centric Bacillariophyceae (Euk OTU3) had a positive lag-time correlation with *Methylophaga* (Prok OTU8). *Methylophaga* (Prok OTU8) was found to be the most abundant organism within the Thiotrichales order that had a distinct response dependent on environment (Figures 22 & 24).

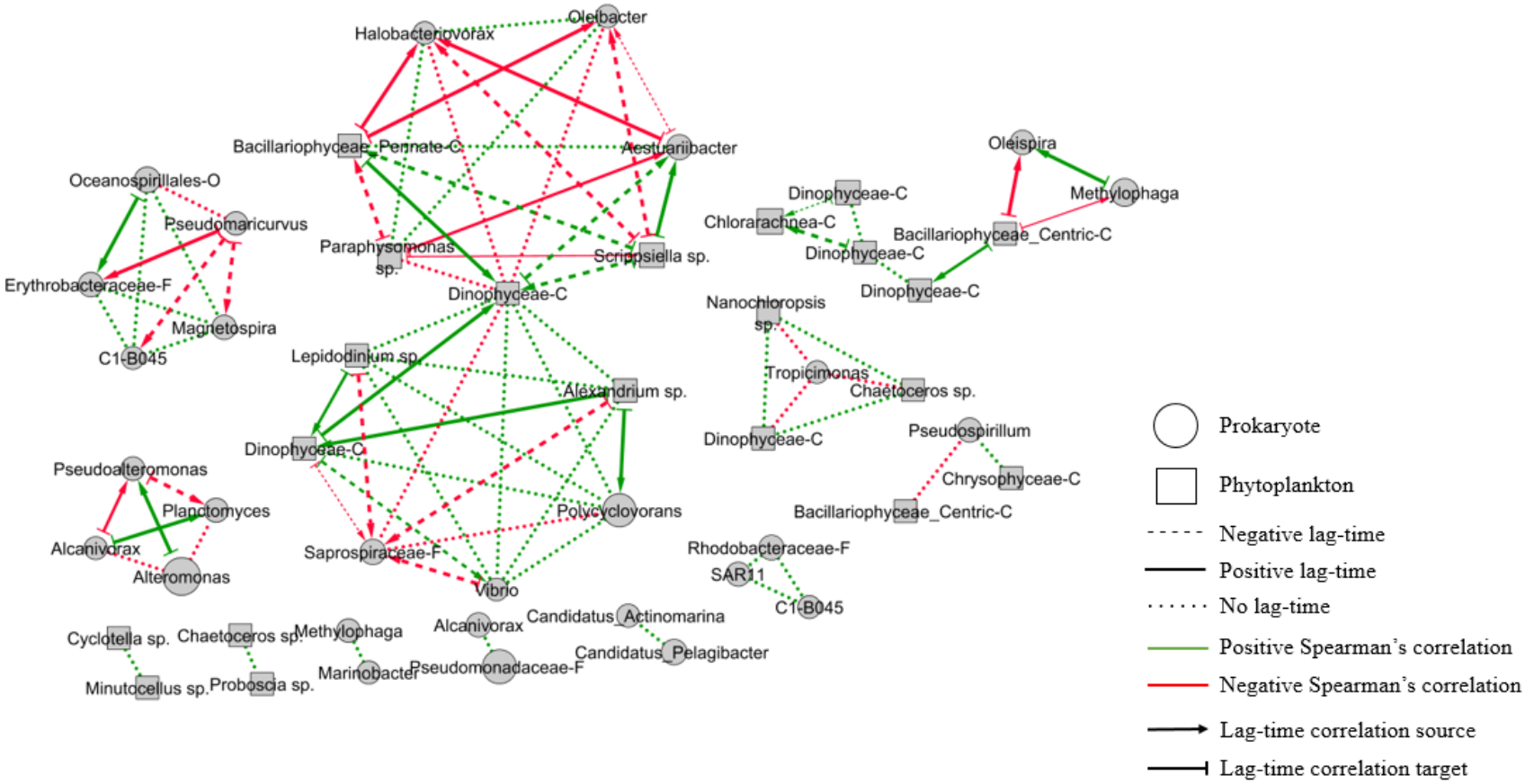

Figure 24: Network analysis in of the control treatment in the open ocean experiment, legend is on the bottom right. Only significant correlations are shown (Spearman's rho > | 0.5|, p > 0.05, q > 0.05). Prokaryotes are represented with circular nodes, phytoplankton with square nodes including labels indicating the genus (or lowest classification). If classification couldn't be made down to genus an extension was added to indicate taxonomic level (i.e. Phylum=K, Class=C, Order=O). Positive correlations are shown with green solid lines, negative with dashed red lines, and no lag time with black dots. Darker shading of green or red shows longer lag-time correlations, up to 4. An arrow with a T at the end (see legend) indicate the node is the source of the correlation and in the case of a lag-time, time-point zero. While an arrow head pointed towards a node (see legend) indicates the target of a lag-time correlation, where the correlation is directed. The size of each node is the mean relative abundance of each OTU across time-points.

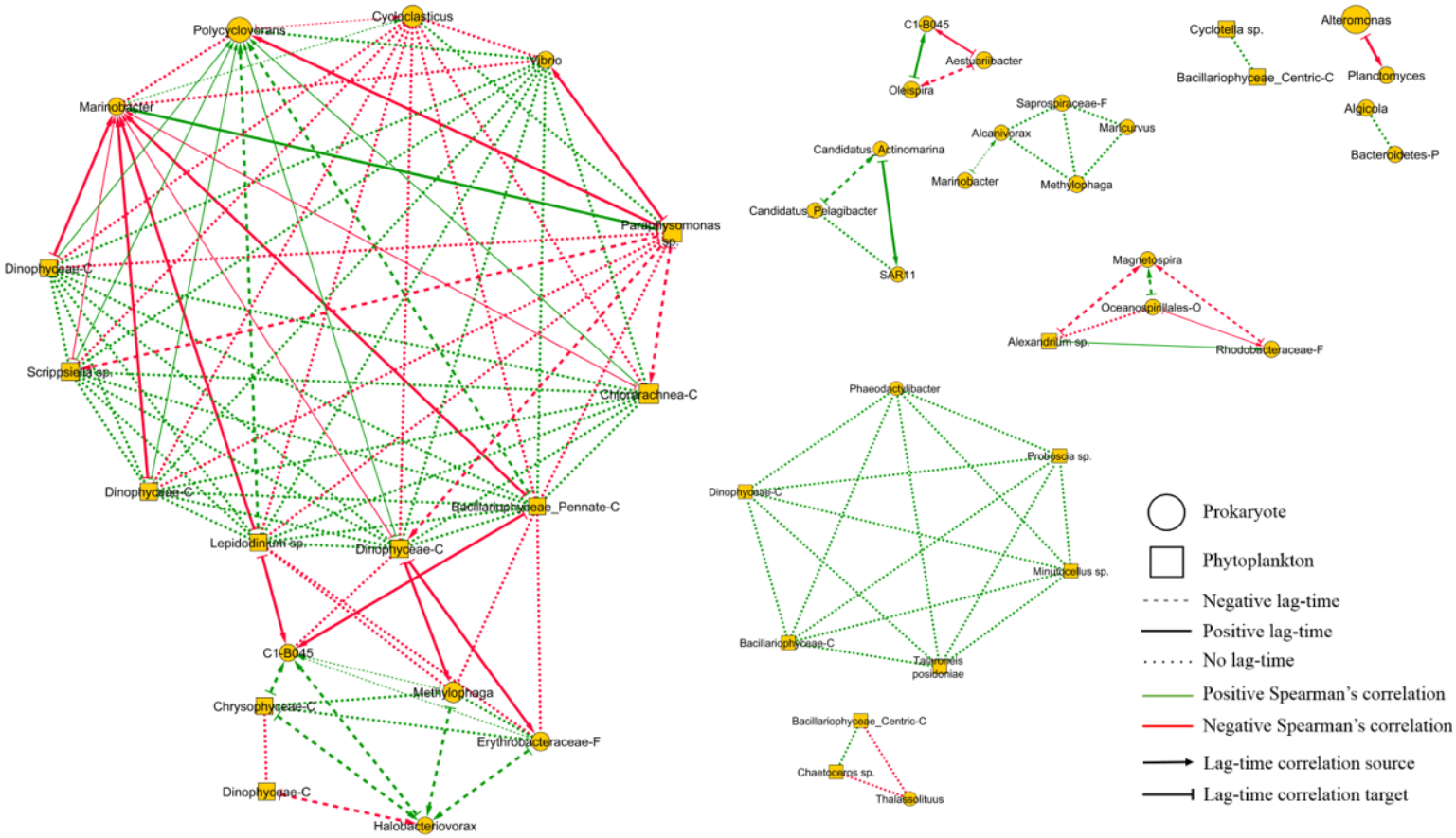

Figure 25: Network analysis in of the WAF treatment in the open ocean experiment, legend is on the bottom right. Only significant correlations are shown (Spearman's rho > | 0.5|, p > 0.05, q > 0.05). Prokaryotes are represented with circular nodes, phytoplankton with square nodes including labels indicating the genus (or lowest classification). If classification couldn't be made down to genus an extension was added to indicate taxonomic level (i.e. Phylum=K, Class=C, Order=O). Positive correlations are shown with green solid lines, negative with dashed red lines, and no lag time with black dots. Darker shading of green or red shows longer lag-time correlations, up to 4. An arrow with a T at the end (see legend) indicate the node is the source of the correlation and in the case of a lag-time, time-point zero. While an arrow head pointed towards a node (see legend) indicates the target of a lag-time correlation, where the correlation is directed. The size of each node is the mean relative abundance of each OTU across time-points.

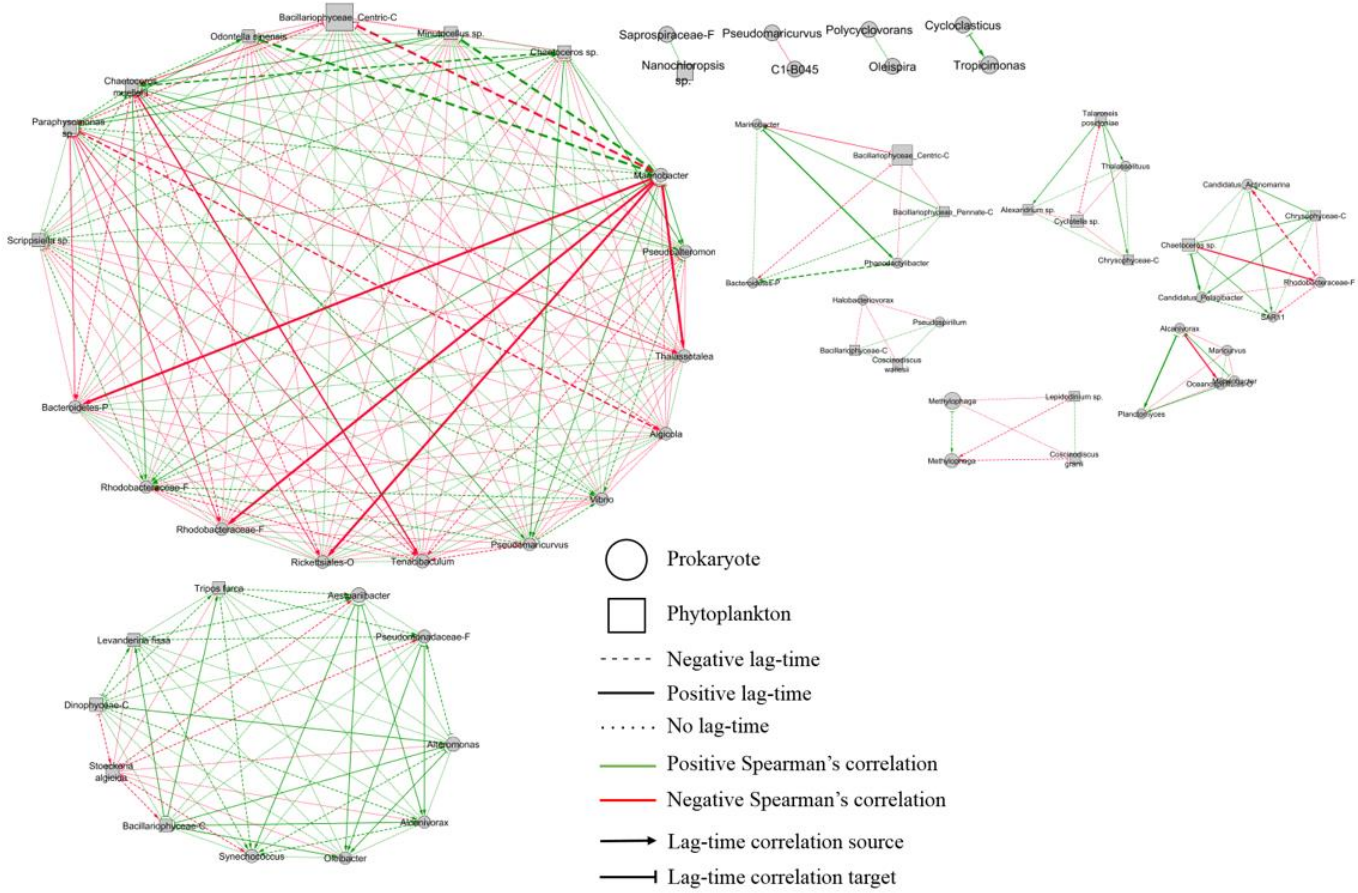

Figure 26: Network analysis in of the control treatment in the coastal experiment, legend is in the bottom center of the figure. Only significant correlations are shown (Spearman's rho > | 0.5|, p > 0.05, q > 0.05). Prokaryotes are represented with circular nodes, phytoplankton with square nodes including labels indicating the genus (or lowest classification). If classification couldn't be made down to genus an extension was added to indicate taxonomic level (i.e. Phylum=K, Class=C, Order=O). Positive correlations are shown with green solid lines, negative with dashed red lines, and no lag time with black dots. Darker shading of green or red shows longer lag-time correlations, up to 4. An arrow with a T at the end (see legend) indicate the node is the source of the correlation and in the case of a lag-time, time-point zero. While an arrow head pointed towards a node (see legend) indicates the target of a lag-time correlation, where the correlation is directed. The size of each node is the mean relative abundance of each OTU across time-points.

Within the coastal experiment there were more interactions between *Methylophaga* (Prok OTU7 & OTU8) and other phytoplankton and bacteria as oil concentration increased. This relationship was not seen in the open ocean experiment, likely because the phytoplankton were not as abundant during this experiment (Figure 25). Likewise, in the WAF treatments putative hydrocarbon degraders also have significant correlations with *Methylophaga* (Prok OTU7 & OTU8) (Figure 25).

While, in the coastal experiment control treatment, *Coscindodiscus granni* (Euk OTU192), and *Lepidodinium sp* (Euk OTU80) had a negative lag-time correlation with *Methylophaga* (Prok OTU8) (Figure 26). *Methylophaga* (Prok OTU7) concurrently had a negative lag-time correlation with the other *Methylophaga* OTU (Prok OTU8) (Figure 26). The WAF treatment in the open ocean environment, Dinophyceae (Euk OTU28) had a negative impact on *Methylophaga* (Prok OTU7), and in turn *Methylophaga* (Prok OTU7) had a negative impact on *Halobacteriovorax* (Prok OTU38) (Figure 25).

There were no other significant lag-time correlations with *Methylophaga* (Prok OTU7 or OTU8) in the open ocean environment (Figures 32 & 33). The WAF treatment in the coastal experiment included negative lag-time correlations between *Marinobacter* (Prok OTU2) and *Methylophaga* (Prok OTU7) as well as between *Aestuariibacter* (Prok OTU5) and *Methylophaga* (Prok OTU8) (Figure 27). Moreover, *Aestuariibacter* (Prok OTU5) also had a positive lag-time correlation with *Methylophaga* (Prok OTU7).

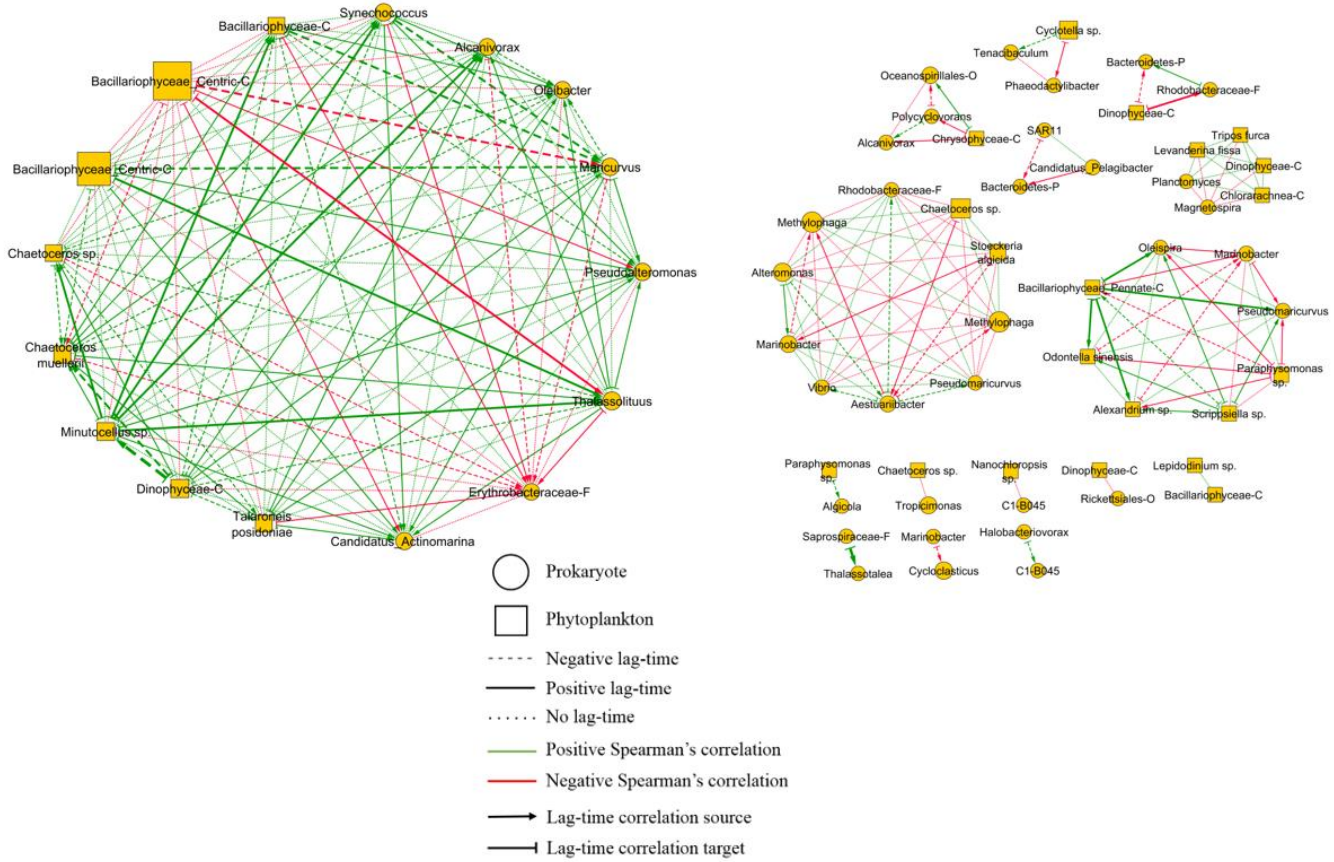

Figure 27: Network analysis in of the WAF treatment in the coastal experiment, legend is on the bottom right. Only significant correlations are shown (Spearman's rho > | 0.5|, p > 0.05, q > 0.05). Prokaryotes are represented with circular nodes, phytoplankton with square nodes including labels indicating the genus (or lowest classification). If classification couldn't be made down to genus an extension was added to indicate taxonomic level (i.e. Phylum=K, Class=C, Order=O). Positive correlations are shown with green solid lines, negative with dashed red lines, and no lag time with black dots. Darker shading of green or red shows longer lag-time correlations, up to 4. An arrow with a T at the end (see legend) indicate the node is the source of the correlation and in the case of a lag-time, time-point zero. While an arrow head pointed towards a node (see legend) indicates the target of a lag-time correlation, where the correlation is directed. The size of each node is the mean relative abundance of each OTU across time-points.

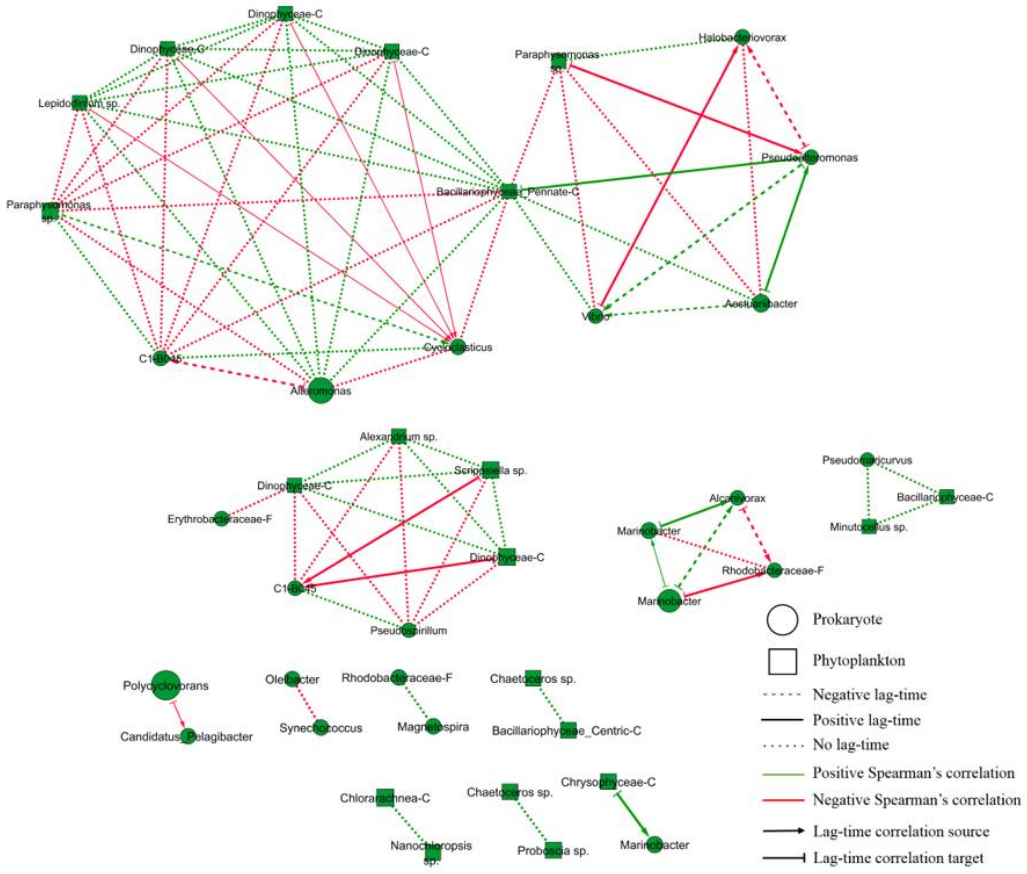

Figure 28: Network analysis in of the DCEWAF treatment in the open ocean experiment, legend is on the bottom right. Only significant correlations are shown (Spearman's rho > | 0.5|, p > 0.05, q > 0.05). Prokaryotes are represented with circular nodes, phytoplankton with square nodes including labels indicating the genus (or lowest classification). If classification couldn't be made down to genus an extension was added to indicate taxonomic level (i.e. Phylum=K, Class=C, Order=O). Positive correlations are shown with green solid lines, negative with dashed red lines, and no lag time with black dots. Darker shading of green or red shows longer lag-time correlations, up to 4. An arrow with a T at the end (see legend) indicate the node is the source of the correlation and in the case of a lag-time, time-point zero. While an arrow head pointed towards a node (see legend) indicates the target of a lag-time correlation, where the correlation is directed. The size of each node is the mean relative abundance of each OTU across time-points.

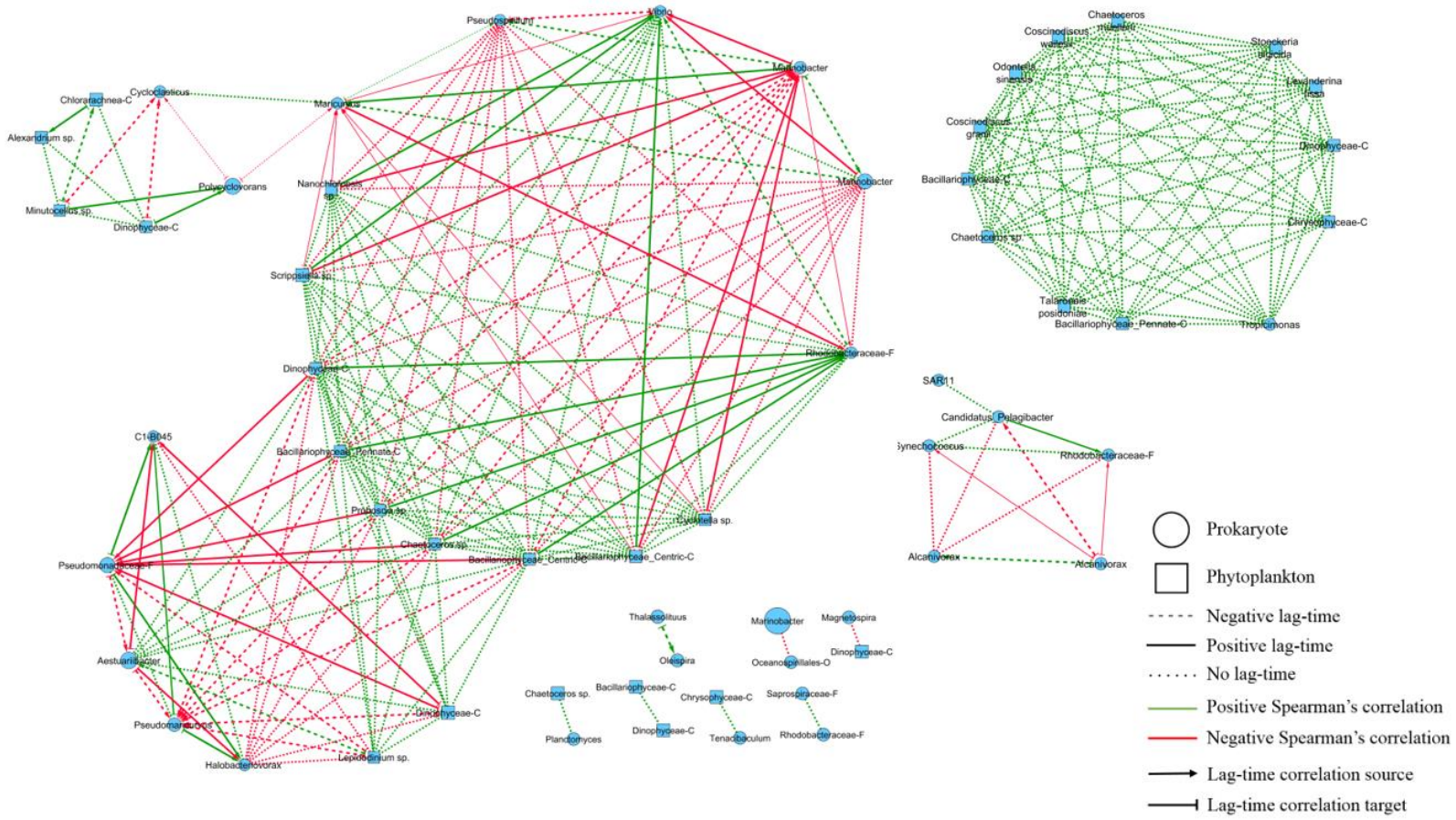

Figure 29: Network analysis in of the CEWAF treatment in the open ocean experiment, legend is on the right. Only significant correlations are shown (Spearman's rho > | 0.5|, p > 0.05, q > 0.05). Prokaryotes are represented with circle nodes, phytoplankton with squares nodes including labels indicating the genus (or lowest classification). If classification couldn't be made down to genus an extension was added to indicate taxonomic level (i.e. Phylum=K, Class=C, Order=O). Positive correlations are shown with green solid lines, negative with dashed red lines, and no lag time with black dots. Darker shading of green or red shows longer lag-time correlations, up to 4. An arrow with a T at the end (see legend) indicate the node is the source of the correlation and in the case of a lag-time, time-point zero. While an arrow head pointed towards a node (see legend) indicates the target of a lag-time correlation and where the correlation is directed. The size of each node is the mean relative abundance of each OTU across time-points.

In the coastal experiment, there were also significant correlations between *Methylophaga* (Prok OTU7 & OTU8) and both eukaryotic and prokaryotic OTUs in the DCEWAF and CEWAF treatments. Again, within the DCEWAF treatment of the coastal experiment, the negative lag-time correlation between *Methylophaga* (Prok OTU7) and *Methylophaga* (Prok OTU8) was seen (Figure 30). *Marinobacter* (Prok OTU2) and Dinophyceae (Euk OTU10) also had a negative lag-time correlation with *Methylophaga* (Prok OTU8) (Figure 30). *Methylophaga* (Prok OTU8) in turn, had a negative lag-time correlation with *Alcanivorax* (Prok OTU15) and Bacteroidetes (Prok OTU72) (Figure 30). *Aestuariibacter* (Prok OTU5), *Polycyclovorans* (Prok OTU4), *Chaetoceros muellerii* (Euk OTU49), and *Chaetoceros* sp. (Euk OTU38) all had a positive lag-time correlation with *Methylophaga* (Prok OTU8) (Figure 30). Meaning each of the aforementioned OTUs increased at one time-point resulting in an increase in *Methylophaga* (Prok OTU8) at subsequent timepoints. Finally, *Aestuariibacter* (Prok OTU5) also had a negative lag-time correlation with the other *Methylophaga* OTU (Prok OTU7) (Figure 30).

In the CEWAF treatment of the coastal experiment, *Methylophaga* (Prok OTU7) had more lag-time correlations compared to *Methylophaga* (Prok OTU8) (Figure 31). *Alexandrium sp.* (Euk OTU54) had a negative lag-time correlation with *Methylophaga* (Prok OTU8), which in turn had a positive lag-time correlation with *Pseudomaricurvus* (Euk OTU12) (Figure 31). *Methylophaga* (Prok OTU7) had negative lag-time correlations with *Oceanospirillales* (Prok OTU14) and *Cycloclasticus* (Prok OTU9), and a positive lag-time correlation with *Candidatus Pelagibacter* (Prok OTU20) (Figure 31). Three phytoplankton, *Chaetoceros sp.* (Euk OTU38), Bacillariophyceae (Euk OTU63), and *Lepidodinium sp.* (Euk OTU80) had a positive lag-time correlation with Methylophaga (Prok OTU7).

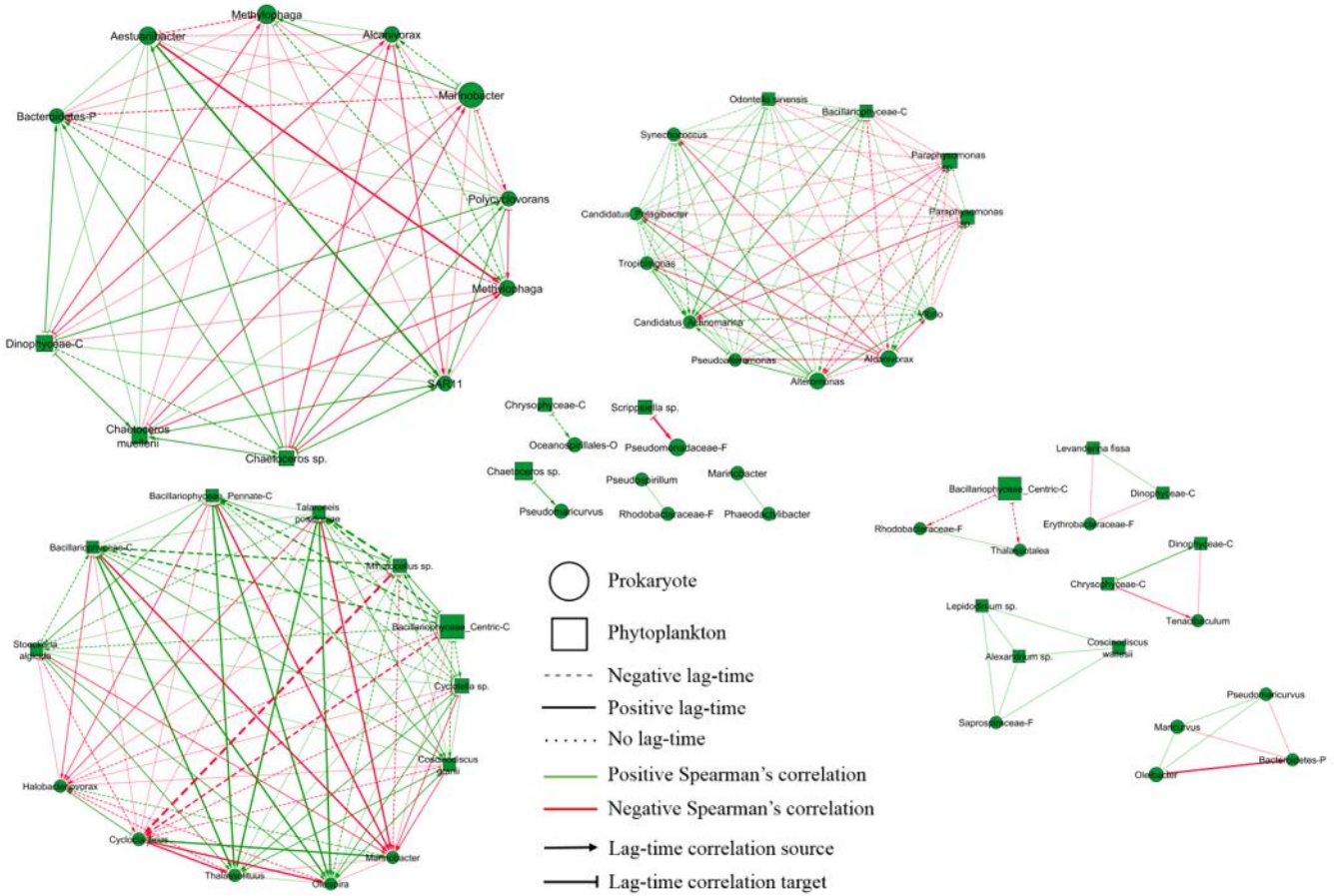

Figure 30: Network analysis in of the DCEWAF treatment in the coastal experiment, legend is on the bottom right. Only significant correlations are shown (Spearman's rho > | 0.5|, p > 0.05, q > 0.05). Prokaryotes are represented with circular nodes, phytoplankton with square nodes including labels indicating the genus (or lowest classification). If classification couldn't be made down to genus an extension was added to indicate taxonomic level (i.e. Phylum=K, Class=C, Order=O). Positive correlations are shown with green solid lines, negative with dashed red lines, and no lag time with black dots. Darker shading of green or red shows longer lag-time correlations, up to 4. An arrow with a T at the end (see legend) indicate the node is the source of the correlation and in the case of a lag-time, time-point zero. While an arrow head pointed towards a node (see legend) indicates the target of a lag-time correlation, where the correlation is directed. The size of each node is the mean relative abundance of each OTU across time-points.

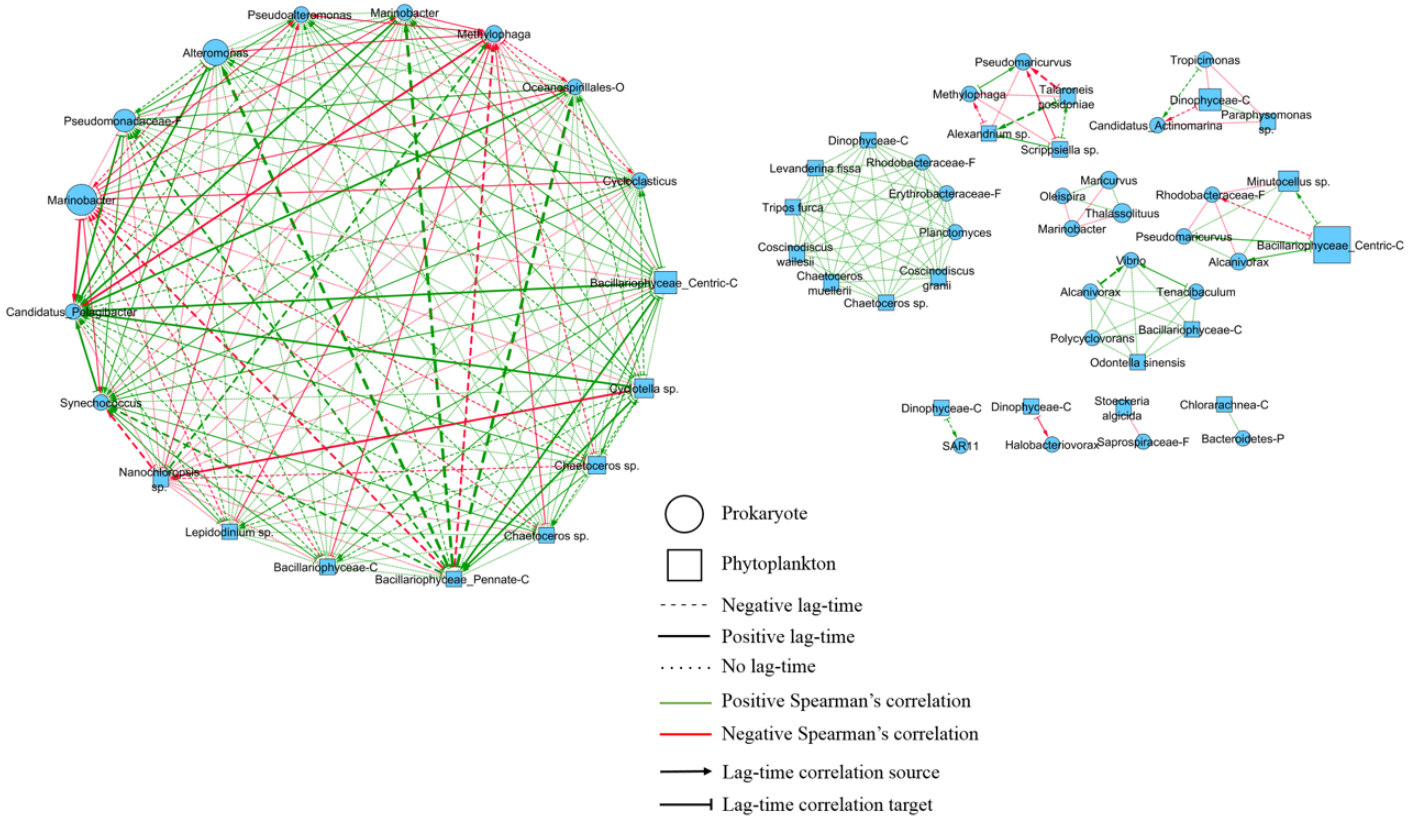

Figure 31: Network analysis in of the CEWAF treatment in the coastal experiment, legend is at the bottom in the center of the figure. Only significant correlations are shown (Spearman's rho > | 0.5|, p > 0.05, q > 0.05). Prokaryotes are represented with circular nodes, phytoplankton with square nodes including labels indicating the genus (or lowest classification). If classification couldn't be made down to genus an extension was added to indicate taxonomic level (i.e. Phylum=K, Class=C, Order=O). Positive correlations are shown with green solid lines, negative with dashed red lines, and no lag time with black dots. Darker shading of green or red shows longer lag-time correlations, up to 4. An arrow with a T at the end (see legend) indicate the node is the source of the correlation and in the case of a lag-time, time-point zero. While an arrow head pointed towards a node (see legend) indicates the target of a lag-time correlation, where the correlation is directed. The size of each node is the mean relative abundance of each OTU across time-points.

While three other phytoplankton, *Chaetoceros sp.* (Euk OTU8), *Nannochloropsis* (Euk OTU134), and pennate *Bacillariophyceae* (Euk OTU24) all had a negative lag-time correlation with *Methylophaga* (Prok OTU7). Altogether there were more significant lag-time correlations between *Methylophaga* (Prok OTU7 & OTU8) and both bacteria and phytoplankton in the dispersed oil treatments (DCEWAF & CEWAF) in the coastal environment. While the only significant lag-time correlations in the coastal experiment with Methylophaga were in the Control and WAF treatment.

Contrastingly, *Pseudoalteromonas* (Prok OTU21) had significant lag-time correlations in all four treatments in both experiments, except for the coastal CEWAF treatment (Figure 31). Open ocean control saw significant positive correlations with both *Alteromonas* (Prok OTU1), and *Alcanivorax* (Prok OTU13) on *Pseudoalteromonas* (Prok OTU21) (Figure 24). This interaction was also seen in the WAF treatment (Figure 25). Additionally, in the control treatment *Pseudoalteromonas* (Prok OTU21) had a negative lag-time correlation with *Planctomyces* (Prok OTU78) (Figure 24). In the WAF treatment there was also a positive lag-time correlation between *Pseudoalteromonas* (Prok OTU21) and *Candidatus actinomarina* (Prok OTU28) (Figure 25). Finally, in the DCEWAF treatment the community correlations were not similar to other treatments like that of the Control and WAF. *Aestuariibacter* (Prok OTU5), and *Paraphysomonas* (Euk OTU35) had a positive lag-time correlation with *Pseudoalteromonas* (Prok OTU21) (Figure 28). While, *Pseudoalteromonas* (Prok OTU21) in turn had a negative lag-time correlation with both *Vibrio* (Prok OTU33), and *Halobacteriovorax* (Prok OTU38) (Figure 28).

In the coastal environment, *Pseudoalteromonas* (Prok OTU21) did not show similar correlations between treatments like that of the aforementioned open ocean environment.

However, there were some similarities between open ocean and coastal environment interactions. In the control treatment in the coastal experiment, *Vibrio* (Prok OTU33), *Tenacibaculum* (Prok OTU32), and *Rhodobacteraceae* (Prok OTU44) had negative lag-time correlations with *Pseudoalteromonas* (Prok OTU21) (Figure 26). The correlation between *Vibrio* (Prok OTU33) and *Pseudoalteromonas* (Prok OTU21) was also seen in the open ocean DCEWAF treatment (Figure 28). *Chaetoceros muelerii* (Euk OTU49) and *Chaetoceros* sp. (Euk OTU38) showed a positive lag-time correlation with *Pseudoalteromonas* (Prok OTU21) (Figure 26). On the other hand, the coastal WAF treatment had one negative lag-time correlation with Bacillariophyceae (Euk OTU63) and *Pseudoalteromonas* (Prok OTU21) (Figure 27). The rest of the significant lag-time correlations were positive among *Maricurvus* (Prok OTU17), *Synechococcus* (Prok OTU16), *Thalassolituus* (Prok OTU11), *Minutocellus* (Euk OTU17), *Talaroneis podidonae* (Euk OTU42), and centric Bacillariophyceae (Euk OTU2 & OTU3) on *Pseudoalteromonas* (Prok OTU21) (Figure 27). In the coastal DCWAF treatment there were multiple consistencies across environments. There were significant, positive, lag-time correlations with both *Alteromonas* (Prok OTU1), and *Alcanivorax* (Prok OTU13) on *Pseudoalteromonas* (Prok OTU21) (Figure 30). This correlation was also seen in the control and WAF treatment in the open ocean environment (Figures 28 & 29). Additionally, *Pseudoalteromonas* (Prok OTU21) had a positive lag-time correlation with *Candidatus actinomarina* (Prok OTU28) in the coastal DCEWAF treatment similar to the open ocean WAF treatment (Figures 29 & 34). Contrastingly, in the coastal CEWAF treatment there were no similarities between environments and many interactions were between phytoplankton and bacteria. Pseudomonadadaceae (Prok OTU3), *Marinobacter* (Prok OTU2), centric Bacillariophyceae (Euk OTU3), *Cyclotella* (Euk OTU9), and *Nannochloropsis* (Euk OTU28) all had a positive lag-time correlation with

Pseudoalteromonas (Prok OTU21) (Figure 31). Lastly, *Candidatus pelagibacter* (Prok OTU21), and pennate Bacillariophyceae (Euk OTU20) had a negative lag-time correlation with *Pseudoalteromonas* (Prok OTU21) (Figure 31). There were more correlations with both bacteria and phytoplankton in the DCEWAF and CEWAF treatments in both open ocean and control experiments. Furthermore, multiple shared interactions were seen between the two environments suggesting conserved interactions throughout different environments.

Paraphysomonas (of the Class Chrysophyceae) was also an abundant phytoplankton group within both experiments and is known to be heterotrophic (Lim et al., 1999). The only significant lag-time correlations within this group were in the control, WAF, and DCEWAF treatments in both experiments. In the open ocean control there were only negative lag time correlations between *Paraphysomonas sp.* (Euk OTU5) and both *Aestuariibacter* (Prok OTU5) and centric Bacillariophyceae (Euk OTU24) (Figure 24). In the open ocean WAF treatment, *Paraphysomonas* sp. (Euk OTU5) had a negative lag-time correlation with *Chlorarachnea* (Euk OTU29), Dinophyceae (OTU28), and *Scrippsiella* sp (Euk OTU20) (Figure 25). While, all of the positive lag-time correlations starting with *Paraphysomonas* sp. (Euk OTU5) involve three prokaryotes, *Marinobacter* (Prok OTU2), *Polycyclovorans* (Prok OTU4), and *Vibrio* (Prok OTU33) (Figure 25). Within the open ocean DCEWAF treatment all of the correlations were between Parphysomonas (eukaryotic mixotroph) and prokaryotes (Figure 28). Both *Aestuariibacter* (Prok OTU5) and *Paraphysomonas* sp. (Euk OTU35) had a negative lag-time correlation with *Pseudoalteromonas* (mentioned above) (Figure 28). Additionally, *Paraphysomonas* sp. (Euk OTU5) had a negative lag-time correlation with *Cycloclasticus* (Prok OTU9) (Figure 28).

Although many OTUs that have a lag-time correlation with *Paraphysomonas* sp. (Euk OTU5), the pattern of mixed algal and bacterial correlations in all but the DCEWAF treatment were consistent in both environments. Within the coastal control, *Paraphysomonas* sp. (Euk OTU5) had a negative lag-time correlation with *Chaetoceros muellerii* (Euk OTU49), *Marinobacter* (Prok OTU2), *Algicola* (Prok OTU98), and *Vibrio* (Prok OTU38) (Figure 26). *Paraphysomonas* sp (Euk OTU5) also had negative lag-time correlations with *Odontella synensis* (Euk OTU60), *Minutocellus* sp. (Euk OTU17), *Thalassotalea* (Prok OTU130), *Tenacibaculum* (Prok OTU32), *Rickettsiales* (Prok OTU123), Rhodobacteraceae (Prok OTU23), and *Bacteriodetes* (Prok OTU82) in the control (Figure 26). Moreover, there was one lag-time correlation between centric Bacillariophyceae (Euk OTU2) and *Paraphysomonas* sp. (Euk OTU5) (Figure 27). In the coastal WAF treatment there were primarily positive lag-time correlations between *Paraphysomonas* sp. (Euk OTU5) and *Pseudomaricurvus* (Prok OTU12), *Oleispira* (Prok OTU25), *Odeontella sinensis* (Euk OTU60), and *Alexandrium* sp. (Euk OTU54) (Figure 27). While there was one negative lag-time correlation between *Paraphysomonas* sp. (Euk OTU5) and a pennate Bacillariophyceae (Euk OTU24) (Figure 27). Finally, the correlations seen in the coastal DCEWAF treatment were similar to those seen in the *Pseudoalteromonas* (Prok OTU21) interactions in the previous section in the coastal control and WAF treatments (Figures 28 & 29). There was also an additional *Paraphysomonas* sp. (Euk OTU35) interaction only in the coastal DCEWAF treatment (Figure 30). Both *Paraphysomonas* sp. (Euk OTU5 & OTU35) had a positive correlation on *Candidatus actinomarina* (Prok OTU28), and a negative correlation with *Alcanivorax* (Prok OTU13) and *Alteromonas* (OTU1) (Figure 30). The consistency between these bacteria and both *Paraphysomonas* sp (Euk OTU5 & OTU35) and *Pseudoalteromonas* (Prok OTU21), indicate a common interaction across

environments and treatments. Furthermore, there were consistencies in the DCEWAF treatment in which *Paraphysomonas* sp. (Euk OTU5 & OTU35) were only correlated with bacteria with an absence of correlations in CEWAF.

Chlorarachnea and Dinophyceae in the open ocean experiment were found to interact in this study as well as that by Stoecker et al., (2017). It is notable that although both organisms are present in the coastal experiment, there were no lag-time correlations between Chlorarachnea and any other organism (Figures 30, 31, 34, & 35). Within the WAF treatment in the open ocean experiment, Chlorarachnea (Euk OTU29), had a positive lag-time correlation with *Marinobacter* (Prok OTU2), and *Polycyclovorans* (Prok OTU4) (Figure 25). Additionally, *Paraphysomonas* sp (Euk OTU5), another known mixotroph, had a negative lag-time correlation with Chlorarachnea (Euk OTU29) (Figure 25). Lastly, in the CEWAF treatment there was a positive lag-time correlation between another Chlorarachnea (Euk OTU49) and *Alexandrium* sp. (OTU54) (Figure 29). The interactions with Chlorarachnea in the WAF and CEWAF are due to correlations with other prominent mixotrophs and putative hydrocarbon degraders.

There were many OTUs within each network that did not have any lag time and responded similarly to treatments rather than interacting after a certain time period, represented by dotted lines for edges (Figures 28 - 33). Moreover, there were also nodes of OTUs that did not significantly correlate with any other OTUs and are included in Tables 7-9. The phytoplankton–bacterial networks examined above provide a more detailed analysis of the interactions between key-players responding to oil spills, built upon by the NMDS plots, bar graphs, and statistical analyses of changes within major functional groups.

DISCUSSION

During the DwH oil spill, unprecedented MOS was observed on the surface ocean (Passow et al. 2012). MOS serves as a hot spot for microbes when aggregates form, and transport oil and dispersant to depths as they sink (Doyle et al. 2018). Within these aggregates microbes degrade hydrocarbons resulting in the release of low molecular weight organic matter, known as EPS, for use in the microbial loop. Therefore, determining the microbial community composition change in response to oils spills is vital to understanding and mitigating the effects of future oil spills, especially in regards to the use of dispersants. The microbial community composition change in open ocean and coastal experiments was investigated using NMDS plots, stacked bar graphs, three diversity indices with associated ANOVA statistical tests, and network analyses. These data will aid determining the key players in phytoplankton–bacterial interactions responding to oil spills in both open ocean and coastal zones of the Gulf of Mexico.

Putative hydrocarbon degraders will be referred to by their respective orders in the rest of this section for consistency, that is, Oceanospiralles (*Alcanivorax* & *Thalassiolituus*) and Thiotrichales (*Cycloclasticus*). However, it should be mentioned that not all organisms within each order are hydrocarbon degraders but lower taxonomic classifications will be discussed with network analyses in relation to prominent phytoplankton groups. Additionally, *Alcanivorax* (Prok OTU13 & OTU15), and *Thalassolituus* (Prok OTU11) accounted for a large fraction of the observed order Oceanospiralles, while the order Thiotrichales was comprised of *Methylophaga* (Prok OTU7, OTU8, OTU94, OTU96, OTU97) and *Cycloclasticus* (Prok OTU9).

HYPOTHESIS # 1

In response to oil, bacterial growth will increase rapidly and communities will shift to species that degrade branched alkanes (e.g., Alcanivorax), followed by those that degrade PAHs (e.g., Cycloclasticus), and finally n-alkane degraders (e.g., Thalassiolituus).

Although bacterial growth was not directly measured, the relative abundance in concert with dissimilarity metrics were used to determine community composition change and shift over time. The community succession generally seen in response to oil spills, *Alcanivorax* (branched alkane degrader), followed by *Cyclocasticus* (PAH degrader), and *Thalassiolituus* (n-alkane degrader) (McKew et al., 2007) was also observed in both the open ocean and coastal experiment. Dubinsky et al. (2013) noted the abundance of the heterotrophic bacteria *Methylophaga* after the DwH oil spill likely resulted from the large abundance of high molecular weight organic matter from hydrocarbon degradation by other microbes, rather than an increase in methane oxidation (Dubinsky et al., 2013). Albeit the high abundance of Thiotrichales within each experiment was due to the abundant *Methylophaga* (Prok OTU7 & OTU8) rather than the hydrocarbon degrader *Cycloclasticus* (Prok OTU9). Thiotrichales had the highest abundance in the later time-points of each treatment in both experiments, a result of the increasing availability from hydrocarbon degrading organisms and release of low-molecular weight organic matter from eukaryotes. One exploration for the network analysis in the proceeding sections includes the correlation between *Methylophaga* (Prok OTU7 & OTU8) and the dominant centric Bacillariophyceae, which release exudates (EPS) and low-molecular weight organic matter (Shniukova & Zolotareva, 2015; van Eenennaam et al., 2016). The release of phytoplankton EPS can affect the microbial community as organisms like *Methylophaga* in Thiotrichales take advantage of the organic matter from this and oil spill degradation (Dubinsky et al., 2013).

However, *Methylophaga* has previously been shown to degrade oil spill hydrocarbons in laboratory experiments and therefore may be reacting to the oiled treatments (Gutierrez & Aitken, 2014)

Besides the aforementioned hydrocarbon degraders, during the DwH oil spill, the community of hydrocarbon degraders were made up of the orders Alteromonadales, Flavobacteriales, Pseudomonadales, Cellvibrionales, and Rhodobacteriales. All of these were found in both the open ocean and coastal experiments, and Alteromonadales, Flavobacteriales, Pseudomonoadales, and Cellvibrionales all increased with increasing oil and dispersed oil (Figures 22 & 24). Throughout the experiment Alteromonadales was in relatively high abundance and was comprised of *Alteromonas* (Prok OTU1)*, Marinobacter* (Prok OTU2, OTU6, & OTU10)*, Pseudoalteromonas* (Prok OTU21)*, and Aestuariibacter* (Prok OTU40), most of which are putative hydrocarbon degraders. However, *Pseudoalteromonas* is also known to release an algicidal protease for certain diatoms (Gutierrez et al., 2013; Lee et al., 2000; Paul & Pohnert, 2011). Putative hydrocarbon degraders, Rhodobacterales, were surprisingly low in the DCEWAF and CEWAF treatments in both experiments, indicating a potential toxic affect to dispersed oil (Joye et al., 2014). However, this order is also commonly found during phytoplankton blooms and might be influenced by the phytoplankton community, which will be explored in the network analysis (Buchan et al., 2014).

Although the environment (open ocean versus coastal) was not statistically significant for the rare prokaryotes (Tables 2, 3, & 4), it was significant for the abundant prokaryotes (Inverse Simpson) highlighting the importance of functional redundancy in the microbial response in the event of an oil spill (Doyle et al., 2018). The three organisms predicted to be seen in community succession over time (*Alcanivorax, Cycloclasticus,* followed by *Thalassiolituus*), were in fact

found at low abundance throughout the duration of both experiments (Figures 22 & 24). The components of oil within the experiment were likely broken down in the first 24 hours of the experimental set-up, which was not captured in this experiment (Doyle et al., 2018). Because of this rapid break down followed by a slower hydrocarbon degradation, a shift in community composition was not seen (Doyle et al., 2018). However, the variety in prokaryotic community composition was due to the mixture of oil components seen during the DwH and that of the Macondo oil used in these experiments, in consortia with affects from abundant phytoplankton (McGenity et al., 2012). Multiple organisms are important in degradation of different components of oil in the event of an oil spill, which can result in functional redundancy of several bacterial groups. The differences in the bacterial community's response in the open ocean and coastal experiment for abundant groups could also be a result of this functional redundancy. Nevertheless, because of the consistency with results in these experiments compared to that during the DwH oil spill, these are likely representative of a potential community response during the DwH oil spill.

HYPOTHESIS # 2

Phytoplankton community composition in order of highest abundance to lowest will include diatoms, phytoflagellates, cryptomonads, cyanobacteria, and dinoflagellates in mesocosms conducted during spring/summer in coastal zones and dominated by picoplankton in the open ocean experiment.

In the coastal community, the phytoplankton abundance from lowest to highest was centric Bacillariophyceae (all four treatments), followed by Dinophyceae and Chrysophyceae (in DCEWAF & CEWAF) (Figure 16). Additionally, the abundance of cyanobacteria although not

directly comparable to the other phytoplankton groups (because detected using 16S rather than 18S), were highest in the control treatment and decreased with increasing dispersed oil.

The phytoflagellates are a diverse group of algae that retain chloroplasts but are also able to consume particulate organic matter, and are therefore mixotrophic (Stoecker et al., 2017). Included in this group are some chrysophytes, haptophytes, silicoflagellates and chlorophytes (Stoecker et al., 2017). Therefore, in order to address hypothesis #2, the phytoflagellates herein follow the definition stated in Stoecker et al. (2017) such that the cryptomonads and dinoflagellates are considered separately. In the open ocean experiment within the phytoflagellates, Chrysophyceae were the most abundant group only in the DCEWAF treatment (Figure 16). Haptophytes, silicoflagellates, and cryptomonads were not part of the top 1 % relative abundance in the bar graphs. These groups were likely not present during the experiments due to the dominance of centric Bacillariophyceae (Figure 16).

The hypothesis of phytoplankton abundance in coastal zones was proven correct in the representative abundant groups of diatoms, phytoflagellates (Chrysophyceae), and dinoflagellates. However, some predicted groups were not present and relative abundance in the order predicted. The temporal evolution and final community composition is reliant on starting community, which in this case was primarily centric Bacillariophyceae (González et al., 2009). Within the phytoflagellates, Chrysophyceae was a large constituent of the community only in the dispersed oil treatment and was comprised primarily of *Paraphysomonas* (Euk OTU21) (Figure 16). *Paraphysomonas*, is heterotrophic and able to consume other algae (especially diatoms) which were also abundant in the DCEWAF treatment (Figure 16) (González et al., 2009). The Dinophyceae group was resilient in the oil and dispersed oil treatments compared to the results from Ozhan et al. (2014). Dinophyceae is mixotrophic and able to ingest particulate organic

matter and prey (Stoecker et al., 2017). Although Dinophyceae and Chrysophyceae were not predicted to have one of the highest relative abundances of the phytoplankton, these group and centric Bacillariophyceae dominated. Centric Bacillariophyceae are commonly found to be resilient to oil spills in coastal zones and present during the same time of year (late spring/early summer) in the area of the DwH (González et al., 2009; Hu et al., 2011; Parsons et al., 2015). The Chrysophyceae group dominated in the DCEWAF treatment, but in the CEWAF Dinophyceae out-competed other mixotrophic organisms. The coastal experiment was the story of a dominant group of Centric Bacillariophyceae with mixotrophic and heterotrophic constituents (Chrysophyceae and Dinophyceae) able to ingest the dominant primary producers depending on sensitivity to dispersed oil.

In the hypothesis for the open ocean experiment, picoplankton refers to phototrophic picoeukaryotes comprised of Prasinophyceae, Chlorophyceae, Prymnesiophyceae Pelagophyceae, and Cyanobacteria (Diez et al., 2001). The open ocean community did not have a dominant phytoplankton community, unlike that of the coastal experiment. Nonetheless, the low abundance phytoplankton groups that were present included, Dinophyceae, Chrysophyceae, Chlorarachnea, Centric Bacillariophyceae, and Pennate Bacillariophyceae (Figure 17). Contrary to the hypothesis that picoeukarotes would dominate, none of the aforementioned eukaryotes (or Cyanobacteria) were present in high abundance in this experiment. This dichotomy is likely a result of the starting community, similar to the affects in the coastal experiment (González et al., 2009).

Analogous to the coastal experiment, Dinophyceae had a high abundance especially in the DCEWAF and CEWAF treatments, while Chrysophyceae was abundant in the WAF and DCEWAF treatments (Figure 17). Again, likely a result of the resiliency and mixotrophy in both

groups (Ozhan et al., 2014; Stoecker et al., 2017). The Centric Bacillariophyceae were highest in the CEWAF treatment, contributing further to the resiliency of this group to dispersed oil (González et al., 2009). These findings can be attributed to the varying response at the individual phytoplankton level and due to competition in a natural community (Bretherton et al., 2018; González et al., 2009; Stoecker et al., 2017).

Chlorarachnea are known to be mixotrophic and all lack cell coverings like that of the diatoms or dinoflagellates (Graham et al., 2016; Stoecker et al., 2017). The class Chlorarachnea was the lowest taxonomic level that could be assigned to these organisms, so mixotrophy in this abundant individual can't be confirmed. At the same time, the prevalence of both Chlorarachnea and Dinophyceae during the open ocean experiment is likely a result of competition between mixotrophs, which was explored further in the network analysis (Figure 17) (Stoecker et al., 2017). The results from the open ocean experiment, was a story of starting community and competition. Unlike the coastal experiment, the open ocean experiment also had dominance of two other groups involved in trophic interactions.

Ciliates and grazers were abundant in the open ocean experiment and are important to trophic interactions. Like that of the mixotrophic phytoplankton, the ciliates and grazers feeding habitats might increase their resiliency to dispersed oil treatments. Bicoecea, Oligohymenophorea, and Granofilosea were the highest abundance of eukaryotes seen in the open ocean experiment (Figure 15). Bicoecea are phagotrophic flagellates and have a typically protozoan diet, and can be resilient at higher salinities but are sensitive to disturbances (Cavalier-Smith & Chao, 2006; Filker et al., 2017; Zhang et al., 2017). Within the Bicoeceae, the most abundant organisms were *Pseudobodo sp.* (Euk OTU4, OTU23, OTU34, OTU51, OTU96), *Bicosoeca sp*. (Euk OTU92), and *Cafeteria roenbergensis* (Euk OTU21, and OTU422). Of

these, *Pseudobodo* is known to be prevalent in oil polluted systems, and *Cafeteria roenbergensis* has previously been shown to do well in oil-only treatments (no dispersed oil) (Dalby et al., 2008; Gertler et al., 2010). Additionally, Dinoflagellates are known to feed on *Cafeteria roenbergensis*, which in turn feeds on heterotrophic bacteria and has the potential to release nutrients for microalgal communities from these bacteria (Plötner et al., 2014). These results are consistent with those seen in the open ocean experiment, with the highest abundance of Bicoeceae in the control and WAF treatments (Figure 15). Bicoecea is also affected by salinity and was not present in the coastal experiment due to salinity differences compared to the open ocean (Figures 19 & 20) (Filker et al., 2017; Zhang et al., 2017). The highest abundance of Oligohymenophorea was in the dispersed oil treatments (Figure 15). Organisms within Oligohymenophorea included *Uronema marinium* (Euk OTU6), *Miamiensis* sp. (Euk OTU11), *Metanophyrs sinensis* (OTU71), *Pseudocohnilembus persalinus* (Euk OTU93) all ciliate filter feeders (Verni & Gualtieri, 1997). Of these *Uronema marinium* is found in oil polluted waters, whereas *Pseudocohnilembus persalinus* is found in sewage sludge but both were found in oiled treatments in Gertler et al. (2010). Furthermore, *Uronema marinium* is grazed on by dinoflagellates, and is a very efficient bacteriovore (Bacosa et al., 2015; Sherr et al., 1988). Granofilosea only in high abundance in the DCEWAF and CEWAF treatments was comprised entirely of *Massisteria marina* Larsen & Patterson 1990, generally associated with sediment but known to colonize detrital aggregates in response to stressors (Patterson et al., 1990). This organism can therefore take advantage of aggregates containing detritus that formed in the dispersed oil treatment. The high abundance of these three heterotrophic grazers and ciliates was a response to prominent communities (both prokaryotic and eukaryotic), as well as a response to treatment.

Fungi can also correlate with nutrient availability and organic matter, similar to phytoplankton and heterotrophic microbes (Orsi et al., 2013; Tisthammer et al., 2016). These two classes steadily decreased in the control and WAF treatments, while they increased in the CEWAF (Figure 15). The fungal community is impacted by the abundance of phytoplankton and peak in biomass after a phytoplankton peak (Gutiérrez et al., 2011). Fungi can also correlate with nutrient availability and organic matter, similar to phytoplankton and heterotrophic microbes (Orsi et al., 2013; Tisthammer et al., 2016). Although Eurotiomycetes and Microbotryomycetes were abundant in all four treatments, by the last time-point their relative abundance dropped to zero (Figure 15). There were fewer abundant classes in the DCEWAF and CEWAF treatments after the fungi abundance decreased (Figure 15). Moreover, the fungi initially increased in the CEWAF treatment indicating these communities were likely not sensitive to dispersed oil (Figure 15). Eurotiomycetes is known to be tolerant to polycyclic aromatic hydrocarbons (PAHs) and a potential hydrocarbon degrader (Aranda, 2016; de Menezes et al., 2012; Zafra et al., 2014). However, less is known about Microbotryomycetes in relation to oil spills and hydrocarbon degradation, but one study by Ferrari et al (2011) linked increasing diesel fuel concentrations with increasing abundance of Microbotryomycetes (Ferrari et al., 2011). The high abundance of these organisms in these dispersed oil treatments could be the result of higher tolerance to oil spills as well as an increase in decaying organic matter, similar to the response of the aforementioned Granofilosea (Figure 15).

The hypothesis for both coastal and open ocean communities was not proven correct, as the highest abundance in each ecosystem was dependent on starting community and prevalent prokaryotic community members. The phytoplankton communities were dominated by diatoms and mixotrophic communities of dinoflagellates, Chrysophytes, and Chlororachnea.

Additionally, the open ocean experiment resulted in a dominance of grazers and fungi that resulted from trophic interactions with bacteria, phytoplankton, and detritus. These results were seen in the three diversity indices that suggested environment, treatment, and time-point have an effect on diversity. All three factors also affect the aforementioned trophic interactions between eukaryotes and prokaryotes. These trophic interactions have implications in the result of an oil spill, as organisms known to release exudates and EPS (diatoms) dominate. Detritus, oil, and dispersed oil accumulate in aggregates that can then be degraded by certain heterotrophic grazers and bacteria. Organisms that take advantage of these organic matter sources are able to out-compete those that can't and transfer organic matter up the food chain.

HYPOTHESIS # 3

Changes in phytoplankton communities will be paralleled by those in bacterial communities and driven heavily by treatment; any divergences in this trend will be driven by the water masses (open ocean versus coastal) in phytoplankton communities and treatment in bacterial communities.

The OTU abundance data from each experiment and treatment were used for several network analyses to investigate correlations between the highest abundance phytoplankton and bacteria. To answer the hypothesis stated above and further detail trends seen in previous sections, several organisms from each network were emphasized including 1) *Methylophaga* (Prok OTU7 & OTU8) 2) *Pseudoalteromonas* (Prok OTU21) 3) *Paraphysomonas* (Euk OTU5) and 4) *Chlorarachnea* (Euk OTU29 & OTU49).

Methylophaga (Prok OTU7 & OTU8) was found in both experiments and during the DwH oil spill, a response to availability of low molecular weight organic matter presumably

from hydrocarbon degrading organisms or organic matter released by abundant organisms (Dubinsky et al., 2013). Although *Methylophaga* were suspected to be positively affected by increasing diatom abundance (and other phytoplankton) these patterns were not evident within the networks. For instance, in the coastal control, *Lepidodinium* sp. (Euk OTU80) had a negative lag-time correlation with *Methylophaga* (Prok OTU8), but in WAF had a positive lag-time correlation (Figure 26 & Figure 27). Moreover, *Chaetoceros* sp. (OTUs 49 & 38) generally had a positive lag-time correlation with *Methylophaga* (Prok OTU7 & OTU8) in the DCEWAF and CEWAF treatments but in some cases (Euk OTU8) negatively impacted *Methylophaga* (Prok OTU7 & OTU8) (Figure 30 & Figure 31). In addition to *Chaetoceros* spp., Bacillariophyceae was also commonly involved in lag-time correlations, however there was no consensus between centric, or pennate reactions. This discrepancy could be a result of the potential for hydrocarbon degredation in Methylophaga, adding another component to the associations between organisms (Gutierrez & Aitken, 2014) In the open ocean environment there were fewer phytoplankton interactions (likely due to lower relative abundance), but centric Bacillariophyceae (Euk OTU3) had a positive lag-time correlation in the control (Figure 24).

This correlation highlights the ability of *Methylophaga* (Prok OTU3) to take advantage of the EPS released by centric Bacillariophyceae (Euk OTU3). While, Dinophyceae (Euk OTU28) had a negative lag-time correlation, potentially grazing on the abundant *Methylophaga* (Prok OTU7) (Figure 25). Notably, there were no correlations with *Methylophaga* (Prok OTU7 or OTU8) in either the CEWAF or DCEWAF treatments but this is likely due to lower overall phytoplankton relative abundance in the open ocean environment (Figure 28 & Figure 29). Most interactions with *Methylophaga* (OTU7 & OTU8) and bacteria involve hydrocarbon degraders, especially in the oil and dispersed oil treatments. Of these lag-time correlations, negative

influences on *Methylophaga* (Prok OTU7 or OTU8) might be due to competition in oil or dispersed oil treatments. Positive lag-time correlations might be a result of the release of low-molecular weight organic matter during hydrocarbon degradation (Dubinsky et al., 2013). However, the only way to determine the differences between these two bacterial interactions are laboratory experimentation as these results are inconsistent in the networks presented. Furthermore, these results accentuate the need for detailed laboratory studies to elucidate relationships between these microorganisms and organic matter cycling in the marine environment.

The prokaryote, *Pseudoalteromonas* (Prok OTU21) was also suspected of influencing the phytoplankton community in these experiments, as this organism has been shown to produce an algicidal protease (Lee et al., 2000). Correlations between *Pseudoalteromonas* (Prok OTU21) and phytoplankton were more common in the coastal environment compared to the open ocean environment, due to the higher relative abundance of phytoplankton. However, *Pseudoalteromonas* (Prok OTU21) was not found to have any negative lag-time correlations with diatoms or other phytoplankton groups. In fact, the only negative lag-time correlations between *Pseudoalteromonas* (Prok OTU21) were with other bacteria, namely *Vibrio* (Prok OTU33), *Plantomyces* (Prok OTU78), *Rhodobacteraceae* (Prok OTU44), *Halobacteriocorax* (Prok OTU38), and the Flavobacterium *Tenacibaculum* (Prok OTU32) (Figures 28 - 35). This is potentially a story of competition in response to oil spills, although it is possible that the negative correlations do not represent causation. Within the coastal experiment centric Bacillariophyceae (Euk OTU2 & OTU3), *Chaetoceros muelerii* (OTU49), and *Chaetoceros* sp. (OTU38) had a positive correlation with *Pseudoalteromonas* (Prok OTU21) across treatments (Figures 30, 31, 34, & 35). Although *Pseudalteromonas* is known to release an algicidal protease, this is

dependent on environmental parameters and algal abundance (Lee et al., 2000). Pseudoalteromonas could also be responding to increased organic matter from the abundant centric Bacillariophyceae. Therefore, the added stressor of an oil spill may reinforce positive interactions between diatoms and *Pseudoalteromonas,* rather than antagonistic. Furthermore, there were consistent relationships between the two environments. For example, *Alcanivorax* (Prok OTU13) and *Alteromonas* (Prok OTU1) have a positive lag-time correlation with *Pseudoalteromonas* (Prok OTU21) seen in the coastal DCEWAF as well as the open ocean control and WAF treatments (Figures 28, 29, & 34). Another consistent interaction seen in the open ocean WAF treatment and coastal DCEWAF *Pseudoalteromonas* (Prok OTU21) was the positive lag-time correlation with *Candidatus actinobacter* (Prok OTU28) (Figures 29 & 34). Although these correlations were found in both environments there are not similarities between unoiled, oiled, or dispersed oil treatments. The community response by phytoplankton to *Pseudoalteromonas* (Prok OTU21) was generally positive, contrary to the suggested negative response based on the release of algicidal proteases (Lee et al., 2000). Consistencies in correlations between environment rather than treatment suggest that the aforementioned hypothesis might not be correct. Interactions between phytoplankton and bacteria are reinforced by treatment but are present across environments.

In addition to the bacteria *Methylophaga* and *Pseudoalteromonas*, the heterotrophic Chrysophyceae, *Paraphymonas* (Euk OTU5 & OTU35) were also thought to affect many of the interactions between other phytoplankton groups. Overall, there were more lag-time correlations driven by *Paraphysomonas* (Euk OTU5 & OTU35) rather than impacting the group of interest (as seen in previous sections) (Figures 28 – 35). Notably, there were no lag-time correlations in the CEWAF treatment in both the open ocean and coastal environment (Figures 33 & 35).

Additionally, the only lag-time correlations between *Paraphysomonas* (Euk OTU5 & OTU35) were with other putative hydrocarbon degraders (Figures 32 & 34). All of the lag-time correlations with phytoplankton in the open ocean experiment are negative, suggesting grazing by *Paraphysomonas* (Euk OTU5) (Figures 28 & 29). However, in the coastal environment where phytoplankton groups dominated *Paraphysomonas* (Euk OTU5) had a positive lag-time correlation with *Odontella* Synensis (Euk OTU60), *Minutocellus* sp. (Euk OTU17), and *Alexandrium* sp. (Euk OTU54) (Figure 26 & Figure 27). Potentially the release of nutrients as Paraphysomonas preys on smaller phytoplankton and bacteria results in an increase in these larger phytoplankton groups (Plötner et al., 2014). However, this assumption would need to be tested in a laboratory setting similar to the presumptions from the *Methylophaga* networks. Contrastingly, the *Paraphysomonas* correlations were consistent within environment and were affected by treatment. Therefore, the hypothesis was again disproven as environment and treatment played a role in the interaction between *Paraphymonas* and other prevalent phytoplankton and bacteria.

One last comparison between mixotrophs investigated the correlation between Chlorarachnea and Dinophyceae as both were abundant in the open ocean oil and dispersed oil treatments. As suspected, the only significant lag-time correlations with Chlorarachnea (Euk OTU29 & OTU49) were found in the WAF and CEWAF treatments in the open ocean experiments (Figure 25 & Figure 29). *Paraphysomonas* (Euk OTU5) had a negative lag-time correlation with Chlorarachnea (Euk OTU29), Dinophyceae (Euk OTU28), and *Scripsiella* sp. (Euk OTU20) (Figure 25). Although competition between the two groups was suspected this correlation suggests competitive exclusion by another mixotroph (*Paraphysomonas* OTU5) (Stoecker et al., 2017). Additionally, in the open ocean CEWAF treatment Chlorarachnea (Euk

OTU49) had a positive lag-time correlation with *Alexandrium* sp. (Euk OTU54) (Figure 29). This interaction reinforces the results from the WAF treatment, and instead of competing the Chlorarachneae and *Dinophyceae* respond similarly to treatments and other competitors.

Finally, throughout all of the microbial networks there appears to be more connections between communities in CEWAF treatments. This might be the result of tighter interactions between organisms as each is trying to survive rather than actively seeking to exclude other groups (like releasing algicidal proteases). Although a large claim, the aforementioned results in the *Methylophaga* (Prok OTU7 & OTU8), *Pseudoalteromonas* (Prok OTU21), *Paraphysomonas* (Euk OTU5), and Chlorarachnea (Euk OTU29 & OTU49) support this. Furthermore, the interactions between phytoplankton and bacteria in the open ocean environment are less complex, with less significant correlations overall (Figures 28, 29, 32, & 33). The open ocean experiment was also dominated by grazers and fungi which should be considered in experiments such as this and might be impacting the lack of complexity in the open ocean networks. Moreover, the Bacillariophyceae (centric/pennate) and Dinophyceae are commonly found as nodes that connect large networks (Figure 24- Figure 29). These communities are more resilient to oil and dispersed oil, and are also known to release EPS (González et al., 2009; Ozhan et al., 2014). Dispersed oil treatments also have a high abundance of oil droplets within the water column allowing microbial recruitment and degradation tied to microbial EPS production (Doyle et al., 2018). Although the viral community was not sampled, viral lysis is likely to have a strong effect on microbial composition and EPS release/production (Fenchel, 2008; Jiao et al., 2010). Moreover, EPS release/production and community composition can be impacted by predators present during the experiments but was not sampled during the two experiments. The

EPS released by microbial communities can play an important role in the microbial loop and carbon cycling (Fenchel, 2008; Jiao et al., 2010).

CONCLUSION

During an oil spill, prokaryotes that are able to take advantage of the mixture of oil components, or the low molecular weight organic matter from both degradation and EPS are favored. Key players among the prokaryotes include dominant hydrocarbon degraders in the classes Alpha- and Gammaproteobacteria, especially *Methylophaga*, and *Pseudoalteromonas*. Key players of the phytoplankton community that are resilient to oil spills (Dinophyceae, Bacillariophyceae, *Paraphysomonas*, and Chlorarachnea) are more likely to dominate the community in coastal areas. However, in an open ocean environment, additional key players become important (Fungi, and grazers). The more resilient phytoplankton like Dinophyceae and Bacillariophyceae release EPS in response to stressors like that of an oil spill. These communities are also some of the most interconnected nodes in the dispersed oil networks suggesting EPS release could result in more interactions between both phytoplankton–associated and water column microbes. Moreover, food web interactions were important in microbial interactions as heterotrophic and mixotrophic eukaryotes able to obtain food from multiple sources dominated dispersed oil treatments. During an oil spill the interactions between microbial communities are affected depending on dominant groups and environment. These dominant microbial communities can release EPS that forms aggregates, especially in the event of an oil spill. This has implications for large scale carbon cycling as organic matter is cycled through the microbial loop dependent on starting community, and environment. During the 2010 DwH oil spill MOS (oil aggregates) formed, allowing the transport of microbes, hydrocarbons, and dispersant through the water column. These interactions at the surface can impact carbon cycling to depth and help degrade otherwise harmful oil and dispersant before it reaches the deep ocean. Although the interaction between phytoplankton and bacteria was investigated in these

experiments, further laboratory analysis including fungi, grazers, and viruses should be conducted for a complete picture of carbon cycling in the event of an oil spill.

REFERENCES

Acuna Alverez, L., Exton, D.A., Timmis, K.N., Suggett, D.J., McGenity, T.J. Characterization of marine isoprene-degrading communities. *Environ Microbiol*. 2009. 11:3280-32291.

Alldredge, A. L., Silver, M. W. Characteristics, Dynamics and Significance of Marine Snow. *Prog. Oceanog.* 1988. 20: 41–82.

Amaral-Zettler, L. A., McCliment, E. A., Ducklow, H. W., Huse, S. M. A method for studying protistan diversity using massively parallel sequencing of V9 hypervariable regions of small-subunit ribosomal RNA Genes. *PLoS ONE*. 2009. 4(7): 1–9.

Amin, S. A., Parker, M. S., Armbrust, E. V. Interactions between Diatoms and Bacteria. *Microbiology and Molecular Biology Reviews*. 2012. 76(3): 667–684.

Amin, S. A., Green, D. H., Hart, M. C., Küpper, F. C., Sunda, W. G., Carrano, C. J. Photolysis of iron, siderophore chelates promotes bacterial, algal mutualism. *Proceedings of the National Academy of Sciences.* 2009. 106(40): 17071–17076.

Apprill A, McNally S, Parsons R, Weber L. Minor revision to V4 region SSU rRNA 806R gene primer greatly increases detection of SAR11 bacterioplankton. *Aquat Microb Ecol.* 2015. 75:129-137.

Aranda, E. Promising approaches towards biotransformation of polycyclic aromatic hydrocarbons with Ascomycota fungi. *Current Opinion in Biotechnology*. 2016. *38*, 1–8. Arumugam, M., Raes, J., Pelletier, E., Le Paslier, D., Yamada, T., Mende, D. R. Fernandes, G. R., Tap, J. Bruls, T., Batto, J.M., Bertalan, M., Borruel, N., Casellas, F., Fernandez, L., Gautier, L., Hansen, T., Hattori, M., Hayashi, T., Kleerebezem, M., Kurokawa, K., Leclerc, M., Levenez, F., Manichanh, C., Nielsen, H.B., Nielsen, T., Pons, N., Poulain, J., Qin, J., Sicheritz-Ponten, T., Tims, S., Torrents, D., Ugarte, E., Zoetendal, E.G. Wang, J., Guarner, F., Pedersen, O., De Vos, W.M., Brunak, S., Doré, J., Weissenbach, J., Ehrlich, S.D., Bork, P. Enterotypes of the human gut microbiome. *Nature*. 2011. *473*(7346), 174–180.

Atlas, R. M., & Hazen, T. C. Oil Biodegradation and Bioremediation : A Tale of the Two Worst Spills in U . S . History. *Environmental Science & Technology.* 2011. 45: 6709–6715.

Azam, F., Fenchel, T., Field, J., Gray, J., Meyer-Reil, L., Thingstad, F. The Ecological Role of Water-Column Microbes in the Sea. *Marine Ecology Progress Series.* 1983. 10: 257–263.

Bacosa, H. P., Liu, Z., & Erdner, D. L. (2015). Natural sunlight shapes crude oil-degrading bacterial communities in northern Gulf of Mexico surface waters. *Frontiers in Microbiology*. 2015.

Bradley, I. M., Pinto, A. J., Guest, J. S. Design and evaluation of illumina MiSeq-compatible, 18S rRNA gene-specific primers for improved characterization of mixed phototrophic communities. *Applied and Environmental Microbiology.* 2016. 82(19): 5878–5891.

Bretherton, L., Williams, A., Genzer, J., Hillhouse, J., Kamalanathan, M., Finkel, Z., & Quigg, A. Physiological response of 10 phytoplankton species exposed to macondo oil and corexit. *Journal of Phycology*. 2018. *1*(506), 0–2.

Brussaard, C. P. D., Peperzak, L., Beggah, S., Wick, L. Y., Wuerz, B., Weber, Arey J.S., van der Burg, B., Jonas, A., Huisman, J., van der Meer, J. R. Immediate ecotoxicological effects of short-lived oil spills on marine biota. *Nature Communications*. 2016. 7: 11206.

Buchan, A., LeCleir, G. R., Gulvik, C. A., & Gonzalez, J. M. Master recyclers: features and functions of bacteria associated with phytoplankton blooms. *Nature Reviews Microbiology*. 2014. *12*(10).

Caporaso, J.G., Lauber, C.L., Walters, W.A., Berg-Lyons, D., Huntley, J., Fierer, N., Owens, S.M., Betley, J., Fraser, L., Bauer, M., Gormley, N., Gilbert, J.A., Smith, G., Knight, R. Ultra-high-throughput microbial community analysis on the Illumina HiSeq and MiSeq platforms. *ISME*. 2012. 6: 1621-1624.

Castro-Nallar, E., Bendall, M. L., Pérez-Losada, M., Sabuncyan, S., Severance, E. G., Dickerson, F. B., Schroeder J.R., Yolken R.H., Crandall, K. A. Composition, taxonomy and functional diversity of the oropharynx microbiome in individuals with schizophrenia and controls. *PeerJ*. 2014. 3: e1140.

Cavalier-Smith, T., & Chao, E. E. Y. Phylogeny and megasystematics of phagotrophic heterokonts (kingdom Chromista). *Journal of Molecular Evolution*. 2006. *62*(4): 388–420.

Clarke, K. R., Place, P., Hoe, W., & Kingdom, U. Non-parametric multivariate analyses of changes in community structure. *Australian Journal of Ecology*. 1993. 18:117–143.

Cole, J.J. Interactions between bacteria and algae in aquatic ecosystems. *Ann Rev. Ecol. Syst*. 1982. 13:291-314.

Cram, J. A., Xia, L. C., Needham, D. M., Sachdeva, R., Sun, F., & Fuhrman, J. A. Cross-depth analysis of marine bacterial networks suggests downward propagation of temporal changes. *ISME Journal*. 2015. 9 (12): 2573–2586.

Croft, M. T., Lawrence, A. D., Raux-Deery, E., Warren, M. J., & Smith, A. G. Algae acquire vitamin B12 through a symbiotic relationship with bacteria. *Nature*. 2005. *438*(7064): 90–93.

Crone, T. J., & Tolstoy, M. Magnitude of the 2010 Gulf of Mexico Oil Leak. *Science*. 2010. 330 (6004): 634–634.

Dalby, A. P., Kormas, K. A., Christaki, U., & Karayanni, H. Cosmopolitan heterotrophic microeukaryotes are active bacterial grazers in experimental oil-polluted systems. *Environmental Microbiology*. 2008. 10(1): 47–56.

Daly, K. L., Passow, U., Chanton, J., Hollander, D. Assessing the impacts of oil-associated marine snow formation and sedimentation during and after the Deepwater Horizon oil spill. *Anthropocene.* 2016. 13: 18–33.

Danger, M., Daufresne, T., & Pissard, S. Does Liebig's law of the minimum scale up from species to communities? *Oikos.* 2008. 117:1741–1751.

Deasi, S.R., Verlecar, X.N., Ansari, Z.A., Jagtap, T.G., Sarkar, A., Vashistha, D., Dalal, S.G. Evaluation of genotoxic response of Chaeotoceros tenuissimus and Skeletonema costatum to water accommodated fraction of petroleum hydrocarbons as biomarker of exposure. *Water Research*. 2010. 44:2235-2244.

de Menezes, A., Clipson, N., & Doyle, E. Comparative metatranscriptomics reveals widespread community responses during phenanthrene degradation in soil. *Environmental Microbiology*. 2012. 14(9): 2577–2588.

de Vargas, C., Audic, S., Henry, N., Decelle, J., Mahe, F., Logares, R., Enrique, L., Berney, C., Bescot, N.L., Probert I., Carmichael, M., Poulain, J., Romac, S., Colin, S., Aury, J., Bittner, L., Chaffron, S., Duntrhorn, M., Engelen, S., Flegontova, O., Guidi, L., Horak, A., Jaillon, O., Lima-Mendez, G., Lukes, J., Malviya, S., Morard, R., Mulot, M., Scalco, E., Siano R., Vincent, F., Zingone, A., Dimier, C., Picheral, M., Searson, S., Kandels-Lewis, S., Acinas., S.G., Bork, P., Bowler, C., Gorsky, G., Grimsley, N., Hingamp, P., Iudicone, D., Not, F., Ogata, H., Pesant, S., Raes, J., Sieracki, M.E., Speich, S., Stemmann, L., Sunagawa, S., Weissenbach, J., Wincker, P., Karsenti, E. Eukaryotic plankton diversity in the sunlit ocean. Sc*ience.* 2015. 348(6237): 1261605–1261605.

Doyle, S.M., E.A. Whitaker, V. De Pascuale, T.L. Wade, A.H. Knap, P.H. Santschi, A. Quigg, and J.B. Sylvan. in review. Corexit 9500® Enhances Formation of Microbe-Oil Micro-aggregates in Coastal Surface Water.

Dubinsky, E. A., Conrad, M. E., Chakraborty, R., Bill, M., Borglin, S. E., Hollibaugh, J. T., Mason, O.U., Piceno, Y.M., Reid, F.C., Stringfellow, W.T., Tom, L.M., Hazen, T.C., Andersen, G. L. Succession of hydrocarbon-degrading bacteria in the aftermath of the deepwater horizon oil spill in the gulf of Mexico. *Environmental Science and Technology*. 2013. 47(19), 10860–10867.

Edvardsen, B., Egge, E.S. & Vaulot, D. Diversity and distribution of haptophytes revealed by environmental sequencing and metabarcoding – a review. *Perspect. Phycol.* in press.

Falkowski, P. G., Barber, R.T., Smetacek, V. 1998. Biogeochemical Controls and Feedbacks on Ocean Primary Production. *Science*. 2016. 281(5374): 200–206.

Fenchel, T. 2008. The microbial loop - 25 years later. *Journal of Experimental Marine Biology and Ecology*. 366(1–2): 99–103.

Ferrari, B. C., Zhang, C., & van Dorst, J. Recovering greater fungal diversity from pristine and diesel fuel contaminated sub-antarctic soil through cultivation using both a high and a low nutrient media approach. *Frontiers in Microbiology*. 2011. 1–14.

Field, C. B., Behrenfeld, M.J., Randerson, J.T., Falkowski, P. Primary Production of the Biosphere: Integrating Terrestrial and Oceanic Components. *Science.* 1998. 281(5374): 237–240.

Filker, S., Forster, D., Weinisch, L., Mora-Ruiz, M., González, B., Farías, M. E., Rosselio-Moira, Stoeck, T. Transition boundaries for protistan species turnover in hypersaline waters of different biogeographic regions. *Environmental Microbiology*. 2017. *19*(8): 3186–3200.

Foster, R. A., Kuypers, M. M. M., Vagner, T., Paerl, R. W., Musat, N., Zehr, J. P. Nitrogen fixation and transfer in open ocean diatom–cyanobacterial symbioses. *The ISME Journal.* 2011. 5(9): 1484–1493.

Fuhrman, J. A., & Azam, F. Bacterio Plankton Secondary Production Estimates for Coastal Waters of British-Columbia Canada Antarctica and California USA. *Applied and Environmental Microbiology*. 1980. 39(6): 1085–1095.

Fuhrman, J. A., & Steele, J. A. Community structure of marine bacterioplankton: patterns, networks, and relationships to function. *Aquatic Microbial Ecology*. 2008. 53(1): 69–81.

Gärdes, A., Iversen, M. H., Grossart, H.P., Passow, U., Ullrich, M. S. Diatom-associated bacteria are required for aggregation of Thalassiosira weissflogii. *The ISME Journal*. 2011. 5(3): 436–445.

Garr, A. L., Laramore, S., Krebs, W. Toxic effects of oil and dispersant on marine microalgae. *Bulletin of Environmental Contamination and Toxicology.* 2014. 93(6): 654–659.

Gertler, C., Näther, D. J., Gerdts, G., Malpass, M. C., & Golyshin, P. N. A mesocosm study of the changes in marine flagellate and ciliate communities in a crude oil bioremediation trial. *Microbial Ecology*. 2010. 60(1): 180–191.

González, J., Figueiras, F. G., Aranguren-Gassis, M., Crespo, B. G., Fernández, E., Morán, X. A. G., Nieto-Cid, M. Effect of a simulated oil spill on natural assemblages of marine phytoplankton enclosed in microcosms. Estuarine, Coastal and Shelf Science. 2009. 83(3): 265–276.

Guidi, L., Chaffron, S., Bittner, L., Eveillard, D., Larhlimi, A., Roux, S., Darzi, Y., Audic, S., Berline, L., Brum, J.R., Coelho, L.P., Espinoza, J.C., Malviya, S., Sunagawa, S., Dimier, C., Kandels-Lewis, S., Picheral, M., Poulain, J., Searson, S., Stemmann, L., Not, F, Hingamp, P., SPeich, S., Follows, M., Karp-Boss, L., Boss, E., Ogata, H., Pesant, S., Weissenbach, J., Wincker, P., Acinas, S.G., Bork, P., de Vargas C, ludicone, D, Sullivan, M.B., Raes, J., Karsenti, E., Bowler, C., Gorskey, G. Plankton networks driving carbon export in the oligotrophic ocean. *Nature.* 2016. 532(7600): 465–470.

Laure Guillou, Dipankar Bachar, Stéphane Audic, David Bass, Cédric Berney, Lucie Bittner, Christophe Boutte, Gaétan Burgaud, Colomban de Vargas, Johan Decelle, Javier del Campo, John R. Dolan, Micah Dunthorn, Bente Edvardsen, Maria Holzmann, Wiebe H.C.F. Kooistra, Enrique Lara, Noan Le Bescot, Ramiro Logares, Frédéric Mahé, Ramon Massana, Marina Montresor, Raphael Morard, Fabrice Not, Jan Pawlowski, Ian Probert, Anne-Laure Sauvadet, Raffaele Siano, Thorsten Stoeck, Daniel Vaulot, Pascal Zimmermann, Richard Christen; The Protist Ribosomal Reference database (PR^2): a catalog of unicellular eukaryote Small Sub-Unit rRNA sequences with curated taxonomy. *Nucleic Acids Research.* 2013. 41(D1): D597–604.

Gutiérrez, M. H., Pantoja, S., Tejos, E., & Quiñones, R. A. The role of fungi in processing marine organic matter in the upwelling ecosystem off Chile. *Marine Biology*. 2011. 158(1): 205–219.

Gutierrez, T., & Aitken, M. D. Role of methylotrophs in the degradation of hydrocarbons during the Deepwater Horizon oil spill. *ISME Journal*. 2014. 8(12): 2543–2545.

Gutierrez, T., Berry, D., Yang, T., Mishamandani, S., McKay, L., Teske, A., & Aitken, M. D. Role of Bacterial Exopolysaccharides (EPS) in the Fate of the Oil Released during the Deepwater Horizon Oil Spill. *PLoS ONE*. 2013. 8(6): 1–18.

Graham, Graham, Wilcox, Cook. 2016. Algae (3rd ed). Upper Saddle River, NJ. LJLM Press.

Harrison, P. J., Cochlan, W. P., Acreman, J. C., Parsons, T. R., Thompson, P. A., Dovey, H. M. The Effects of Crude-Oil and Corexit 9527 on Marine-Phytoplankton in an Experimental Enclosure. *Marine Environmental Research.* 1986. 18(2): 93–109.

Hibbing, M. E., Fuqua, C., Parsek, M. R., & Peterson, S. B. Bacterial competition: Surviving and thriving in the microbial jungle. *Nature Reviews Microbiology*. 2010. 8(1): 15–25.

Hill, T. C. J., Walsh, K. A., Harris, J. A., Moffet, B.F. Using ecological diversity measures with bacterial communities. *FEMS Microbiology Ecology*. 2003. 43:1–11.

Hook, S. E., & Osborn, H. L. Comparison of toxicity and transcriptomic profiles in a diatom exposed to oil, dispersants, dispersed oil. *Aquatic Toxicology*. 2012. 124–125: 139–151.

Hu, C., Weisberg, R. H., Liu, Y., Zheng, L., Daly, K. L., English, D. C., Zhao, J., Vargo, G. A. Did the northeastern Gulf of Mexico become greener after the Deepwater Horizon oil spill? *Geophysical Research Letters*. 2011. 38: L09601.

Hughes, J. B., Hellmann, J. J., Ricketts, T. H., Bohannan, B. J. M. Counting the Uncountable : Statistical Approaches to Estimating Microbial Diversity MINIREVIEW Counting the Uncountable : Statistical Approaches to Estimating Microbial Diversity. *Applied and Environmental Microbiology*. 2001. 10(1): 4399–4406.

Hutchinson, G. E. The Paradox of the Plankton. *The American Naturalist*. 1961. 95(882), 137–145.

Jiao, N., Herndl, G. J., Hansell, D. A., Benner, R., Kattner, G., Wilhelm, S. W., Kirchman, D.L., Weinbauer, M.G., Luo, T., Chen, F., Azam, F. Microbial production of recalcitrant dissolved organic matter: long-term carbon storage in the global ocean. *Nature Reviews Microbiology*. 2010. 8(8): 593–599.

Jiao, N., Robinson, C., Azam, F., Thomas, H., Baltar, F., Dang, H., Hardman-Mountford, N.J., Johnson, M., Kirchman, D.L., Koch, B.P., Legendre, L., Li, C., Liu, J., Luo, T., Luo, Y.W., Mitra, A., Romanou, A., Tang, K., Wang, X., Zhang, C., Zhang, R. Mechanisms of microbial carbon sequestration in the ocean future research directions. *Biogeosciences.* 2014. 11(19): 5285–5306.

Joye, S. B., Andreas, P., Kostka, J. E. Microbial Dynamics Following the Macondo Oil Well Blowout across Gulf of Mexico Environments. *BioScience.* 2014. 64(9): 766–777.

Koren, O., Knights, D., Gonzalez, A., Waldron, L., Segata, N., Knight, R., Huttenhower, C., Ley, R. E. A Guide to Enterotypes across the Human Body: Meta-Analysis of Microbial Community Structures in Human Microbiome Datasets. *PLoS Computational Biology*. 2013. 9(1).

Kozich, J. J., Westcott, S. L., Baxter, N. T., Highlander, S. K., Schloss, P. D. Development of a dual-index sequencing strategy and curation pipeline for analyzing amplicon sequence data on the miseq illumina sequencing platform. *Applied and Environmental Microbiology*. 2013. 79(17): 5112–5120.

Lau, W. W. Y., Keil, R. G., Armbrust, E. V. Succession and diel transcriptional response of the glycolate-utilizing component of the bacterial community during a spring phytoplankton bloom. *Applied and Environmental Microbiology.* 20007. 73(8): 2440–2450.

Lee, S., Kato, J., Takiguchi, N., Kuroda, A., & Ikeda, T. Involvement of an Extracellular Protease in Algicidal Activity of the Marine Bacterium Involvement of an Extracellular Protease in Algicidal Activity of the Marine Bacterium Pseudoalteromonas sp . Strain A28. *Applied and Environmental Microbiology*. 2010. 66(10): 4334.

Lee. Photo-oxidation and Photo-toxicity of Crude and Refined Oils. *Spill Science & Technology Bulletin*. 2003. 8(2): 157-162.

Lessard, R. R., & Demarco, G. The Significance of Oil Spill Dispersants. *Science*. 2000. 6(1): 59–68.

Lim, E. L., Dennett, M. R., & Caron, D. A. (1999). The ecology of Paraphysomonas imperforate based on studies employing oligonucleotide probe identification in costal water samples and enrichment cultures. *Limnol Oceanogr*, *44*(1), 37–51.

Martin, J. H., & Fitzwater S.E. Iron Deficiency Limits Phytoplankton Growth in the North-East Pacific Subarctic. *Nature.* 1988. 331: 341–343.

Martin-Platero, A. M., Cleary, B., Kauffman, K., Preheim, S. P., McGillicuddy, D. J., Alm, E. J., Polz, M. F. High resolution time series reveals cohesive but short-lived communities in coastal plankton. *Nature Communications*. 2018. 9(1), 1–11.

McGenity, T. J., Folwell, B. D., McKew, B. A., Sanni, G. O. Marine crude-oil biodegradation: a central role for interspecies interactions. *Aquatic Biosystems*. 2012. 8(1): 10.

McKew, B.A., Coulon, F., Osborn, A.M., Timmis, K.N., McGenity, T.J. Determining the identity and roles of oil-metabolizing marine bacteria from the Thames estuary, UK. *Environ Microbiol.* 2007. 9:165-176.

McNutt, M. K., Camilli, R., Crone, T. J., Guthrie, G. D., Hsieh, P. A., Ryerson, T. B., Savas, O., Shaffer, F. Review of flow rate estimates of the Deepwater Horizon oil spill. *Proceedings of the National Academy of Sciences*. 2012. 109(50): 20260–20267.

Moore, C. M., Mills, M. M., Arrigo, K. R., Berman-Frank, I., Bopp, L., Boyd, P. W., Galbraith, E.D., Geider, R.J., Guieu, C., Jaccard, S.L., Jickells, T.D., La Roche, J., Lenton, T.M., Mahowald, N.M., Maranon, E., Marinov, I., Moore, J.K., Nakatsuka, T., Oschlies, A., Saito, M.A., Thingstad, T.F., Tsudo, A., Ulloa, O. Processes and patterns of oceanic nutrient limitation. *Nature Geoscience*. 2013. 6(9): 701–710.

Morales-McDevitt, M. E. Enriched mesocosm experiments to study the production of marine oil snow in the presence of BP surrogate oil and corexit 9500A. Master's Thesis, Texas A & M Univeristy. 2017.

Myklestad, S. M. Release of extracellular products by phytoplankton with special emphasis on polysaccharides. *The Science of the Total Environment*. 1995. 165: 155–164.

Orsi, W. D., Edgcomb, V. P., Christman, G. D., & Biddle, J. F. Gene expression in the deep biosphere. *Nature*. 2013. 499(7457): 205–208.

Ozhan, K., & Bargu, S. Distinct responses of Gulf of Mexico phytoplankton communities to crude oil and the dispersant corexit Ec9500A under different nutrient regimes. *Ecotoxicology*. 2014. 23(3): 370–384.

Ozhan, K., Parsons, M. L., Bargu, S. How were phytoplankton affected by the deepwater horizon oil spill? *BioScience.* 2014. 64(9): 829–836.

Pace, C. B., Clark, J. R., Bragin, G. E. Comparing crude oil toxicity under standard and environmentally realistic exposures. Proceedings of the 1995 International Oil Spill Conference, (Poster Session EW3). 1995. 1003–1004.

Parada AE, Needham DM, Fuhrman JA. Every base matters: assessing small subunit rRNA primers for marine microbiomes with mock communities, time series and global field samples. *Environ Microbiol.* 2015. 18:1403-1414.

Parsons, M. L., Morrison, W., Rabalais, N. N., Turner, R. E., Tyre, K. N. Phytoplankton and the Macondo oil spill: A comparison of the 2010 phytoplankton assemblage to baseline conditions on the Louisiana shelf. *Environmental Pollution*. 2015. 207: 152–160.

Passow, U. Formation of rapidly-sinking, oil-associated marine snow. *Research Part II: Topical Studies in Oceanography*, *129*, 232–240.

Passow, U., Alldredge, A. L., & Logan, B. E. The role of particulate carbohydrate exudates in the flocculation of diatom blooms. *Deep Sea Research I.* 1994. 41(2), 335–357.

Passow, U., Sweet, J., & Quigg, A. How the dispersant Corexit impacts the formation of sinking marine oil snow. *Marine Pollution Bulletin*. 2017. 125(1–2): 139–145.

Passow, U., Ziervogel, K., Asper, V., & Diercks, A. Marine snow formation in the aftermath of the Deepwater Horizon oil spill in the Gulf of Mexico. *Environmental Research Letters*. 2012. 7: 35301.

Patterson, D., Tom Flanchel, & Fenchel, T. Massisteria marina Larsen & Patterson 1990, a widespread and abundant bacterivorous protist associated with marine detritus. *Marine Ecology Progress Series. Oldendorf*. 1990. 62: 11–19.

Paul, C., & Pohnert, G. Interactions of the algicidal bacterium Kordia algicida with diatoms: Regulated protease excretion for specific algal lysis. *PLoS ONE*: 2011. *6*(6).

Plötner, W. A., Hillebrand, H., Ptacnikova, R., Ptacnik, R. Heterotrophic flagellates increase microalgal biomass yield. *Journal of Applied Phycology*. 2014. 27(1): 87–96.

Prowe, F, Pahlow, M, Dutkiewicz, S, Follows, M, Oschlies, A. Top-down control of marine phytoplankton diversity in a global ecosystem model. *Progress in Oceanography*. 2012. 101(1):1-13.

Quast C, Pruesse E, Yilmaz P, Gerken J, Schweer T, Yarza P, Peplies J, Glöckner FO. The SILVA ribosomal RNA gene database project: improved data processing and web-based tools. *Nucl. Acids Res.* 2014. 41(D1): D590-D596.

Quigg, A., Passow, U., Chin, W.C., Xu, C., Doyle, S., Bretherton, L., Kamalanathan, M., Williams, A.K., Sylvan, J.B., Finkel, Z.V., Knap, A.H., Schwehr, K.A., Zhang, S., Sun, L., Wade, T.L., Obeid, W., Hatcher, P.G., Santschi, P. H. The role of microbial exopolymers in determining the fate of oil and chemical dispersants in the ocean. *Limnology and Oceanography Letter*s. 2016. 3–26.

Quigg, A., Sylvan, J. B., Gustafson, A. B., Fisher, T. R., Tozzi, S. Ammerman, J. W. Going west: Nutrient limitation of primary production in the Northern Gulf of Mexico and the Importance of the Atchafalaya River. *Aquat Geochem*. 2011. 17: 519.

Quinn, G. P., & Keough, M. J. *Experimental Design and Data Analysis for Biologists*. 2002. Cambridge University Press.

Ramachandran, S. D., Hodson, P. V., Khan, C. W., Lee, K. Oil dispersant increases PAH uptake by fish exposed to crude oil. *Ecotoxicology and Environmental Safety*. 2004. 59(3): 300–308.

Reddy, C. M., Arey, J. S., Seewald, J. S., Sylva, S. P., Lemkau, K. L., Nelson, R. K., Carmichael, C.A., McIntyre, C.P., Fenwick, J., Ventura, G.T., Van Mooy, B.A.S., Camilli, R. (2012). Composition and fate of gas and oil released to the water column during the Deepwater Horizon oil spill. *Proceedings of the National Academy of Sciences*. 2012. 109(50): 20229–20234.

Ruan Q, Dutta D, Schwalbach MS, Steele JA, Fuhrman JA, Sun FZ. Local similarity analysis reveals unique associations among marine bacterioplankton species and environmental factors. *Bioinformatics.* 2006. 22: 2532–2538.

Schloss, P. D., Westcott, S. L., Ryabin, T., Hall, J. R., Hartmann, M., Hollister, E. B., Lesniewski, R.A., Oakly, B.B., Parks, D.H., Robinson, C.J., Sahl, J., Stres, B., Thallinger, G.G., Van Horn, D.J., Weber, C.F. Introducing mothur: Open-source, platform-independent, community-supported software for describing and comparing microbial communities. *Applied and Environmental Microbiology*. 2009. 75(23), 7537–7541.

Shannon, P., Markiel, A., Ozier, O., Baliga, N. S., Wang, J. T., Ramage, D., Amin, N., Schwikowski, B. Ideker, T. Cytoscape: a software environment for integrated models of biomolecular interaction networks. *Genome Research*. 2003. (13): 2498–2504.

Sherr, B. F., Sherr, E. B., & Hopkinson, C. S. Trophic interactions within pelagic microbial communities: Indications of feedback regulation of carbon flow. *Hydrobiologia*. 1988. 159(1): 19–26.

Shniukova, E. I., & Zolotareva, E. K. Diatom Exopolysaccharides: a Review. *International Journal on Algae*. 2015. 17(1): 50–67.

Stoecker, T., Bass, D., Nebel, M., Christen, R., Jones, M. D. M., Breiner, H. W., Richards, T. A. Multiple marker parallel tag environmental DNA sequencing reveals a highly complex eukaryotic community in marine anoxic water. *Molecular Ecology*. 2010. 19: 21–31.

Sylvan, J. B., Quigg, A., Tozzi, S. Ammerman, J.W. Eutrophication induced phosphorus limitation in the Mississippi River Plume: Evidence from fast repetition rate fluorometry. *Limnology and Oceanography*. 2007. 52: 2679-2685.

Sylvan, J. B., Quigg, A., Tozzi, S. Ammerman, J.W. Mapping phytoplankton community physiology on a river impacted continental shelf: testing a multifaceted approach. *Estuaries and Coasts*. 2011. 34:1220–1233

Tisthammer, K. H., Cobian, G. M., Amend, A. S. Global biogeography of marine fungi is shaped by the environment. *Fungal Ecology*. 2016. 19:39–46.

Thornton, D. Diatom aggregation in the sea: mechanisms and ecological implications. *Eur. J. Phycol*. 2002. 37: 149–161.

Tragin, M., Lopes dos Santos, A., Christen, R. Vaulot, D. Diversity and ecology of green microalgae in marine systems: an overview based on 18S rRNA gene sequences. *Perspect. Phycol*. 2016. 3(3): 141-154.

U.S. Coast Guard. On scene coordinator report - Deepwater Horizon oil spill: Submitted to the National Response Team. 2011. 244.

Valentine, David L., Kessler, John D., Redmond, Molly C., Mendes, Stephanie D., Heintz, Monica B., Farwell, Christopher, Hu, Lei, Kinnaman, Franklin S., Yvon-Lewis, Shari, Du, Mengran, Chan, Eric W., Tigreros, Fenix Garcia, Villanueva, C. J. Propane Respiration Jump-Starts Microbial Response to a Deep Oil Spill. *Science*. 2010. 330: 208–211.

van Eenennaam, J. S., Wei, Y., Grolle, K. C. F., Foekema, E. M., Murk, A. T. J. Oil spill dispersants induce formation of marine snow by phytoplankton–associated bacteria. *Marine Pollution Bulletin*. 2016. 104(1–2): 294–302.

Verni, F., & Gualtieri, P. Feeding behaviour in ciliated protists. *Micron*. 1997. 28(6): 487–504.

Wade, T. L., Morales-McDevitt, M., Bera, G., Shi, D., Sweet, S., Wang, B., Gold-Bouchot, G., Quigg, A., Knap, A. H. A method for the production of large volumes of WAF and CEWAF for dosing mesocosms to understand marine oil snow formation. *Heliyon*. 2017. 3(10): e00419.

Walters W, Hyde, E.R., Berg-Lyons, D., Ackermann, G., Humphrey, G., Parada, A., Gilbert, J.A., Jansson, J.K., Caporaso, J.G., Fuhrman, J.A., Apprill, A., Knight, R. Improved Bacterial 16S rRNA Gene (V4 and V4-5) and Fungal Internal Transcribed Spacer Marker Gene Primers for Microbial Community Surveys. *mSystems*. 2015. 1:1-10.

Weiss, S., Xu, Z. Z., Peddada, S., Amir, A., Bittinger, K., Gonzalez, A., Lozupone, C., Zaneveld, J.R., Vazquez-Baeza, Y., Birmingham, A., Hyde, E.R., Knight, R. Normalization and microbial differential abundance strategies depend upon data characteristics. *Microbiome*. 2017. 5(1): 1–18.

Wilhelm, S.W. and Suttle, C.A. Viruses and Nutrient Cycles in the Sea. *BioScience*. 1999. 49 (10): 781-788.

Wells, M. L., Trick, C. G., Cochlan, W. P., Hughes, M. P., Trainer, V. L. Domoic acid: The synergy of iron, copper, and the toxicity of diatoms. *Limnology and Oceanography*. 2005. 50(6): 1908–1917.

Xia, L. C., Steele, J. A., Cram, J. A., Cardon, Z. G., Simmons, S. L., Vallino, J. J., Fuhrman, J.A., Sun, F. Extended local similarity analysis (eLSA) of microbial community and other time series data with replicates. *BMC Systems Biology*. 2011. *5*(SUPPL2):S15.

Zafra, G., Absalón, Á. E., Cuevas, M. D. C., Cortés-Espinosa, D. V. Isolation and selection of a highly tolerant microbial consortium with potential for PAH biodegradation from heavy crude oil-contaminated soils. *Water, Air, and Soil Pollution*. 2015. 225(2).

Zhao, Y., & Quigg, A. Nutrient Limitation in Northern Gulf of Mexico (NGOM): Phytoplankton Communities and Photosynthesis Respond to Nutrient Pulse. *PLoS ONE*. 2014. 9(2).

Zhang, N., Xiao, X., Pei, M., Liu, X., & Liang, Y. Discordant temporal turnovers of sediment bacterial and eukaryotic communities in response to dredging: Nonresilience and functional changes. *Applied and Environmental Microbiology*. 2017. 83(1): 1–15.

Zurr, A., Ieno, E.N. Walker, N. Saveliev, A.A., Smith, G.M. Mixed Effects Models and Extensions in Ecology with R. New York City: Springer, 2009. Print.

APPENDIX

List A-1: Eukaryotic community composition commands for sample processing in mothur. Detailed notes on commands used in mothur for the Eukaryotic community.

make.contigs(file=file.file, processors=48)
summary.seqs(fasta=current, processors=48)
screen.seqs(fasta=current, group=current, maxambig=0, maxhomop=8, maxlength=350, processors=48)
unique.seqs(fasta=current)
count.seqs(name=current, group=current, processors=48)
align.seqs(fasta=current, reference=silva.nr_v123.pcr.align, processors=48)
summary.seqs(fasta=current, count=current, processors=48)
screen.seqs(fasta=current, count=current, start=2052, end=5810, processors=48)
filter.seqs(fasta=current, vertical=T, trump=., processors=48)
unique.seqs(fasta=current, count=current)
pre.cluster(fasta=current, count=current, diffs=3, processors=48)
chimera.uchime(fasta=current, count=current, dereplicate=T, processors=48)
remove.seqs(fasta=current, accnos=current)
classify.seqs(fasta=current, count=current, reference=silva.nr_v123.pcr.align, taxonomy=silva.nr_v123_delete.tax, cutoff=80, processors=48) #After classify.seqs, taxonomy file downloaded, removed Metazoa and uploaded again.
remove.lineage(fasta=current, count=current, taxonomy=RemoveMetazoa.taxonomy, taxon=Archaea-Bacteria-Chloroplast-Mitochondria-unknown-Metazoa)
summary.tax(taxonomy=current, count=current)
dist.seqs(fasta=current, cutoff=0.05, processors=48)
cluster.split(column=current, count=current, cutoff=0.05, processors=48)
make.shared(list=current, count=current, label=0.05)
get.oturep(column=current, list=current, count=current, fasta=current, method=distance, label=0.05)
classify.seqs(fasta=current, template=pr2_version_4.7_mothur_Eukaryota.fasta, taxonomy=pr2_version_4.7_mothur_Eukaryota.tax, processors=48)
classify.otu(taxonomy=current, list=current, label=0.05)
sub.sample(shared="the original shared file", size=8196) #The output shared file is called "the subsampled shared file".
summary.single(shared="the subsampled shared file", calc=nseqs-coverage-sobs-invsimpson-ace-chao)
rarefaction.single(shared=Euk.shared, calc=sobs, freq=100)

List A-2: Prokaryotic community composition commands for sample processing in mothur. Detailed notes on commands used in mothur for the prokaryotic community.

make.file(inputdir=file.fastq, type=fastq, prefix=meso3and4)
make.contigs(file=file.files, processors=20)
summary.seqs(fasta=current, processors=20)
screen.seqs(fasta=current, group=meso3and4.groups, maxambig=0, maxlength=275, maxhomop=8)
unique.seqs(fasta=current)
count.seqs(name=current, group=meso3and4.good.groups)
align.seqs(fasta=current, reference=silva.nr_v123.pcr.align)
summary.seqs(fasta=current, processors=20)
screen.seqs(fasta=current, count=current, start=1968, end=11550)
filter.seqs(fasta=meso3and4.good.unique.good.align, vertical=T, trump=.)

unique.seqs(fasta=current, count=current)
pre.cluster(fasta=current, count=current, diffs=2)
chimera.vsearch(fasta=current, count=current, dereplicate=t)
remove.seqs(fasta=current, accnos=current)
classify.seqs(fasta=current, count=current, reference=silva.nr_v123.pcr.align,
taxonomy=silva.nr_v123.tax, cutoff=80)
remove.lineage(fasta=current, count=current,
taxonomy=meso3and4.good.unique.good.filter.unique.precluster.pick.nr_v123.wang.taxonomy,
taxon=Chloroplast-Mitochondria-unknown-Eukayota)
cluster.split(fasta=current, count=current,
taxonomy=meso3and4.good.unique.good.filter.unique.precluster.pick.nr_v123.wang.pick.taxonomy,
splitmethod=classify, taxlevel=2, cutoff=0.03, method=opti, processors=20)
make.shared(list=current, count=current, label=0.03)
classify.otu(list=current, count=current,
taxonomy=meso3and4.good.unique.good.filter.unique.precluster.pick.nr_v123.wang.pick.taxonomy,
label=0.03)
count.groups(shared=current)
sub.sample(shared= Prok_meso3and4.shared, size=1114)
summary.single(shared=Prok_meso3and4_subsample.shared, calc=nseqs-coverage-sobs-invsimpson-ace-chao)
rarefaction.single(shared=Prok_meso3and4.shared, calc=sobs, freq=100)

Table A-1: Eukaryotic OTU (Operational Taxonomic Unit) table. Table includes taxonomy for the top 99% abundant eukaryotic OTUs.

Kingdom	**Phylum**	**ClassW**	**PR2 Genus and Species**	**Group**
Chromista	Stramenopiles-Ochrophyta	Bacillariophyceae-Centric	unknown	Otu00002
Chromista	Stramenopiles-Ochrophyta	Bacillariophyceae-Centric	unknown	Otu00003
Chromista	Stramenopiles-Bigyra	Bicoecea	*Pseudobodo* sp.	Otu00004
Chromista	Stramenopiles-Ochrophyta	Chrysophyceae	*Paraphysomonas* sp.	Otu00005
Chromista	Rhizaria-Cercozoa	Granofilosea	*Massisteria marina*	Otu00007
Chromista	Stramenopiles-Ochrophyta	Bacillariophyceae-Centric	*Chaetoceros* sp.	Otu00008
Chromista	Stramenopiles-Ochrophyta	Bacillariophyceae-Centric	*Cyclotella* sp.	Otu00009
Chromista	Alveolata-Myzozoa	Dinophyceae	unknown	Otu00010
Chromista	Alveolata-Ciliophora	Oligohymenophorea	*Miamiensis* sp.	Otu00011
Fungi	Basidiomycota	Microbotryomycetes	*Rhodotorula glutinis*	Otu00012

Kingdom	**Phylum**	**ClassW**	**PR2 Genus and Species**	**Group**
Chromista	Stramenopiles-Ochrophyta	Bacillariophyceae-Centric	*Minutocellus* sp.	Otu00017
Unclassified	unknown	Unclassified	unknown	Otu00018
Fungi	Ascomycota	Eurotiomycetes	*Aspergillus flavipes*	Otu00019
Chromista	Alveolata-Myzozoa	Dinophyceae	*Scrippsiella* sp.	Otu00020
Chromista	Stramenopiles-Bigyra	Bicoecea	*Cafeteria roenbergensis*	Otu00021
Chromista	Rhizaria-Cercozoa	Granofilosea	*Massisteria marina*	Otu00022
Chromista	Stramenopiles-Bigyra	Bicoecea	*Pseudobodo* sp.	Otu00023
Chromista	Stramenopiles-Ochrophyta	Bacillariophyceae-Pennate	unknown	Otu00024
Chromista	Alveolata-Myzozoa	unknown	unknown	Otu00026
Chromista	Stramenopiles-Ochrophyta	Bacillariophyceae-Centric	*Coscinodiscus wailesii*	Otu00027
Chromista	Alveolata-Myzozoa	Dinophyceae	unknown	Otu00028
Chromista	Rhizaria-Cercozoa	Chlorarachnea	unknown	Otu00029
Chromista	Stramenopiles-Bigyra	Labyrinthulea	*Aplanochytrium* sp.	Otu00031

Kingdom	**Phylum**	**ClassW**	**PR2 Genus and Species**	**Group**
Protozoa	Choanozoa	Ichthyosporea	uncultured marine ichthyosporeans group 1	Otu00032
Chromista	Alveolata-Ciliophora	Oligohymenophorea	unknown	Otu00033
Chromista	Stramenopiles-Bigyra	Bicoecea	*Pseudobodo* sp.	Otu00034
Chromista	Stramenopiles-Ochrophyta	Chrysophyceae	*Paraphysomonas* sp.	Otu00035
Unclassified	unknown	Unclassified	unknown	Otu00036
Chromista	Alveolata-Myzozoa	Dinophyceae	*Stoeckeria algicida*	Otu00037
Chromista	Stramenopiles-Ochrophyta	Bacillariophyceae-Centric	*Chaetoceros* sp.	Otu00038
Protozoa	Choanozoa	Ichthyosporea	uncultured marine ichthyosporeans group 1	Otu00040
Chromista-Heterokonta	Stramenopiles-unclassified	Stramenopiles(IK)-Unclassified	MAST-12D	Otu00041
Chromista	Stramenopiles-Ochrophyta	Bacillariophyceae-Pennate	*Talaroneis posidoniae*	Otu00042
Fungi	Ascomycota	Dothideomycetes	unknown	Otu00043
Fungi	Ascomycota	Dothideomycetes	unknown	Otu00044

Kingdom	**Phylum**	**ClassW**	**PR2 Genus and Species**	**Group**
Chromista	Stramenopiles-Bigyra	Labyrinthulea	unknown	Otu00046
Chromista	Stramenopiles-Ochrophyta	Bacillariophyceae-Centric	*Chaetoceros muellerii*	Otu00049
Chromista	Stramenopiles-Bigyra	Bicoecea	*Pseudobodo* sp.	Otu00051
Fungi	unknown	Fungi(K)-Unclassified	unknown	Otu00052
Chromista	Alveolata-Myzozoa	Dinophyceae	*Alexandrium* sp.	Otu00054
Chromista	Stramenopiles-Bigyra	Bicoecea	unknown	Otu00056
Chromista	Stramenopiles-Bigyra	Bicoecea	*Caecitellus paraparvulus*	Otu00057
Chromista	Stramenopiles-Ochrophyta	Ochrophyta(P)-Unclassified	MOCH-5	Otu00059
Chromista	Stramenopiles-Ochrophyta	Bacillariophyceae-Centric	*Odontella sinensis*	Otu00060
Chromista	Stramenopiles-Ochrophyta	Ochrophyta(P)-Unclassified	unknown	Otu00062
Chromista	Stramenopiles-Ochrophyta	Bacillariophyceae	unknown	Otu00063

Kingdom	**Phylum**	**ClassW**	**PR2 Genus and Species**	**Group**
Unclassified	unknown	Unclassified	unknown	Otu00064
Chromista-Heterokonta	Stramenopiles-unclassified	Stramenopiles(IK)-Unclassified	MAST-2C	Otu00065
Unclassified	unknown	Unclassified	unknown	Otu00067
Fungi	Ascomycota	Sordariomycetes	unknown	Otu00068
Chromista	Alveolata-Ciliophora	Oligohymenophorea	*Metanophyrs sinensis*	Otu00071
Fungi	unknown	Fungi(K)-Unclassified	unknown	Otu00073
Chromista	Stramenopiles-Ochrophyta	Ochrophyta(P)-Unclassified	unknown	Otu00074
Fungi	unknown	Fungi(K)-Unclassified	unknown	Otu00075
Unclassified	unknown	Unclassified	unknown	Otu00076
Chromista	Stramenopiles-Ochrophyta	Chrysophyceae	unknown	Otu00077
Chromista	Alveolata-Ciliophora	Phyllopharyngea	*Chlamydodon* sp.	Otu00078
Chromista	Alveolata-Myzozoa	Dinophyceae	*Lepidodinium* sp.	Otu00080

Kingdom	**Phylum**	**ClassW**	**PR2 Genus and Species**	**Group**
Chromista	Stramenopiles-Ochrophyta	Bacillariophyceae-Centric	*Chaetoceros* sp.	Otu00084
Chromista	Alveolata-Ciliophora	Oligotricea	*Favella panamensis*	Otu00087
Chromista	Stramenopiles-Ochrophyta	Ochrophyta(P)-Unclassified	unknown	Otu00088
Chromista	Alveolata-Myzozoa	Dinophyceae	unknown	Otu00089
Chromista-Heterokonta	Stramenopiles-unclassified	Stramenopiles(IK)-Unclassified	MAST-9C	Otu00090
Unclassified	unknown	Unclassified	unknown	Otu00091
Chromista	Stramenopiles-Bigyra	Bicoecea	*Bicosoeca* sp.	Otu00092
Chromista	Alveolata-Ciliophora	Oligohymenophorea	*Pseudocohnilembus persalinus*	Otu00093
Chromista	Stramenopiles-unclassified	Stramenopiles(IK)-Unclassified	unknown	Otu00094
Chromista	Stramenopiles-Bigyra	Bicoecea	*Pseudobodo* sp.	Otu00096
Unclassified	unknown	Unclassified	unknown	Otu00099
Fungi	Basidiomycota	Ustilaginomycetes	unknown	Otu00100

Kingdom	**Phylum**	**ClassW**	**PR2 Genus and Species**	**Group**
Chromista-Heterokonta	Stramenopiles-unclassified	Stramenopiles(IK)-Unclassified	MAST-12A	Otu00104
Chromista	Rhizaria-Cercozoa	Granofilosea	*Massisteria marina*	Otu00105
Chromista	Stramenopiles-Ochrophyta	Ochrophyta(P)-Unclassified	MOCH-3	Otu00106
Chromista	Alveolata-Myzozoa	Dinophyceae	*Gyrodinium instriatum*	Otu00107
Chromista	Stramenopiles-Bigyra	Labyrinthulea	*Aplanochytrium stocchinoi*	Otu00109
Chromista	Stramenopiles-Ochrophyta	Chrysophyceae	unknown	Otu00110
Chromista	Alveolata-Myzozoa	Dinophyceae	unknown	Otu00112
Fungi	Basidiomycota	Tremellomycetes	*Cryptococcus aureus*	Otu00113
Chromista	Stramenopiles-Ochrophyta	Ochrophyta(P)-Unclassified	MOCH-5	Otu00114
Chromista	Stramenopiles-Ochrophyta	Ochrophyta(P)-Unclassified	MOCH-5	Otu00117
Chromista	Alveolata-Ciliophora	unknown	unknown	Otu00120

Kingdom	**Phylum**	**ClassW**	**PR2 Genus and Species**	**Group**
Unclassified	unknown	Unclassified	unknown	Otu00123
Chromista	Alveolata-Ciliophora	Spirotrichea	*Holosticha* sp.	Otu00126
Unclassified	unknown	Unclassified	unknown	Otu00128
Chromista	Stramenopiles-Ochrophyta	Bacillariophyceae-Centric	unknown	Otu00129
Protozoa	Amoebozoa	Variosea	unknown	Otu00131
Chromista	Stramenopiles-Ochrophyta	Eustigmatophyceae	*Nanochloropsis* sp.	Otu00134
Chromista	Stramenopiles-Bigyra	Bicoecea	unknown	Otu00138
Chromista	Alveolata-Myzozoa	Dinophyceae	*Neoceratium furca*	Otu00140
Unclassified	unknown	Unclassified	unknown	Otu00143
Chromista	Stramenopiles-Bigyra	Bicoecea	unknown	Otu00148
Chromista	Stramenopiles-Bigyra	Labyrinthulea	unknown	Otu00152
Unclassified	unknown	Unclassified	unknown	Otu00153
Chromista-Heterokonta	Stramenopiles-unclassified	Stramenopiles(IK)-Unclassified	MAST-1C	Otu00154

Kingdom	**Phylum**	**ClassW**	**PR2 Genus and Species**	**Group**
Protozoa	Amoebozoa	Discosea	*Vannella aberdonica*	Otu00155
Chromista	Stramenopiles-unclassified	Stramenopiles(IK)-Unclassified	unknown	Otu00158
Chromista	Alveolata-Ciliophora	Oligohymenophorea	unknown	Otu00160
Chromista	Alveolata-Myzozoa	Dinophyceae	unknown	Otu00169
Chromista	Alveolata-Myzozoa	Dinophyceae	unknown	Otu00172
Unclassified	unknown	Unclassified	unknown	Otu00173
Chromista	Stramenopiles-Ochrophyta	Bacillariophyceae-Centric	*Coscinodiscus granii*	Otu00192
Unclassified	unknown	Unclassified	unknown	Otu00194
Chromista	Alveolata-Myzozoa	unknown	unknown	Otu00201
Protozoa	Amoebozoa	Discosea	*Vanella plurinucleolus*	Otu00206
Chromista	Rhizaria-Cercozoa	Imbricatea	unknown	Otu00208
Chromista	Stramenopiles-Bigyra	Labyrinthulea	*Aplanochytrium* sp.	Otu00218
Chromista	Stramenopiles-Ochrophyta	Bacillariophyceae-Centric	*Proboscia* sp.	Otu00219

Kingdom	**Phylum**	**ClassW**	**PR2 Genus and Species**	**Group**
Chromista	Stramenopiles-Bigyra	Labyrinthulea	unknown	Otu00227
Chromista	Stramenopiles-Oomycota	Developayella	*Developayella* sp.	Otu00238
Chromista	Alveolata-Ciliophora	Litostomatea	unknown	Otu00239
Chromista	Stramenopiles-Bigyra	Bicoecea	*Caecitellus parvulus*	Otu00255
Chromista	Alveolata-Myzozoa	Conoidasida	unknown	Otu00261
Unclassified	unknown	Unclassified	unknown	Otu00267
Unclassified	unknown	Unclassified	unknown	Otu00399
Chromista	Stramenopiles-Ochrophyta	Bacillariophyceae-Pennate	unknown	Otu00412
Chromista	Stramenopiles-Bigyra	Bicoecea	*Cafeteria roenbergensis*	Otu00422
Unclassified	unknown	Unclassified	unknown	Otu00605

Table A-2: Prokaryotic OTU (Operational Taxonomic Unit) table. Table includes taxonomy for the top 99% abundant prokaryotic OTUs.

Domain	**Phylum**	**Class**	**Order**	**Genus**	**Group**
Bacteria	Proteobacteria	Gammaproteobacteria	Alteromonadales	*Alteromonas*	Otu00001
Bacteria	Proteobacteria	Gammaproteobacteria	Alteromonadales	*Marinobacter*	Otu00002
Bacteria	Proteobacteria	Gammaproteobacteria	Pseudomonadales	unknown	Otu00003
Bacteria	Proteobacteria	Gammaproteobacteria	Xanthomonadales	*Polycyclovorans*	Otu00004
Bacteria	Proteobacteria	Gammaproteobacteria	Alteromonadales	*Aestuariibacter*	Otu00005
Bacteria	Proteobacteria	Gammaproteobacteria	Alteromonadales	*Marinobacter*	Otu00006
Bacteria	Proteobacteria	Gammaproteobacteria	Thiotrichales	*Methylophaga*	Otu00007
Bacteria	Proteobacteria	Gammaproteobacteria	Thiotrichales	*Methylophaga*	Otu00008
Bacteria	Proteobacteria	Gammaproteobacteria	Thiotrichales	*Cycloclasticus*	Otu00009
Bacteria	Proteobacteria	Gammaproteobacteria	Alteromonadales	*Marinobacter*	Otu00010
Bacteria	Proteobacteria	Gammaproteobacteria	Oceanospirillales	*Thalassolituus*	Otu00011
Bacteria	Proteobacteria	Gammaproteobacteria	Cellvibrionales	*Pseudomaricurvus*	Otu00012
Bacteria	Proteobacteria	Gammaproteobacteria	Oceanospirillales	*Alcanivorax*	Otu00013
Bacteria	Proteobacteria	Gammaproteobacteria	Oceanospirillales	unknown	Otu00014
Bacteria	Proteobacteria	Gammaproteobacteria	Oceanospirillales	*Alcanivorax*	Otu00015

Domain	**Phylum**	**Class**	**Order**	**Genus**	**Group**
Bacteria	Cyanobacteria	Cyanobacteria	Cyanobacteria(P)-Unclassified	*Synechococcus*	Otu00016
Bacteria	Proteobacteria	Gammaproteobacteria	Cellvibrionales	*Maricurvus*	Otu00017
Bacteria	Proteobacteria	Gammaproteobacteria	Oceanospirillales	*Oleibacter*	Otu00018
Bacteria	Proteobacteria	Alphaproteobacteria	Rhodobacterales	*Tropicimonas*	Otu00019
Bacteria	Proteobacteria	Alphaproteobacteria	SAR11_clade	*Candidatus pelagibacter*	Otu00020
Bacteria	Proteobacteria	Gammaproteobacteria	Alteromonadales	*Pseudoalteromonas*	Otu00021
Bacteria	Proteobacteria	Gammaproteobacteria	Alteromonadales	*Alteromonas*	Otu00022
Bacteria	Proteobacteria	Alphaproteobacteria	Rhodobacterales	unknown	Otu00023
Bacteria	Proteobacteria	Alphaproteobacteria	Rhodobacterales	unknown	Otu00024
Bacteria	Proteobacteria	Gammaproteobacteria	Oceanospirillales	*Oleispira*	Otu00025
Bacteria	Proteobacteria	Alphaproteobacteria	Rhodobacterales	unknown	Otu00026
Bacteria	Proteobacteria	Alphaproteobacteria	Rhodobacterales	unknown	Otu00027
Bacteria	Actinobacteria	Acidimicrobiia	Acidimicrobiales	*Candidatus actinomarina*	Otu00028
Bacteria	Proteobacteria	Alphaproteobacteria	Sphingomonadales	Erythrobacteraceae unclassified	Otu00029
Bacteria	Proteobacteria	Alphaproteobacteria	Rhodospirillales	AEGEAN-169_marine_group	Otu00030

Domain	**Phylum**	**Class**	**Order**	**Genus**	**Group**
Bacteria	Proteobacteria	Alphaproteobacteria	Rhodobacterales	unknown	Otu00031
Bacteria	Bacteroidetes	Flavobacteriia	Flavobacteriales	*Tenacibaculum*	Otu00032
Bacteria	Proteobacteria	Gammaproteobacteria	Vibrionales	*Vibrio*	Otu00033
Bacteria	Bacteroidetes	Sphingobacteriia	Sphingobacteriales	unknown	Otu00034
Bacteria	Proteobacteria	Alphaproteobacteria	Caulobacterales	*Ponticaulis*	Otu00035
Bacteria	Proteobacteria	Alphaproteobacteria	Rhodobacterales	unknown	Otu00036
Bacteria	Proteobacteria	Alphaproteobacteria	Rhodobacterales	*Ruegeria*	Otu00037
Bacteria	Proteobacteria	Deltaproteobacteria	Bdellovibrionales	*Halobacteriovorax*	Otu00038
Bacteria	Proteobacteria	Gammaproteobacteria	Oceanospirillales	*Pseudospirillum*	Otu00039
Bacteria	Proteobacteria	Gammaproteobacteria	Alteromonadales	*Aestuariibacter*	Otu00040
Bacteria	Proteobacteria	Gammaproteobacteria	Salinisphaerales	*Salinisphaera*	Otu00041
Bacteria	Proteobacteria	Gammaproteobacteria	Cellvibrionales	OM60_clade	Otu00042
Bacteria	Proteobacteria	Deltaproteobacteria	Deltaproteobacteria(C)-Unclassified	unknown	Otu00043
Bacteria	Proteobacteria	Alphaproteobacteria	Rhodobacterales	unknown	Otu00044
Bacteria	Proteobacteria	Alphaproteobacteria	Rhodospirillales	*Thalassospira*	Otu00045

Domain	**Phylum**	**Class**	**Order**	**Genus**	**Group**
Bacteria	Bacteroidetes	Flavobacteriia	Flavobacteriales	*Owenweeksia*	Otu00046
Bacteria	Proteobacteria	Alphaproteobacteria	SAR11_clade	unknown	Otu00047
Bacteria	Proteobacteria	Alphaproteobacteria	4-Org1-14	4-Org1-14_unclassified	Otu00048
Bacteria	Bacteroidetes	Sphingobacteriia	Sphingobacteriales	unknown	Otu00049
Bacteria	Proteobacteria	Gammaproteobacteria	Salinisphaerales	*Salinisphaera*	Otu00050
Bacteria	Proteobacteria	Alphaproteobacteria	Caulobacterales	*Hyphomonas*	Otu00051
Bacteria	Proteobacteria	Alphaproteobacteria	Rhodospirillales	*Magnetospira*	Otu00052
Bacteria	Proteobacteria	Gammaproteobacteria	Gammaproteobacteria(C)-Unclassified	unknown	Otu00053
Bacteria	Bacteroidetes	Flavobacteriia	Flavobacteriales	unknown	Otu00054
Bacteria	Proteobacteria	Gammaproteobacteria	Cellvibrionales	C1-B045	Otu00055
Bacteria	Proteobacteria	Gammaproteobacteria	Gammaproteobacteria(C)-Unclassified	*Marinicella*	Otu00056
Bacteria	Cyanobacteria	Cyanobacteria	Cyanobacteria(P)-Unclassified	*Synechococcus*	Otu00057
Bacteria	Proteobacteria	Gammaproteobacteria	Oceanospirillales	*Neptuniibacter*	Otu00058
Bacteria	Proteobacteria	AEGEAN-245	AEGEAN-245(C)-Unclassified	AEGEAN-245 unclassified	Otu00059

Domain	**Phylum**	**Class**	**Order**	**Genus**	**Group**
Bacteria	Proteobacteria	Alphaproteobacteria	Rhodobacterales	*Pseudophaeobacter*	Otu00060
Bacteria	Proteobacteria	Alphaproteobacteria	Caulobacterales	*Maricaulis*	Otu00061
Bacteria	Bacteroidetes	Sphingobacteriia	Sphingobacteriales	unknown	Otu00062
Bacteria	Proteobacteria	Alphaproteobacteria	Parvularculales	*Parvularcula*	Otu00063
Bacteria	Proteobacteria	Gammaproteobacteria	Cellvibrionales	C1-B045	Otu00064
Bacteria	Bacteroidetes	Flavobacteriia	Flavobacteriales	NS5_marine_group	Otu00065
Bacteria	Proteobacteria	Alphaproteobacteria	SAR11_clade	unknown	Otu00066
Bacteria	Cyanobacteria	Cyanobacteria	Cyanobacteria(P)-Unclassified	*Synechococcus*	Otu00067
Bacteria	Proteobacteria	Gammaproteobacteria	Oceanospirillales	unknown	Otu00068
Bacteria	Bacteroidetes	Sphingobacteriia	Sphingobacteriales	unknown	Otu00069
Bacteria	Proteobacteria	Gammaproteobacteria	Cellvibrionales	*Pseudomaricurvus*	Otu00070
Bacteria	Proteobacteria	Gammaproteobacteria	Cellvibrionales	*Luminiphilus*	Otu00071
Bacteria	Bacteroidetes	Bacteroidetes(P)-Unclassified	Bacteroidetes(P)-Unclassified	unknown	Otu00072
Bacteria	Bacteroidetes	Cytophagia	Cytophagales	Fabibacter	Otu00074
Bacteria	Proteobacteria	Gammaproteobacteria	Cellvibrionales	OM60_clade	Otu00076

Domain	**Phylum**	**Class**	**Order**	**Genus**	**Group**
Bacteria	Proteobacteria	Alphaproteobacteria	Rhodospirillales	*Thalassospira*	Otu00077
Bacteria	Planctomycetes	Planctomycetacia	Planctomycetales	*Planctomyces*	Otu00078
Bacteria	Bacteroidetes	Sphingobacteriia	Sphingobacteriales	*Phaeodactylibacter*	Otu00079
Bacteria	Planctomycetes	OM190	OM190(C)-Unclassified	OM190_unclassified	Otu00080
Bacteria	Bacteroidetes	Bacteroidetes(P)-Unclassified	Bacteroidetes(P)-Unclassified	unknown	Otu00082
Bacteria	Cyanobacteria	Cyanobacteria	Cyanobacteria(P)-Unclassified	*Synechococcus*	Otu00083
Bacteria	Proteobacteria	Alphaproteobacteria	Rhodobacterales	unknown	Otu00087
Bacteria	Proteobacteria	Gammaproteobacteria	Oceanospirillales	unknown	Otu00088
Bacteria	Bacteroidetes	Flavobacteriia	Flavobacteriales	unknown	Otu00089
Bacteria	Cyanobacteria	Cyanobacteria	Cyanobacteria(P)-Unclassified	*Synechococcus*	Otu00090
Bacteria	Proteobacteria	Gammaproteobacteria	Oceanospirillales	*Pseudospirillum*	Otu00091
Bacteria	Proteobacteria	Gammaproteobacteria	Thiotrichales	*Methylophaga*	Otu00094
Bacteria	Proteobacteria	Alphaproteobacteria	SAR11_clade	unknown	Otu00095
Bacteria	Proteobacteria	Gammaproteobacteria	Thiotrichales	*Methylophaga*	Otu00096
Bacteria	Proteobacteria	Gammaproteobacteria	Thiotrichales	*Methylophaga*	Otu00097

Domain	**Phylum**	**Class**	**Order**	**Genus**	**Group**
Bacteria	Proteobacteria	Gammaproteobacteria	Alteromonadales	*Algicola*	Otu00098
Bacteria	Bacteroidetes	Flavobacteriia	Flavobacteriales	NS4_marine_group	Otu00102
Bacteria	Proteobacteria	Gammaproteobacteria	Alteromonadales	*Idiomarina*	Otu00103
Bacteria	Actinobacteria	Actinobacteria	PeM15	unknown	Otu00104
Bacteria	Proteobacteria	Alphaproteobacteria	Sphingomonadales	*Altererythrobacter*	Otu00110
Bacteria	Proteobacteria	Gammaproteobacteria	Gammaproteobacteria(C)-Unclassified	unknown	Otu00115
Bacteria	Proteobacteria	Gammaproteobacteria	Oceanospirillales	unknown	Otu00119
Bacteria	Proteobacteria	Alphaproteobacteria	Rickettsiales	LWSR-14_unclassified	Otu00123
Bacteria	Proteobacteria	Gammaproteobacteria	Cellvibrionales	*Pseudomaricurvus*	Otu00127
Bacteria	Proteobacteria	Gammaproteobacteria	Alteromonadales	*Thalassotalea*	Otu00130
Bacteria	Proteobacteria	Proteobacteria(P)-Unclassified	Proteobacteria(P)-Unclassified	unknown	Otu00132
Bacteria	Proteobacteria	Gammaproteobacteria	34P16	34P16_unclassified	Otu00135
Bacteria	Proteobacteria	Alphaproteobacteria	Rickettsiales	S25-593_unclassified	Otu00142
Bacteria	Proteobacteria	Gammaproteobacteria	Oceanospirillales	unknown	Otu00161

Domain	**Phylum**	**Class**	**Order**	**Genus**	**Group**
Bacteria	Bacteroidetes	Flavobacteriia	Flavobacteriales	*Aquibacter*	Otu00167
Bacteria	Proteobacteria	Alphaproteobacteria	Rickettsiales	unknown	Otu00173
Bacteria	Proteobacteria	Alphaproteobacteria	Rickettsiales	unknown	Otu00176
Bacteria	Proteobacteria	Gammaproteobacteria	Oceanospirillales	unknown	Otu00184
Bacteria	Cyanobacteria	Cyanobacteria	Cyanobacteria(P)-Unclassified	*Synechococcus*	Otu00203
Bacteria	Proteobacteria	Gammaproteobacteria	Oceanospirillales	unknown	Otu00204
Bacteria	Bacteroidetes	Flavobacteriia	Flavobacteriales	NS2b_marine_group	Otu00205
Bacteria	Proteobacteria	Deltaproteobacteria	SAR324_clade	unknown	Otu00212
Bacteria	Proteobacteria	Alphaproteobacteria	Alphaproteobacteria(C)-Unclassified	unknown	Otu00226
Archaea	Euryarchaeota	Thermoplasmata	Thermoplasmatales	Marine_Group_II_unclassified	Otu00264
Bacteria	Proteobacteria	Gammaproteobacteria	Gammaproteobacteria(C)-Unclassified	unknown	Otu00365